NTNU

Norwegian University of
Science and Technology

Petrophysical Characterization of Reservoirs in the Pil and Bue area,Norwegian Sea

Endrias Hailu Berhe

Petroleum Engineering
Submission date: July 2017
Supervisor: Erik Skogen, IGP

Norwegian University of Science and Technology
Department of Geoscience and Petroleum

Acknowledgment

First and foremost, I would like to thank the Almighty God and His Mother St. Mary for the grace, love and mercy throughout my life. Whatever the challenges faced in my life I never walked alone His protection and guidance has led me up to now.

I would like to express my deepest gratitude to my supervisor Professor Erik Skogen for his guidance, encouragement, and an overall support have been invaluable throughout my thesis. I really appreciate his nice treatment though it is common in NTNU but most of my exposure was with him and this gives me great experience how to treat and respect your student. In addition, I would like to thank Professor Carl Fredrik for his Invaluable help in answering to my confusions on the thesis.

I would like to thank the Norwegian government for the scholarship, for every limit less service I got and for every resource I use in the two years of my study. I really appreciate that everything in Norway was a great exposure for me and the knowledge I got is a great input to serve my country.

Finally, I would like to express my sincere gratitude to my dear mother for everything she has done for me throughout my life!!

Abstract

This thesis presents Petrophysical characterization of Pil and Bue oil and gas bearing shaly sand reservoirs in offshore Norwegian Sea, Norway. In the petroleum industry, interpreting and analyzing logs from shaly sand formations are difficult tasks. The main challenges of water saturation estimation and general petrophysical analysis of rock properties in shaly sand reservoirs are mainly caused by the conductive behavior associated with the clay minerals. The presences of these minerals create vertical and horizontal heterogeneity in the geological formation and finally to the physical properties. Moreover, this thesis project assesses the clean sand and shaly sand methods of water saturation, correcting and correlating of the core porosity and core permeability with the log data results of porosity and permeability. In the analysis of the parameters, Techlog software was used to perform the computations of the petrophysical properties. Three wells (6406/12-3S, 6406/12-3B and 6406/12-3A) were evaluated, and from these wells oil and gas-bearing reservoir was encountered in well 6406/12-3S. However, in well 6406/12-3B and well 6406/12-3A only oil-bearing reservoirs were encountered. Based on general and detailed evaluation of the petrophysical parameters of these wells different values were recorded. The shale volume determined in the reservoirs intervals of well 6406/12-3S, 6406/12-3B and 6406/12-3A lies in a range of 9-20 %, 15-32 %, and 5-33 % respectively. The average grain density used in the log analysis of the three wells was 2.65 g/cc.

The reservoir rock properties of the three wells as calculated from the log analysis and values taken from core analysis report shows good to very good reservoir quality. The porosity in well 6406/12-3S ranges between 9-16 % from log analysis and 14-15% from core analysis, in well 6460/12-3B lies in a range of 9.3-14.5 % from log analysis and 12.9 % from core analysis, and in well 6406/12-3A lies in a range of 9-17 % from log analysis. The water saturation in the reservoir interval of the three wells from Archie, Indonesia and Simandoux equations lies in a range of 40-99 %, 31-95%, and 29-98 % for well 6406/12-3S, 59-98 %, 49-93 %, and 49-91% for well 6406/12-3B, and 82-100 %, 79-99 %, and 81-100 % for well 6406/12-3A respectively. In calculation of water saturation the average formation water resistivity estimated was 0.1 Ohm-m and the deep resistivity reading was taken as the true formation resistivity of the reservoirs by assuming as it is corrected to invasion, thin bed and other effects. In addition to these properties the permeability of the reservoirs has high to very high values.

Key words: Shale volume, water saturation, Porosity, and Permeability

Table of Contents

List of Figures

List of Tables

Nomenclature

NPD = **N**orwegian Petroleum Directorate

MD = Measured depth

TD = Total depth penetrated

RKB = Rotary Kelly Bushing

OBM = Oil Based Mud

GR_{min} = Minimum gamma ray reading in the clean zone

GR_{max} = Maximum gamma ray reading in the shale zone

GR_{log} = Gamma ray log reading

a = Tortuosity factor

m = Cementation exponent

F = Formation resistivity factor

n = Saturation exponent

K= Permeability

RHOB/ ρ_b = Bulk density

ρ_{log} = Density log reading

PHI /ϕ = Porosity

PHIE_D/ϕ_e = Effective porosity from density log

Φ_{tsh} = Shale total porosity

PHIT_D/ϕ_D /DPHI = Total porosity from density log

NMR = Nuclear Magnetic Resonance

CMR = Combinable Magnetic Resonance

TCMR = Total NMR porosity/ Total combinable magnetic resonance

Core_PHI = Core Porosity

GOC = Gas Oil Contact

OWC = Oil Water Contact

Rw = Formation water resistivity

Rwa = Apparent formation water resistivity

Rt = True formation resistivity/ Restivity of partially saturated rock

C_t = Formation conductivity

Rsh = Resistivity of shale

Vsh = Volume of shale

V_p = Pore volume

V_b = Bulk Volume

Sw = Water saturation

Swirr = Irreducible water Saturation

Swe = Effective water saturation

SWE_INDO = Indonesian effective water saturation

SWE_SIM = Simandoux effective water saturation

Swt = Total water saturation

Sw_AR = Archie water saturation

BVW = Bulk volume of water

Curve Mnemonics

CAL= Caliper

GR = Gamma ray

TH = Thorium

K= Potassium

TVD = True Vertical Depth

ZDEN = Formation bulk density

DEN = Compensated bulk density

NEU = Neutron porosity

MPHS = Magnetic resonance total porosity

DMRP = Density-Magnetic resonance porosity

MPRM = Magnetic resonance Permeability

RDEP = Deep resistivity

RMED = Medium resistivity

RMIC = Micro resistivity

Chapter One

1.1. Introduction

The presence of shale distribution in a reservoir leads to numerous challenges in interpretation and evaluation of petrophysical properties. The affinity of clay minerals to bind water in their surface and interlayer bonds affects the electrical conductivity that makes the petrophysical analysis of shaly sand reservoirs complex and prone to some uncertainties of the evaluated parameters. In the petroleum industry, shaly sand interpretation is still the main interest of numerous researchers and different studies have been conducted to investigate the effect of clay minerals on rock conductivity through experimental and theoretical approach. For accurate description of shaly-sand reservoirs, careful analysis of conventional logs with correlation to other data like core analysis should be performed.

Usually well logs are the main source of subsurface information for investigating and evaluating the formation parameters like permeability, porosity and water saturation but none of these variables are measured directly by logs in the well. The estimated variables are used as input in assessing the hydrocarbon content of the target reservoir and volumetric calculation of reserve estimation. Therefore, the first task to be performed is identification of the type of lithology, mineral content, and determination of petrophysical properties. For this study area, identification of lithology from gamma ray response, estimation of porosity from different methods and estimation of water saturation using clean sand method analysis and shaly sand method analysis was performed.

Water saturation can be calculated from deep resistivity log using clean sand model and different shaly sand saturation models. The saturation of hydrocarbon in the formation can be calculated by subtracting the water saturation from 100% fluid content of the formation since the remaining effective pore spaces are filled with hydrocarbon. When the electrical conductivity of a formation comes only from the interstitial water, Archie method is usually used in the estimation of water saturation. However, this model is no longer true in shaly sand formations (clayey formations), because the extra conductivity of clay is not included in the Archie water saturation equation (Bardon and Pied, 1969). Archie model is applicable for clean sand formations that contain saline formation water in their pore spaces and non-conductive matrix. To include the extra conductivity of shale laminae in Pil and Bue shaly sand reservoirs Indonesia and Simandoux models were applied in the estimation of water saturation.

Porosity is a measure of the storage capacity of the reservoir rocks and it can be estimated from different methods like well log analysis and core analysis. In the estimation of porosity using density log derived total and effective porosity (PHIT and PHIE) fluid type and matrix density have great effect in getting correct value. In log analysis, proper fluid density and matrix density should be taken to minimize the errors and uncertainties. The presence of gas phase in a reservoir makes the density porosity to read higher due to its low density, and the NMR porosity reads lower due to low hydrogen index and partial polarization of gas. To address this problem, a new method called density-magnetic resonance porosity (DMRP) was applied that compensates the effects of both responses and gives gas corrected total porosity.

The other rock property is the permeability, which is the measure of the ease to flow fluids in a porous media. There is no logging tool that directly measures permeability of a formation, rather it is determined from indirect methods of logs, cores or combination of the core data and log data. There are different methods for permeability determination like Wyllie-Rose method, Morris Biggs, and Timur Coates method. However, all these methods contain two or more unknowns in their equation, which are not provided in this study. To address this problem, NMR permeability, core porosity and Klinkenberg corrected gas permeability relationship (PoroPerm) was applied to get the permeability of the formations.

1.2. Thesis Outline

This thesis is organized and outlined as follow:

- **Chapter one**: - gives general overview of the study area and lithostratigraphic make-up of Norwegian Sea Jurassic age, the main objectives and aims of the thesis, general overview of clay and shale, and the effect of shale on some well logging measurements.
- **Chapter Two**: – Material and Methods- this chapter includes the methodology and theory part, which gives description of the methods used, literature on the methods and the topics.
- **Chapter Three**: Result of the analysis including figures, tables for each of the wells
- **Chapter Four**: Discussion-this chapter explains the implications of the results
- **Chapter Five**: Conclusions

1.3. Objective of the thesis

1.3.1. Main objective

The main objective of this thesis is to evaluate and estimate the petrophysical properties of the Pil and Bue shaly sand reservoirs. This study mainly focuses on shale volume, water saturation, porosity, and porosity-permeability relationship based on the available well log data, formation pressure data and core report results.

1.3.2. Specific Objectives

The specific objectives to be covered in this study analysis are:

- Lithology identification and shale volume estimation in the three wells
- Identification of fluid type and fluid contacts based on log analysis and formation pressure gradient analysis
- Interpretation of porosity, permeability and water saturation data
- Correlation and comparison of core data and petrophysical log data
    - Core porosity and log porosity
    - Core permeability and log permeability
    - Core permeability and core porosity
- Finally comparing results using clean sand and shaly sand water saturation equations

1.4. Significance of the Study

The main significance of this thesis paper is to give information to researchers who are interested in further study of the recent discovery wells in the Late Jurassic age of Norwegian Sea.

1.5. Study area description

Pil and Bue fields are located in the Southern end of Halten Terrace offshore Norwegian Sea, around 35km and 65kms far from southwest of Njord field and Draugen field respectively. The formations targeted in these fields are part of the Norwegian Sea Lithostratigraphic units. Norwegian Sea comprises Twenty-three units of different formations from the early Jurassic age of Åre formation to Quaternary age of Naust formation as shown (***Fig.1)*** (Vernay et al., 2009). The Jurassic age of the Norwegian Sea is the target of the study area where the formations of the Pil and Bue wells are penetrated. This geological time is classified into Lower, Middle and Late Jurassic age characterized with different formations and depositional environments. The lower Jurassic age sediments were deposited in Halten Terrace and Trøndelang platform, which

comprises the lithostratigraphic unit of Båt group characterized by alternating sandstone and siltstone/shale deposits. However, the dominant lithology is sandstone and the group includes four formations (Åre, Ror, Tilje and Tofte formations) (Dalland et al., 1988).

The other group of lithostratigraphic unit is the Fangst group deposited because of cyclic regression/transgression caused by rapid changes in relative sea level in the Middle Jurassic age. The sedimentary successions of this group are correlated to the Brent group of North Sea and it contains three formations (Not, Ile and Garn formations) (Bøe et al., 2010).

In the Late Jurassic age, the rapid changes in relative sea level started by the end of Middle Jurassic continued to early Cretaceous age and during this major transgression Viking group was deposited in the Haltenbanken and Trænabanken area (Bugge et al., 1984). The depositional environment of this group in the Haltenbanken area is marine environment and the dominant lithologies are shale and mudstone. However, the dominant lithology in the Draugen field of this area is significantly sandstone (Bøe et al., 2010). The Viking group contains three formations: Melke formation, Spekk formation, and Rogn formation. In addition to these formations, there is Intra-Melke sandstone formation, which is categorized under the age of Viking group with the Melke formation.

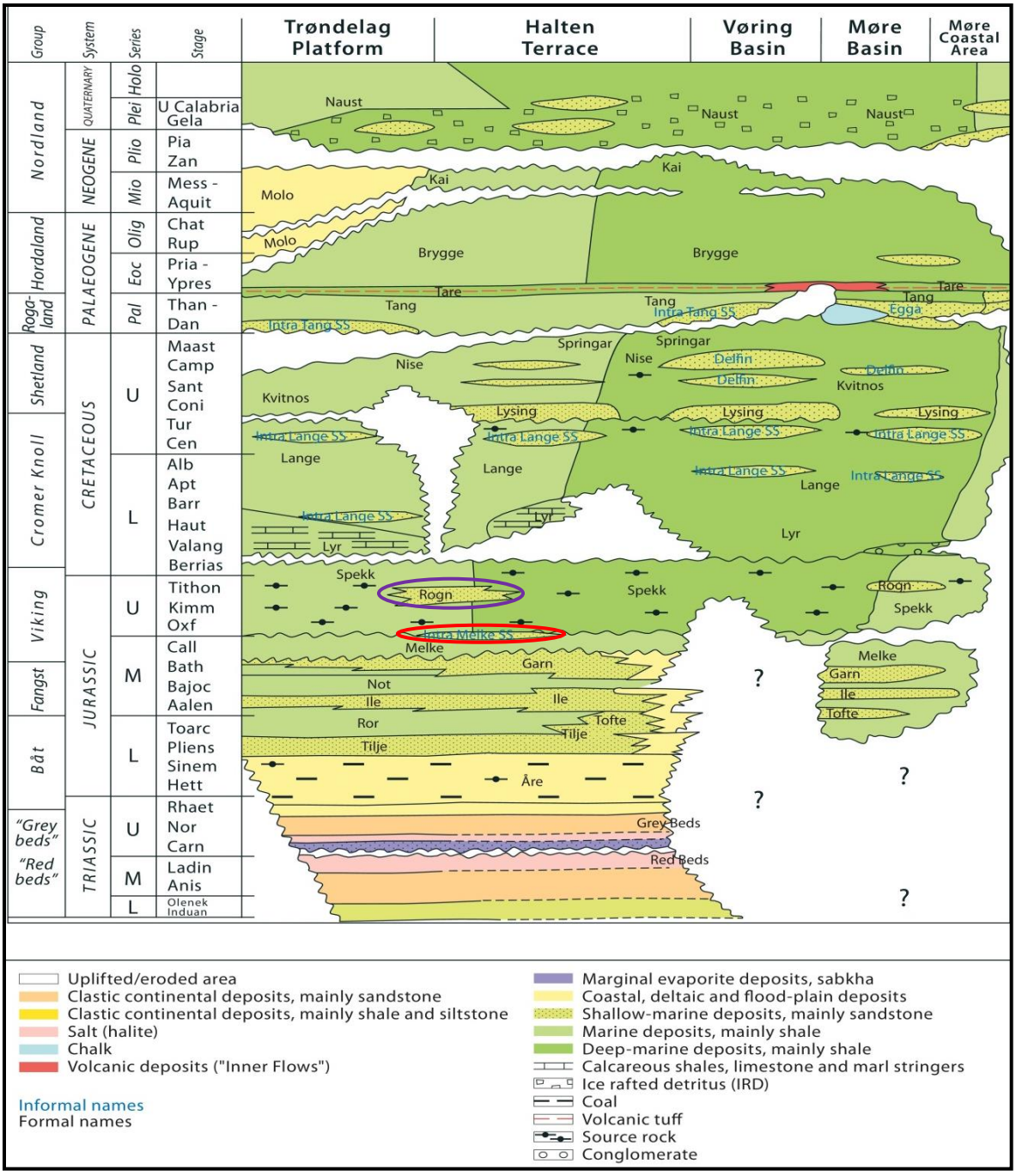

Figure 1: Lithostratigraphic units of Norwegian Sea (NPD, 2017)

Melke formation is deposited in an open marine environment and dominated with lithology of fine-grained gray to dark brown claystone, siltstone and limestone interbeds (Dalland et al., 1988). In terms of organic content it is moderately organic rich but in the Haltenbanken area it is not confirmed as source rock (Heum et al., 1986).

Intra-Melke formation is a sandstone formation found intercalated with Melke formation and this formation is the reservoir target of the study area (NPD, 2017).

Spekk formation is found overlying the Melke formation as shown in (***Fig.1)*** and it is deposited in marine environment with anoxic bottom water condition. This formation consists of predominantly non calcareous dark brown to dark grey shale with high organic content mostly Type II Kerogen and it is confirmed as source rock (Heum et al., 1986).

The Rogn Formation is one of the reservoirs in the Norwegian Sea and it is created within the Spekk Formation. The depositional environment of the formation is shallow marine deposit bars and it is characterized with upward coarsening from siltstone and shale to sandstone (Bøe et al., 2010; Dalland et al., 1988; Ellenor and Mozetic, 1986).

In the wells used for this study, the target formations are the Intra-Melke sandstone formation and Rogn sandstone formation. In these formations three exploration wells were drilled, two of them targeting the Intra-Melke sandstone formation and one well targeting the Rogn formation. Well 6406/12-3S targeted the Pil Prospect and 227m of gross hydrocarbon column (134 m of oil and 93 m of gas) was discovered in the Intra-Melke sandstone formation (all measured depth along the well path)**.** The discovery of hydrocarbon in the well made the operator company to drill an appraisal well, 6406/12-3B (Pil 2). The sidetrack appraisal well was drilled on the Pil discovery 1.7 kilometer northwest of the Pil well in order to appraise the lateral extent of the reservoir. This well again confirmed the presence of hydrocarbons in the upper Jurassic Intra-Melke sandstone formation, which is in pressure communication with 6406/12-3S. The thickness of the Intra-Melke formation encountered in well 6406/12-3B was 500 m but the entire interval is not hydrocarbon bearing. The thickness of the hydrocarbon column of this well is only 82 m (measured depth along the well path). In addition to this well, another side track well (6406/12-3A) was drilled to check the extension of the reservoir, thickness, the reservoir properties, to test and evaluate the fluid contacts in the Bue prospect and its connectivity with the Pil discovery. Well 6406/12-3A was drilled into the Bue prospect at distance of 2.1 Kilometer northwest of the Pil well. However, based on pressure data analysis of the well it has confirmed that the well was not in pressure communication with the Pil discovery and due to this reason the well is considered as an isolated discovery in the Bue area. The other difference of this well from well S

and B is that, the hydrocarbon discovery is in the Intra-Melke formation rather it is in the Rogn sandstone formation and 18 m oil column was discovered in this formation (NPD, 2017)[1].

The position of the wells in the offshore Norwegian Sea is shown in (***Fig.2)***. The green color is an indication of oil discovery and the alternating green and red is oil and gas discovery.

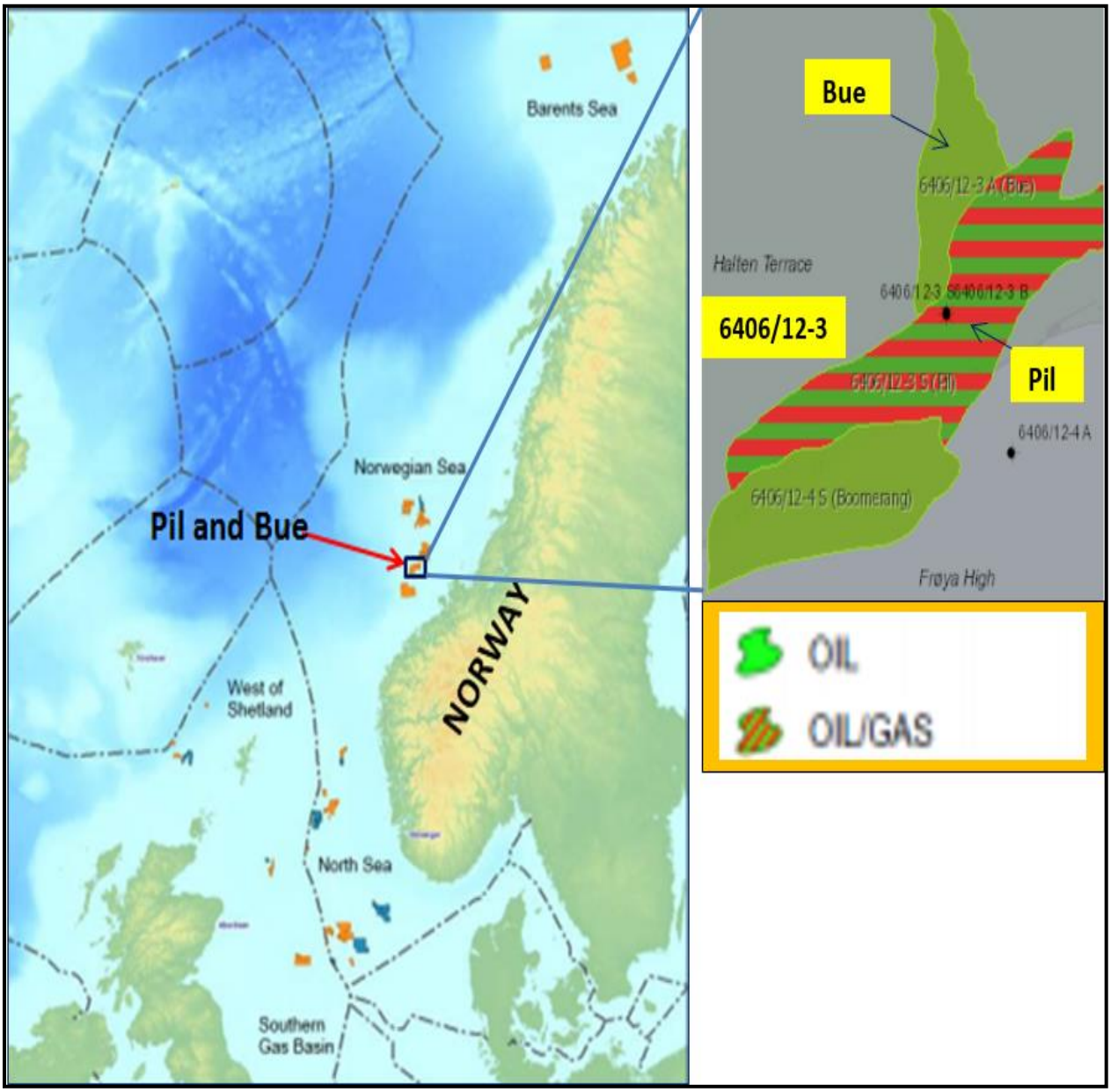

Figure 2: The location of Pil and Bue fields in the Norwegian Sea (modified after Faroe Petroleum Interim presentation, 2015 and NPD, 2017)

[1] http://factpages.npd.no/factpages/

The location co-ordinate of the three wells penetrated in to the Intra-Melke formations and Rogn formations, the maximum inclination of drilling and the type of drilling mud used are given in ***Table 1*.** Based on the latitude and longitude of the wells it is apparent that they all side track from the spud location.

Table 1: Geographical co-ordinates, the total depth (TD) drilled and the maximum inclination of the three wells (NPD, 2017)

Name of wells	Locations	TD (MD)[m RKB]	Maximum Inclination[^{0}]	Drilling Mud Type
6406/12-3 S (Pil)	Latitude: 64^0 01'52.324'' N Longitude: 6^0 45' 17.58'' E	4001	33	OBM
6406/12-3 B (Pil appraisal)	Latitude: 64^0 01'52.324'' N Longitude: 6^0 45' 17.58'' E	4315	44	OBM
6406/12-3 A (Bue)	Latitude: 64^0 01'52.324'' N Longitude: 06^0 45' 17.579''E	4356	45.2	OBM

During the drilling of the wells, different formations were encountered from surface to the total depth penetrated. The formations penetrated and the types of lithology are given in ***Table 2*** and the oldest penetrated formation in the three wells is the Melke formation.

Table 2: Type of formations penetrated and their lithology (NPD, 2017)

Well Name	Top [m]	Bottom [m]	Formation	Lithology	Target reservoir
6406/12-3S	3505	3514	Lyr	Marl	Intra-Melke
	3514	3912	Intra-Melke	Sandstone/shaly sand	
	3912	4001	Melke	Shale	
6406/12-3B	3695	3726	Lyr	Marl	Intra-Melke
	3726	3728	Spekk	Shale	
	3728	3748	Rogn	Sandstone/shaly sand	
	3748	3761	Spekk	Shale	
	3761	4264	Intra-Melke	Sandstone/shaly sand	
	4264	4315	Melke	Shale	
6406/12-3A	4019	4041	Lyr	Marl	Rogn
	4041	4053	Spekk	Shale	
	4053	4114	Rogn	Sandstone/shaly sand	
	4114	4124	Spekk	Shale	
	4124	4180	Intra-Melke	Sandstone/shaly sand	
	4180	4356	Melke	Shale	

The drilling trajectory of the wells, which is the deviation from vertical direction in terms of true vertical depth and measured depth, is given in ***Fig. 3***. When the true vertical depth and measured depth are the same, the well is vertical well but if they are not the same the well is deviated. Therefore, as shown in the plot the wells have vertical alignment to certain depth then start to deviate to an angle of inclination.

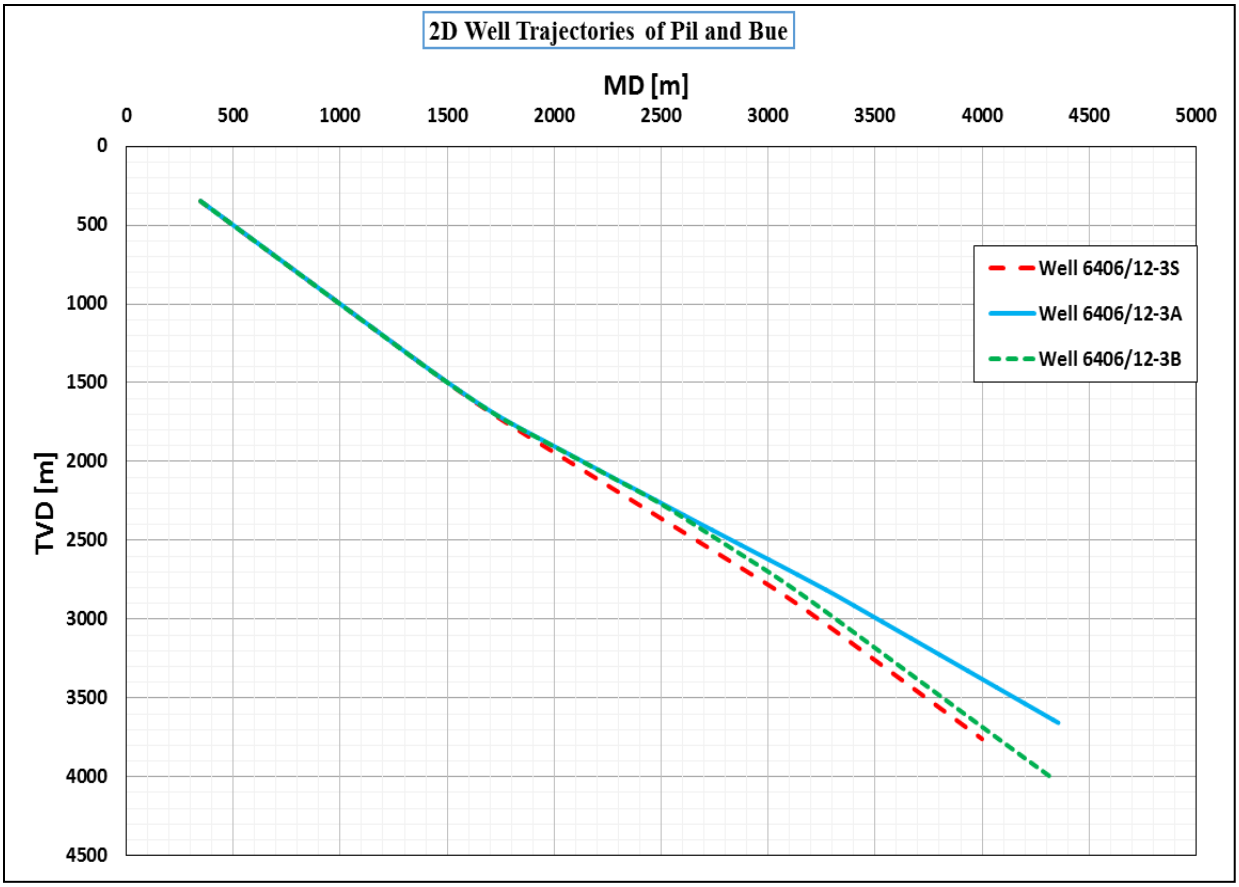

Figure 3: 2D well trajectories of Pil and Bue in terms of TVD and MD

The alignment of the wells in terms of inclination angle (2D view) and plot of 3D view as shown in ***Fig. 4*** and ***5***, they start from one-location but targets different locations in the subsurface. According to the information given in the Norwegian Petroleum Directorate website of the Pil and Bue wells, the two wells (A and B) were kicked off from well 6406/12-3S at a depth of 1259 m (measured depth) and 2355 m for wells 6406/12-3A and 6406/12-3B respectively. This can be clearly seen in ***Fig.4*** how the wells are side tracked from the original well. In addition, the well path data of the wells provided in this study confirms that the local east and local North of the three wells follow the same path to certain depth. The differences of the northing and easting values of the three wells give zero up to 1225 m but after this depth, there are some small variations up to the sidetrack depths.

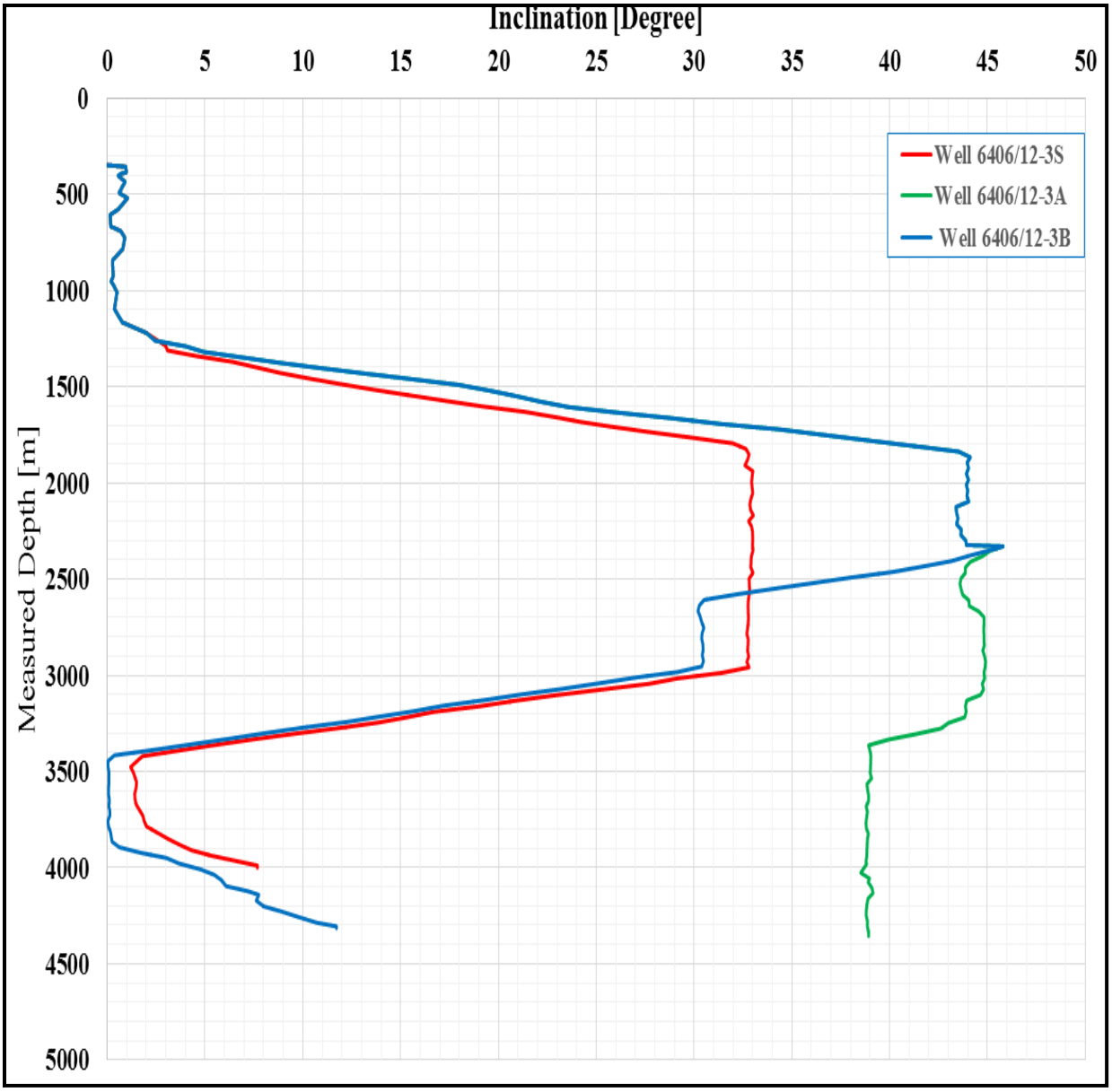

Figure 4: 2D well path alignment of the wells in terms of measured depth and Inclination Depth

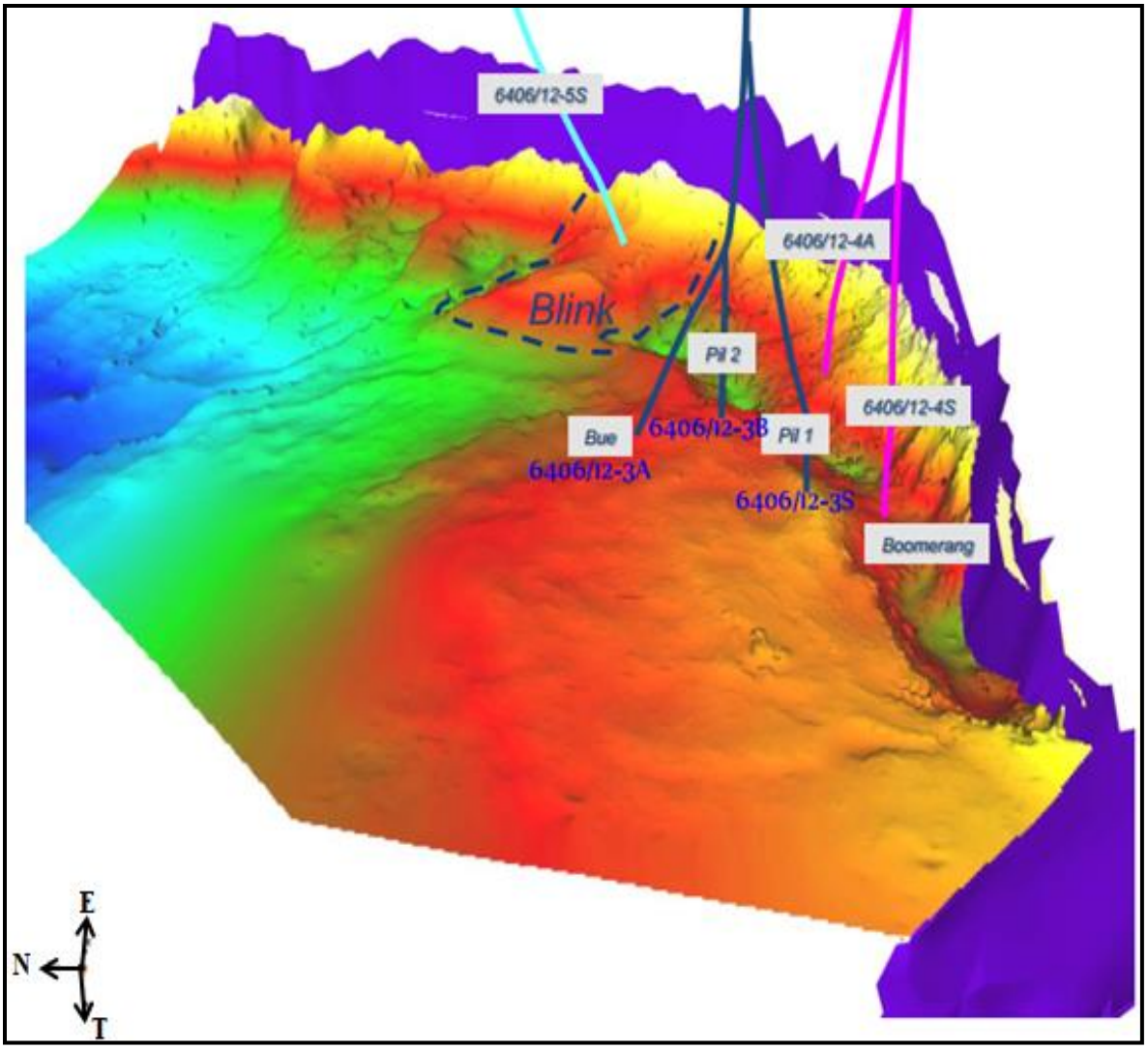

Figure 5: 3D view of Pil and Bue wells and neighboring Boomerang and Blink wells (Adapted from Faroe Petroleum Interim presentation, 2015)[2]

1.6. Shaly sand formations

Shaly sand formations are formations that contain shales distributed in different modes in the sandstone layers. The interpretation and analysis of shaly sand formations should take into account the effect of shale that makes it different from the clean sand reservoirs. Therefore, it is obvious that including the effect of shale and clay minerals in the estimation of petrophysical parameters increases the accuracy in the estimation of hydrocarbon resources of the area.

[2] **http://www.fp.fo/investors/results-centre/**

1.6.1. Clay and clay minerals

Clay has different definitions in different fields and it can be described as a particle or a rock. Considering as a particle it is small size particle which is less than 4 micro meters created from weathering of rocks and as a rock, it is a fine grained material which has plasticity nature when mixed with water. All clay minerals are aluminosilicates and they are classified in to five groups based on structure and composition. These are Illite, chlorite, kaolinite, montmorillonite, and vermiculite. The structure of clay minerals is sheet like, one sheet consists of hydroxyl around a central atom usually aluminum or octahedral unit of oxygen, and the other sheet consists of a central silicon atom surrounded by oxygen. Clay minerals usually contain negative surface charge and this makes them to adsorb cations on their exposed surface, which is responsible for creating a thin layer of altered composition and electrical double layer in the surrounding fluid. This effect is created by, Isomorphous substitution (unbalanced substitution like Mg^{+2} for Al^{+3} or Al^{+3} for Si^{+4}) and the interlayer complex present that have the tendency to fill the charge deficiency. When a clay is immersed in water, the positive ions (cations) like sodium or potassium and polar water molecules are attracted (adsorbed) but the negative ions (chlorine ions) are repelled (Ellis and Singer, 2007).

1.6.2. Shale and their modes of distribution

Shale is a fine-grained clastic sedimentary rock formed from the compaction of silt particles (size of 4-62.5 microns) and clay sized particles (less than 4 microns), and this compaction creates mostly clay dominated mudstone. Shale is distinguished from claystone and mudstone by its fissile and laminated nature which splits along the bedding planes of laminations (Alexander et al., 2011).

The depositional environment has an effect in the type of lithology and in sandstone formation, shales found distributed with in it. In this study, the principle of sand and shale mixture as a shaly sand reservoir is applied.

The distribution of shale in a sandstone formation affects the response of logging measurements and there are three modes of distribution as developed by (Thomas and Stieber, 1975).

- **Laminar shale** - this type of distribution is created when the shale exists as a thin layer/laminae between the clean sandstone layers and it reduces both the volume of matrix and porosity.

- **Dispersed shale** - as the name indicates the shale present is dispersed through out the pore spaces of the clean sand grains. This type of distribution affects the original porosity resulting in reduced porosity without affecting the grain space and it can be distributed in three ways ***Fig. 6***: Pore filling, pore lining and pore bridging.
- **Structural Shale** - this type of distribution is created when the shale is occurs as part of the frame work structure and replaces the rock matrix which leads to confusion in porosity calcula-tion since sometimes it has the same matrix denisty as sand.

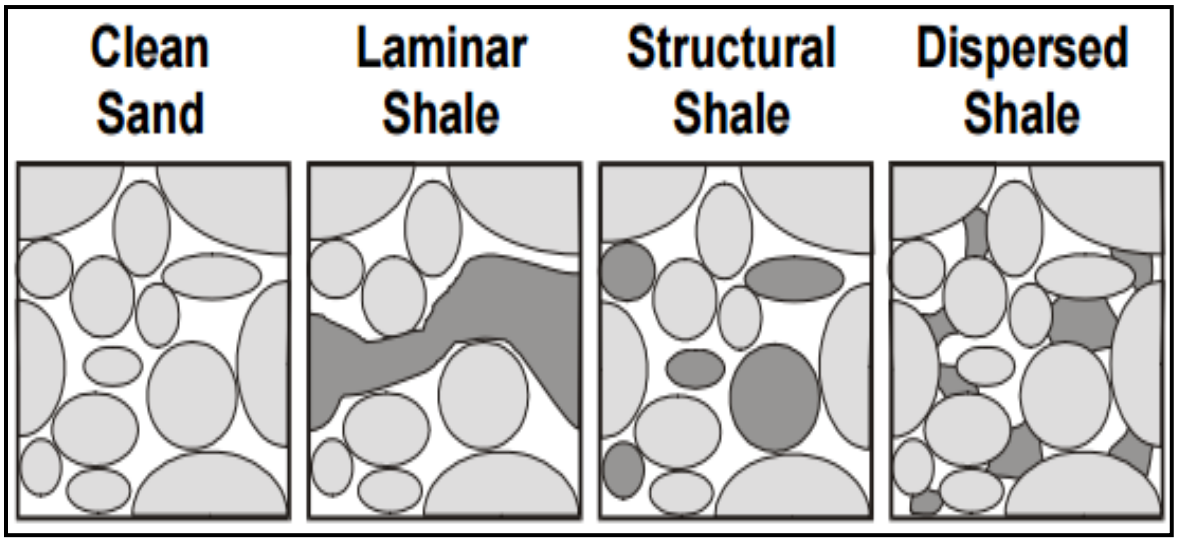

Figure 6: The three modes of shale distribution in sandstone reservoirs (Glover, 2011)

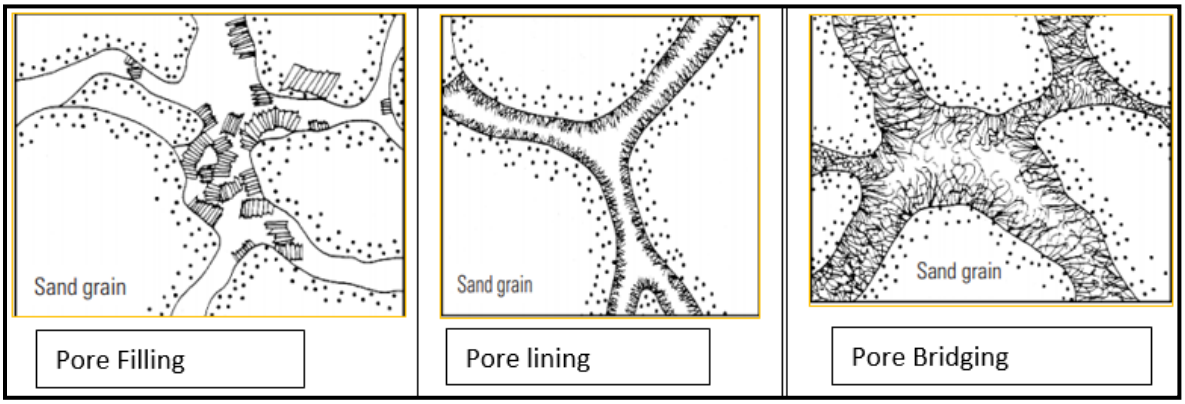

Figure 7: The ways of distribution of dispersed shale in a sandstone reservoir rock (modified after Ellis and singer, 2007)

1.6.3. Log responses in shaly sand reservoirs

The presence of shale in sandstone formations affects the log responses and complicates the interpretation of the readings, which results in erroneous estimated petrophysical parameters. The wrong values considerably affect the characterization of the hydrocarbon-bearing formations by reducing the effective porosity, permeability and by altering the resistivity(Jongkittinarukorn and Tiab, 1997).

The presence of hydrogen as hydroxyl group in the chemical formula of clay minerals affects the response of neutron log, which results in high porosity values in a shale zone. The gamma ray in shale zone gives high reading value, this is due the presence of radioactive elements like Thorium, and Potassium incorporated with the clay minerals. The effect of shale in a density log depends on the distribution modes of the shale in the sandstone layers (Ellis and Singer, 2007). In addition, the water trapped in the clay minerals due to their platy nature creates another conductivity path in the formation and it affects the resistivity log. This makes the resistivity log to read low in the shale containing depth intervals but the degree of effect depends on their amount (Vsh) and their distributions (Glover, 2011).

Chapter Two: Materials and Methods

This chapter clarifies the Methodology applied and discusses the input parameters related to the methods, and literature review on the methods. In the petrophysical analysis of the provided log data and core report results, Techlog 2016.2 (Version 2) of Schlumberger software was used to integrate, correlate, and estimate the petrophysical parameters.

2.1. Data Availability

The data available for the analysis of the present study was the suite of Wireline log data (Las file, DLIS, Asc file and text files) of the three wells, formation pressure data and core analysis report of two wells (well 6406/12-3S and 3B). The Norwegian University of Science and Technology (NTNU) provided these data from NPD's DISKOS database.

The core report data provided includes core porosity, core permeability, total gamma ray, water saturation and oil saturation, lithological description of the core plugs, brine conductivity measurements, and core photographs.

The logging measurements in the wells were performed during drilling (Logging while drilling and measurement while drilling) and after drilling (Wireline logging). The detail of the type of the logging measurements done in the depth intervals of the wells are given in Norwegian Petroleum Directorate (NPD) Website of Pil and Bue wells. However, in this study some of the provided suites of Wireline logs run in the three wells are given in ***Table 3***.

In the provided log data, one curve/variable is given in different names for example; the name gamma ray is given in different nomenclatures and the same for other curves. However, not all of them can be used at a time and appropriate logging curves were chosen from the logging composite data provided to do the analysis.

Table 3: Suite of Wireline log runs in the three wells of Pil and Bue field

Logging curves	Abbreviations	6406/12-3A	6406/12-3B	6406/12-3S
Caliper	CAL	☒	☒	☒
Bulk density	DENS/ZDEN	☒	☒	☒
NMR Porosity	MPHS	☒	☒	☒
Neutron Porosity	CNC/CNCSS/NEU	☒	☒	☒
Gamma Ray	GR/GRSLC/GRSL	☒	☒	☒
Photoelectric Factor	PE	☒	☒	☒
Porosity	PORZ	☒	☒	☒
Travel Time	TTC/TTS	☒	☒	☒
Shear Slowness	DTSM/DTSMR/DTSMX	☒	☒	☒
Compressional Slowness	DT24_I/DTC/DTCR/DTCX	☒	☒	☒
Potassium	K	☒	☒	☒
Thorium	Th	☒	☒	☒
Uranium	U	☒	☒	☒
Deep Resistivity	RDEP	☒	☒	☒
Medium Resistivity	RMED	☒	☒	☒
Micro Resistivity	RMIC	☒	☒	☒
Rate of penetration	ROP	☒	☒	☒
NMR Permeability	MPRM	☒	☒	☒
Cable Speed	SPD	☒	☒	☒
Array of Resistivity	M2R1/M2R2/M2R3/ M2R6/ M2R9/ M2RX/	☒	☒	☒
Temperature	WTBH	☒	☒	☒

The log measurements used in the petrophysical analysis of the water saturation, porosity, and permeability estimation of the three wells are given in ***Table 4.*** In addition, core porosity and

core permeability were used from the core analysis report to correlate and compare with the logging parameters.

Table 4: The logging measurements used in the petrophysical analysis and their application

Logging measurements used	Applications
Measured depth (MD)	Reference depth with reference to Kelley Bushing
Caliper	To locate bad hole, lithology changes and permeability
Gamma ray (GR)	For lithology and shale volume determination
Density log (DEN/ZDEN)	For density porosity estimation and lithology determination
Deep Resistivity (RDEP)	For water saturation estimation in un-invaded zone and to identify hydrocarbon bearing zone
Nuclear Magnetic resonance Porosity log (TCMR/MPHS)	NMR porosity of the formation
Neutron log (NEU)	For porosity and lithology determination
Nuclear magnetic resonance Permeability (MPRM)	For permeability
Density Magnetic Resonance Porosity (DMRP)	Gas corrected porosity estimation

The petrophysical parameters calculated from the above logs were:

- Volume of shale (Vsh)
- Effective porosity (PHIE/ϕe)
- Total porosity (PHIT/ϕt)
- Water saturation (Un-invaded zone) (Sw)
- Permeability (K)

2.2. Workflow to perform the formation evaluation using Techlog

The procedures followed in the petrophysical analysis of this study are:

[1]. Identify the type of lithology and the reservoir interval of the wells based on the log responses in the well interval

[2]. Calculate the shale volume of the three wells

[3]. Identify the Hydrocarbon zones with in the reservoir interval

[4]. Differentiate the fluid types (oil, gas and water) and the fluid contacts (GOC and OWC)

[5]. Evaluate porosity in the reservoir zones using different methods

[6]. Calculate the Formation water resistivity in the water zone

[7]. Water saturation determination of the well using the above inputs

2.3. Depth Shifting

When well log measurements of separate logging runs in the same borehole are combined, some depth discrepancies are observed in the displayed logging track and it is important to correctly correlate the measurements in depth with one another. This log editing should be performed before quantitative interpretation of the measurements. The slight mismatch of the logs from different Wireline tool strings is created because of rig motion during recording, tidal changes in the sea level, cable stretch and others (Hagelberg et al., 1992).

In the logging measurements of this study, no depth shifting was required in any of the three wells except the core data of the two wells (6406/12-3S and 6406/12-3B). The core data was depth matched with the log data and this was done for core porosity and the log porosity only. In the software, one reference curve (Variable) was chosen for depth shifting of the core porosity and both curves were dragged in to an empty layout for matching.

2.4. Lithology determination and shale volume estimation

Determination of lithology is essential to make accurate petrophysical estimation of porosity, water saturation and permeability because the chemical and physical properties of the rock affect the response of the logging tools that used to measure the formation properties. Due to this reason in this study, the first interpretation made in the log analysis was identification of the lithology type. Lithology of the formations was determined from the gamma ray reading response and Density-Neutron crossover (separation) as shown in ***Fig.8***, and Density-Neutron cross plots as shown in ***Fig.11***.

As shown in ***Fig.8*** depth intervals with high GR, high neutron log and positive Density-Neutron separation between the sand layers were identified as shaly sand with shale lamina. The low gamma ray, low neutron and negative Density-Neutron separation are identified as clean sand lithology.

In addition to these responses, Thorium-Potassium cross plot was done to identify the presence of radioactive and heavy minerals like mica, feldspar and to show clay type in the sandstone section of the target reservoirs.

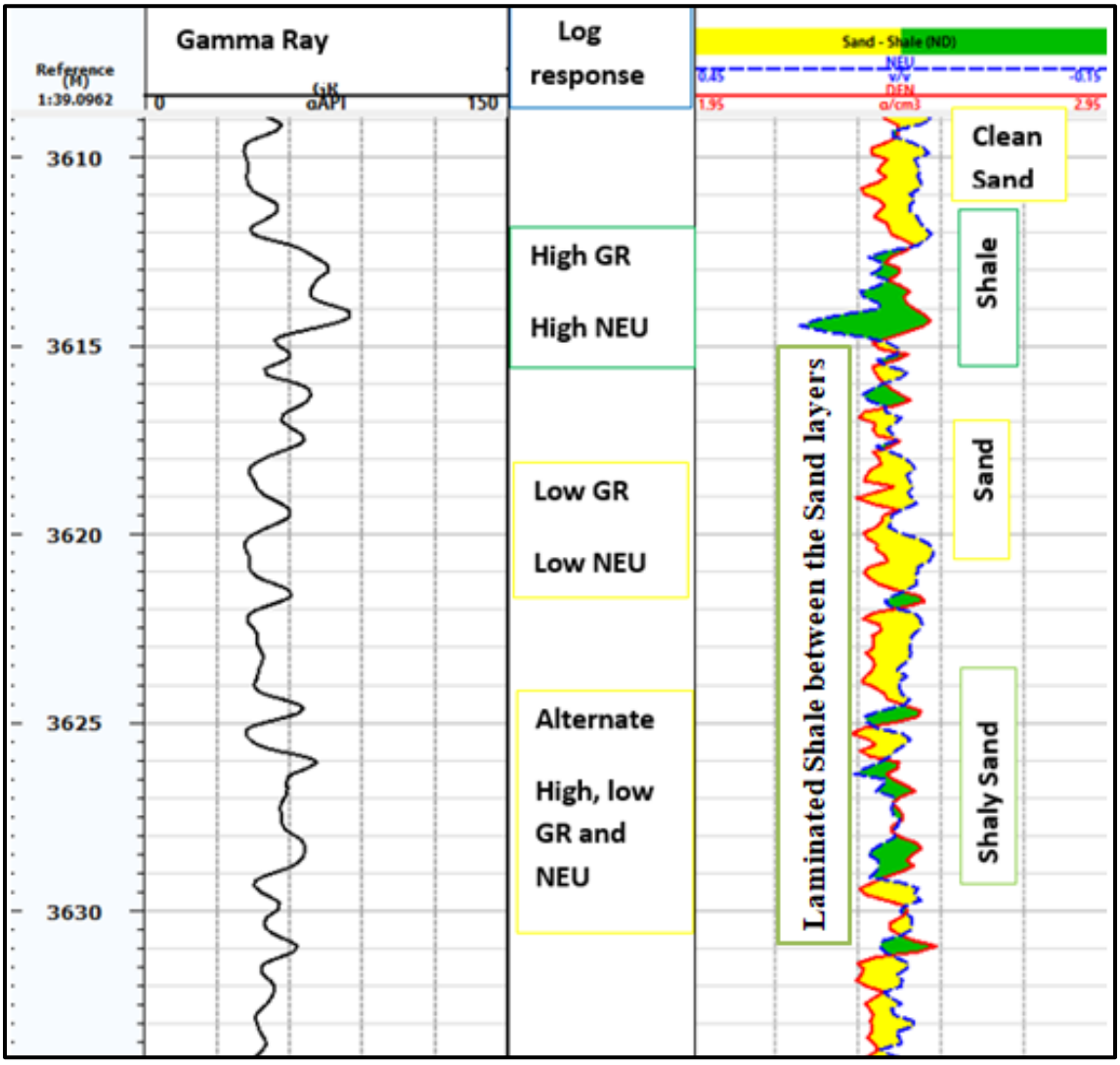

Figure 8: Lithology determination from GR and Density-Neutron crossover responses of well 6406/12-3S

Shale volume estimation

There are different methods of estimating shale volume in a formation and some of the methods are:

- Gamma ray method
- Neutron-density method

- Spontaneous Potential method
- Thorium method

For this study, the shale volume was estimated using the gamma ray method assuming the high gamma ray response in the reservoirs comes from the presence of shale distribution in the sandstone layers. However, there are different computation methods of estimating shale volume from gamma ray like linear method, Larionov (for Tertiary age and older rocks), Clavier, Stieber variation I and II, and Stieber Miocene and Pliocene (Bassiouni and Bassiouni, 1994). All these methods are given in Techlog software as optional methods but in this study, the linear method was used in the estimation of the shale volume.

In the Linear Method, the volume of shale is equal to the gamma ray index calculated and it is given as in the following equation 1:

$$V_{sh} = GR_{index} = \frac{GR_{log} - GR_{min}}{GR_{max} - GR_{min}} \quad [1]$$

Where GR_{log} is the log reading value taken from the gamma ray curve, which is the response in the formation of interest, GR_{min} is the minimum reading in a clean sand zone with 100% sand (0 % shale), and GR_{max} is the maximum reading in a 100% shale bed (0% sand). The maximum and minimum Gamma ray readings in the analysis of the shale volume were chosen from the shale zone below or above the target reservoirs for full maximum deflection and from the clean sand zones for full minimum deflection ***Fig.9***. In well 6406/12-3S and 6406/12-3B the maximum Gamma ray reading was selected from the 100% shale zone of Melke formation below the Intra-Melke formation and the minimum Gamma ray reading was taken from the clean sand part of the Intra-Melke formation. In well 6406/12-3A, the maximum reading was taken from the top shale zone of Spekk formation and the minimum reading was taken from the clean sand zone of Rogn formation.

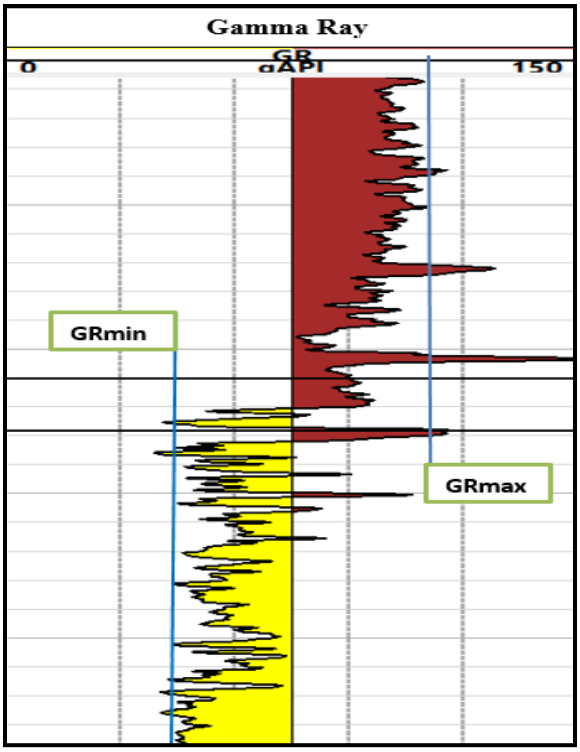

Figure 9: Selecting Maximum and Minimum gamma ray reading (Example taken from the Pil Well)

2.5. Fluid types and fluid contacts identification

2.5.1. From well log responses

Fluid type identification is the basis for estimation of petrophysical parameters. The presence of different fluids in the reservoir have different responses to the logs especially resistivity, density and neutron logs. The identification of fluid types and fluid contacts from logging measurements of this study was done based on the response of resistivity log, density log responses and density-neutron porosity separation. The presence of hydrocarbon bearing zone in a reservoir gives negative separation in a Density-Neutron cross over and higher resistivity log reading. Big negative separation in the cross over is an indication of gas bearing zone and in the oil zone the cross over decreases. In addition to these methods, the nuclear magnetic resonance and density log derived total porosity showed a big separation, which is an indication of gas bearing zone in the reservoir. Moreover, this property was observed only in gas bearing reservoir of well 6406/12-3S.

The identification of the possible fluid contacts (GOC and OWC) in the log analysis of the reservoir intervals was done based on the response of resistivity log and the Density-Neutron

cross over (separation). This was performed by observing the decrease and increase in the resistivity log response accompanied by the gap changes between the Density-Neutron cross over.

2.5.2. From pressure gradient analysis

Formation pressure measurements are used to determine the fluid pressure in the formation and the wellbore. The recorded formation pressure data enables one to calculate the fluid density and to identify the fluid type in the formation, provided that the calculated pressure gradients are dependent only on the fluid density in the formation (Xiaoquan and Yongjie, 2009). In addition to the fluid type interpretation, it can also help to get the fluid interface or fluid contacts between the different phases (gas, oil and water). This is identified from the intersection of two pressure lines corresponding to different pressure gradients (Jackson et al., 2007). The working principles assumed in the pressure gradient analysis are: the frictional flow effects are ignored in the measured pressure and it considers the static pressure, the pressure varies linearly with depth, and the main cause of fluid distribution is gravity separation (Zhou and Mardambek, 2008). Fluid density from pressure gradient was estimated under static and Isothermal conditions assumption using the following equation.

$$\frac{dp}{dz} = \rho_{fluid} * g \qquad [2]$$

Where:

P = Pressure/ formation pressure

Z = Vertical depth / True vertical depth (TVD)

g = gravitational constant

dp/dz = pressure gradient

Fluid type and fluid contact identification from pressure gradient analysis in this thesis was done for the wells 6406/12-3S and 6406/12-3B since the formation pressure data was given for the these wells only. The first task in the estimation of fluid density was plotting the formation pressure data in the x-axis and true vertical depth in the y-axis then linear trend line was inserted to find the point of intersection of the pressure gradient lines. In the calculation, the gravity constant (g) was taken 9.81 m/s^2 and the reverse (1/g) is 0.10194 Kg/N.

The type of fluid identification in the pressure gradient calculation and estimated density was done based on the range of the density values given in ***Table* 5**.

Table 5: Range of densities and pressure gradients for different fluids (Modified after Chen, 2003)

Fluid types	Density [g/cc]	Gradient [psia/ft]
Gas	0.1-0.2	0.04-0.15
Sour gas	0.2-0.6	0.11-0.26
Condensate	0.2-0.55	0.08-0.24
Black oil	0.65-0.85	0.29-0.37
Water	0.95-1.05	0.41-0.45

2.6. Porosity Estimation

Porosity is one of the important reservoir /rock properties defined as the ratio of the pore spaces (voids between grain matrix) volume to the overall bulk volume of the rock. This ratio gives how much (the percentage) of the total volume of the rock is occupied with the voids which contains fluid and without fluid. The distribution of porosity in a rock is affected and controlled by different factors and some of the factors are cementation, shape of the grains, sorting, clay content, over burden pressure (compaction), dissolution of grains and fracturing effect (Amyx et al., 1960). Porosity can be expressed as follow:

$$\text{Porosity}(\emptyset) = \frac{\text{Pore volume}}{\text{bulk volume}} = \frac{V_{Pore}}{V_{Pore}+V_{grain}} \quad [3]$$

Where the pore volume is the total volume of the pore spaces in the rock and bulk volume is the physical volume of the rock, which includes the total pore spaces and matrix materials.

There are different types of porosity classifications and descriptions and based on the timing of the pore spaces genesis, they are classified as primary porosity and secondary porosity. Primary porosity is the original porosity of the rock created at the time of deposition (syn-depositional porosity) and secondary porosity is always created in a post depositional process (Shanmugam, 1985).

In petroleum industry, porosity can be described as total porosity or effective porosity. The general definition of total porosity of a rock is the entire pore spaces of the rock but effective porosity is the interconnected pore spaces of the rock that allow the ease flow of the fluids. They are expressed in formula as:

$$\emptyset_{tot} = \frac{\text{total pore volume,} V_p}{\text{Bulk volume,} V_{bulk}} \quad [4]$$

The effective porosity is given as:

$$\emptyset_{eff} = \frac{\text{Interconneted } V_P \text{ or effective pore volume}}{V_b} \quad [5]$$

These definitions and formulas are not used in Petrophysics rather equation ***7*** and ***9*** are applied in the determination of total porosity and effective porosity.

Porosity determination

In a reservoir evaluation of porosity determination, two approaches are used based on the available data. These approaches are direct measurement of porosity values from core analysis of a sample rock of a target reservoir and porosity values calculated from the down hole log data analysis using different methods (Jenkins, 1966).

In this thesis, the analysis of the porosity estimation was done based on the log data using different methods and comparing the result with the provided core porosity. The methods used in the logging analysis of the porosity estimation were:

- Density log porosity (PHIT_D and PHIE_D)
- Nuclear magnetic resonance Porosity (TCMR/MPHS)
- Density-Magnetic Resonance Porosity (DMRP)
- Density-Neutron cross plot porosity

2.6.1. Density log porosity method

Density logs use a radioactive source at a borehole wall, which emits medium energy gamma rays into the formation that results in Compton scattering. This scattering extent is directly related to the electron density of the formation, which is the number of electrons per unit volume. The electron density depends on the density of matrix, the pore space and the density of the

fluids filling the pore spaces. Based on these inputs the porosity from density log is calculated from the formula given in the following equation (Rider, 1986).

$$\emptyset_{\mathrm{D}}(\mathrm{DPHI}) = \mathrm{PHIT} = \frac{\rho_{\mathrm{matrix}} - \rho_{\mathrm{log}}}{\rho_{\mathrm{matrix}} - \rho_{\mathrm{fluid}}} \quad [7]$$

This calculation of total porosity is applicable for only two components (fluid and matrix) but for the three components that include the effect of shale in the estimation of porosity for shaly sands as shown in ***Fig.10*** and can be expressed in formula as:

$$\rho = \emptyset\rho_{\mathrm{fluid}} + (1 - \emptyset - \mathrm{V_{sh}}) * \rho_{\mathrm{matrix}} + \mathrm{V_{sh}}\rho_{\mathrm{sh}} \quad [8]$$

Re-arranging the equation to give effective porosity:

$$\emptyset_{\mathrm{e}}(\mathrm{PHIE}) = \frac{\rho_{\mathrm{matrix}} - \rho_{\mathrm{log}}}{\rho_{\mathrm{matrix}} - \rho_{\mathrm{fluid}}} - \frac{\mathrm{V_{sh}} * (\rho_{\mathrm{matrix}} - \rho_{\mathrm{sh}})}{(\rho_{\mathrm{matrix}} - \rho_{\mathrm{fluid}})} \quad [9]$$

In Techlog software, the effective porosity is given as:

$$\emptyset_{\mathrm{e}}(\mathrm{PHIE}) = \emptyset_T - \left(\emptyset_{T_{sh}} * Vsh\right)$$

Alternatively, it is defined as the total porosity of the rock minus the pore space occupied by the clays (Clay bound water) i.e.:

$$\emptyset_e = \emptyset_{\mathrm{tot}} - CBW$$

Where:

$\emptyset_{\mathrm{T}}$ = Total porosity, fr.b.v.

$\emptyset_{\mathrm{T_{sh}}}$ = Total porosity in the shale zone, fr.b.v

$\emptyset_{\mathrm{e}}$ = Effective density porosity from density log, fr.b.v.

CBW = Clay Bound Water

ρ_{matrix} = Matrix density/ the average grain density of the matrix, [g/cc]

ρ_{log} = Log reading density, [g/cc]

ρ_{sh} = Density of shale, [g/cc]

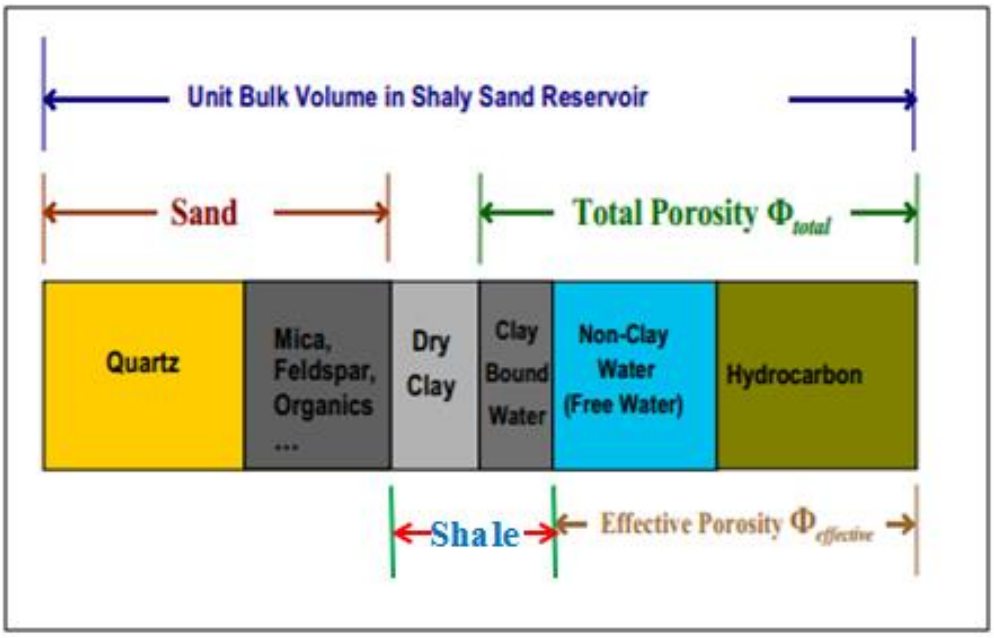

Figure 10: Shaly sand components in a unit bulk-volume of shaly sand formation modified after (AlRuwaili and AlWaheed,2004)

The bulk density of shale/ mudstone given in the core analysis report of lithology description contains pyrite mineral and the presence of this mineral makes the density higher. Therefore, in the effective porosity estimation of the three wells, the bulk density of shale was chosen in the thick shale zone by inserting vertical base line in the density log.

In the estimation of density log porosity, the density of water is used mostly as density of fluid as the density tool measures largely the invaded zone. The invaded zone fluid density depends on the hydrocarbon remaining in the invaded zone (residual hydrocarbon saturation), saturation of mud filtrate and the saturation of saline water. Therefore, it is not unreasonable to use the same density throughout the reservoir interval even where fluids other than water are available since the wells were drilled with OBM (Gaymard and Poupon, 1968).

The procedures of total density porosity estimation in the three wells are given as follow:

- Density log was imported from the given log suite and it was given as ZDEN and Den but both of them show the same thing and Den/ZDEN was selected for the estimation.
- The input parameters were set as density of matrix/grain density =2.65 g/cc which is the density of quartz, density of fluid = 1 g/cc considering denser fluid in the invaded zone.

- For comparison, total porosity was calculated based on the fluid densities estimated from the pressure gradient of well 6406/12-3S and 6406/12-3B

The procedures of effective porosity:

- The density log and shale volume was imported as input parameter
- The fluid density and bulk density of matrix parameters were set the same as the total density porosity.
- Bulk density of shale for 6406/12-3S and 6406/12-3B was selected from Melke formation and for well 6406/12-3A from Spekk formation and in ***Table 6***.

Table 6: Input parameters used in the estimation of effective porosity

Input parameter	Unit	Description	Value
Bulk density of matrix	g/cc	Density log reading in 100% rock matrix	2.65
Bulk density of shale	g/cc	Density log reading in 100% shale	2.51, 2.52
Bulk density of fluid	g/cc	Fluid density	1.0
Shale volume	v/v	Estimated volume of shale from GR	variable

2.6.2. Neutron, NMR and Density-Neutron cross-plot porosity Methods

Neutron log is sensitive to hydrogen index or hydrogen atoms in a formation because the high-energy neutrons emitted from a radioactive source are primarily react with hydrogen atom. However, it is also sensitive to other elements to small extent but most of the time the contributions of these elements are assumed to be negligible. Neutron log is a good indicator of shale, gas and porosity. In clean sand reservoirs, the direct measurement of neutron porosity is a good indicator of porosity in oil and water containing pore spaces. The presence of gas in the pore spaces makes the neutron porosity to read lower because the hydrogen index of gas is much less than the oil and water. The presence of shale also affects the response of the neutron log because the clay minerals contain hydroxyl group in their chemical formula. This makes the hydrogen index of the formation to increase and leads to high neutron porosity even in very low porosity shales (Glover, 2011).

In this study, the neutron and NMR porosities were not estimated rather they were given directly as porosity units in the provided well log suite data. Using these porosities with other estimated porosities give important information of the fluid type in the reservoir, and porosity distribution

in the reservoir. Especially Neutron log is important in lithology determination in combination with density log based on separation and cross plot.

Density-Neutron cross plot was done in the Techlog software by plotting the density log in the Y-axis and the neutron porosity log in the X-axis. To see the distribution of the points in a porosity range and lithology type Baker Hughes, 2420, Thermal/Epithermal compensated Neutron versus Bulk density curve overlay was inserted. The plot contains three lines as shown in ***Fig.11*** that shows sandstone (quartz line), limestone (calcite line), and dolomite lines with porosity readings. Gas or light hydrocarbons should plot above and to the left of the sandstone line and shales plot opposite to gas effect towards the lower right below the dolomite line. The porosity of the study area was estimated based on the density of the points and their distribution in the line or between the lines of the porosity values in the curve. In addition to porosity determination, lithology of the formations were determined from the cross plot based on the distribution of the data points.

NMR porosity gives an alternative option to estimate the total porosity of the reservoirs which is similar to neutron log porosity that responds to hydrogen atoms. However, it is not affected by rock type and hydrogen in the chemical formula of the clay minerals as neutron logs (Abouzaid et al., 2016). In this study, the NMR porosity (MPHS) was used to identify fluid identification (mostly gas) and to see the variation of the density porosity and neutron porosity with the variation of lithology.

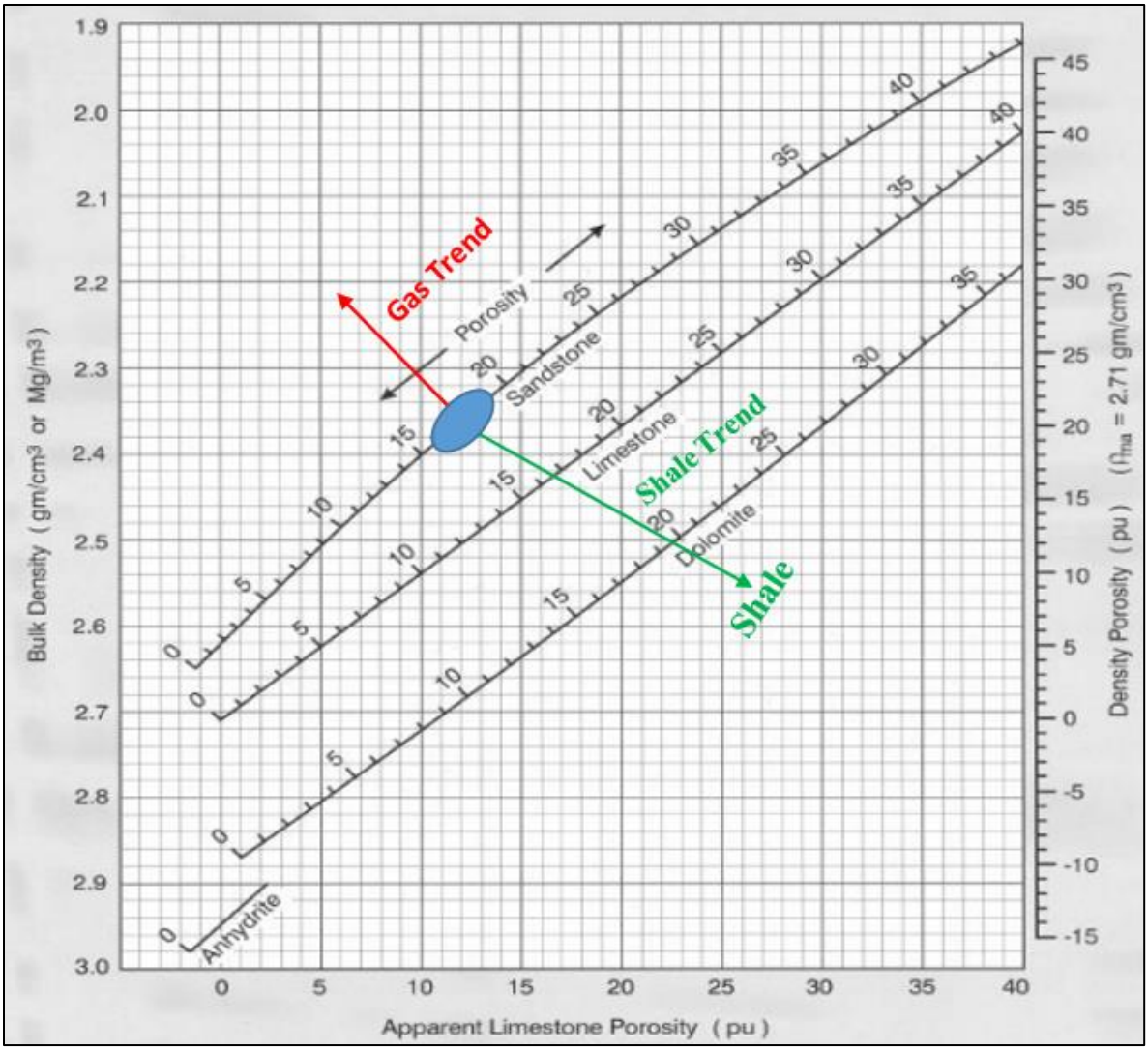

Figure 11: Density-Neutron cross plot modified after (Glover, 2011)

2.6.3. Density-Magnetic Resonance Porosity Method

The presence of gas cap in a reservoir interval of the study area was identified from the logging responses of Nuclear magnetic resonance porosity log, the density log and neutron log and their cross plots. However, the porosity readings of the measurements in the gas zone doesn't show the same value rather a big gap was created between density porosity (DPHI) and Nuclear magnetic resonance porosity(TCMR/MPHS). As shown in ***Fig.12,*** the presence of gas reduces the response of bulk density resulting in high value of apparent porosity and low NMR porosity creating big gap in the gas zone. However, both the total nuclear magnetic resonance porosity and density porosity agrees well in a water filled porosity since the NMR response depends on the total hydrogen content of the formation (Allen et al., 1998). To address the problem of density log porosity in a gas zone a new method was developed that combines the response of

formation bulk density (density log) and response of the total nuclear magnetic resonance porosity (NMR log). This method of porosity computation is called Density-Magnetic Resonance Porosity (DMRP) and it helps to estimate gas corrected total porosity of the formation. The two reasons that make the nuclear magnetic resonance porosity to read too low in a gas reservoir are the low hydrogen index (HI) of gas, long longitudinal relaxation time of gas and high diffusion relaxation (Freedman et al., 1998).

In a gas zone, the bulk density (RHOB) determined from the logging acquisition is the result of adding the contribution of the matrix density, the liquid phase in the invaded zone and the gas phase (Breda et al., 2000).

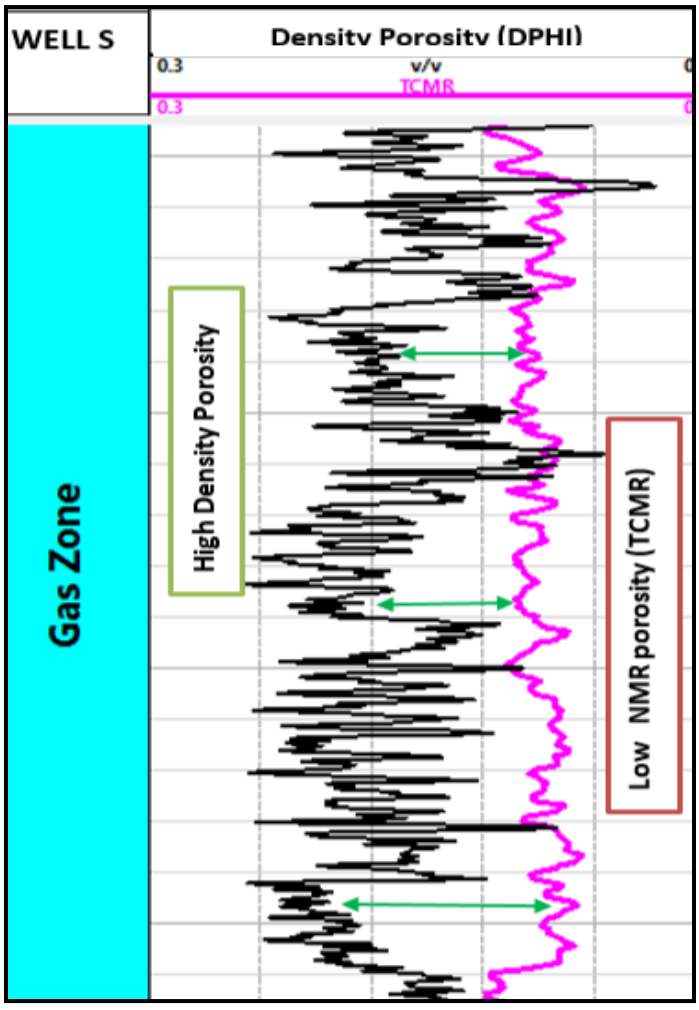

Figure 12: NMR porosity and Density porosity separation in a gas zone taken from well 6406/12-3S

The invaded zone liquid phase includes the mixture of irreducible water saturation left from the displacement of mud filtrate, the gas phase left in the gas reservoir and the mud filtrate itself. Therefore, the two-response equations in the Density-Magnetic resonance are given as follow:

Bulk density response in gas zone:

$$\rho_b = \rho_{ma}(1-\emptyset) + \rho_f\emptyset\left(1-S_{g,xo}\right) + \rho_g\emptyset S_{g,xo} \quad [10]$$

Total NMR porosity response in gas zone:

$$TCMR = (HI)_g.P_g.\emptyset.S_{g,xo} + (HI)_f.\emptyset.\left(1-S_{g,xo}\right) \quad [11]$$

The simultaneous solution of the two equations will give gas-corrected total porosity, which is applicable for reservoirs containing gas (or light hydrocarbons as follow:

$$\Phi = \frac{DPHI.(1-\gamma)+\beta\lambda}{(1-\gamma)+\lambda} \quad [12]$$

Where $\boldsymbol{\lambda}$ is the density difference between the liquid and gas phase, DPHI is the density derived porosity and γ and β are used to simplify the algebra. Four of them are represented as follow:

$$\lambda = \frac{\rho_f-\rho_g}{\rho_{ma}-\rho_f}$$

$$\gamma = \frac{HI_gP_g}{HI_f}$$

$$\beta = \frac{TCMR}{HI_f}$$ And DPHI from equation [7] above

Where:

Φ = The total formation porosity [fraction]

ρ_{ma} = Matrix density of the formation [g/cc]

ρ_f = Liquid phase density in the flushed (invaded) zone at reservoir conditions [g/cc]

$(HI)_g$ = Hydrogen index of gas at reservoir conditions

$(HI)_f$ = Fluid hydrogen index (water +mud filtrate)

$P_{g\,=}$ 1-exp (W/T1, g) is the gas polarization factor

W = the wait time

T1, g = gas longitudinal relaxation time of gas at reservoir conditions

In this study, the challenge was in getting the hydrogen index of gas, hydrogen index of the fluid, density of the fluid, the wait time and the gas longitudinal relaxation. Freedman et al., 1998 in their paper give a solution by approximating the gas-corrected total porosity equation into weighted sum of DPHI and TCMR/ $(HI)_f$ which is given as follow:

$$\emptyset = \mathrm{DPHI} * \mathrm{w} + (1 - \mathrm{w}) * \frac{\mathrm{TCMR}}{(\mathrm{HI})_f} \qquad [13]$$

Where w is given as:

$$\mathrm{w} = \frac{1 - \frac{\mathrm{HI_g} * \mathrm{P_g}}{\mathrm{HI_f}}}{\left(1 - \frac{\mathrm{HI_g} * \mathrm{P_g}}{\mathrm{HI_f}}\right) + \lambda}$$

Taking w ≅ **0.6**, (1-w) ≅ **0.4** and $(HI)_f$ ≅ **1** finally the following approximation equation was developed

$$\mathrm{DMRP} \cong 0.6 * \mathrm{DPHI} + 0.4 * \mathrm{TCMR} \qquad [14]$$

Based on this equation the gas-corrected total porosity always lies between DPHI and TCMR.

Where:

DPHI = Density Porosity estimated from density log, fraction

TCMR = Total Combinable Magnetic Resonance and in this study it is given as MPHS, fraction

DMRP = Density-Magnetic Resonance porosity (gas-corrected total porosity), fraction

In all calculations of water saturation of the well 6406/12-3 S, the gas corrected total porosity (DMRP) was used. For the sake of simplicity in the calculation, the approximated formula was used in creating the DMRP curve in the logging track. However, the well 6406/12-3A and

6406/12-3B does not have gas cap since the only discovery in both wells is oil from different formations.

2.7. Core Porosity

In this study, core data was provided for two wells covering the hydrocarbon bearing zones of Well 6406/12-3B and 6406/12-3S. The provided core porosity was considered as total porosity and it was compared with the calculated log derived total density porosity and DMRP.

2.8. Permeability

Permeability is a measurement of the ease to flow of a fluid through a porous material and it is critical to know the distribution of permeability in a reservoir. However, the distribution of permeability in a reservoir rock is affected by different controlling factors. These factors are distribution of grains and their shape, type of clay and their distribution, cementation, and grain size. The dependence of the reservoir permeability in these factors makes it difficult task in a log analysis and to measure directly using the log measurements. In addition, no log has been yet developed that measures directly the values of subsurface permeability of the reservoir. To address this problem in the oil field, indirect method of intrinsic core permeability is used to describe reservoir permeability (Logan, 1989). However, keeping other factors constant permeability can have direct relationship with grain size and porosity with in the rock. Hence; higher porosity will result in higher permeability and smaller gains will have smaller pores and pore throats which results in lower permeability (Glover, 2011). In the oil and gas industry, rock permeability is an important input parameter in reservoir simulation and characterization. Reasonable determination of permeability is needed because it influences the decision in optimal placement of wells, the hydrocarbon production rate and the economy of the whole sector of development and operation of the oil and gas field (Lacentre and Carrica, 2003).

Permeability in the oil field is given as the Darcy's linear flow/radial equation that relates flow rate with permeability and the pressure difference in the flow as shown in ***Fig.13***. This is given in a formula for linear flow:

$$Q = \frac{K * A * \Delta P}{\mu * L} \qquad [15]$$

Where:

K = Permeability [D]

A = Cross-sectional area [cm^2]

μ = the viscosity of the fluid [cp]

Q = the flow rate [cm/s]

ΔP= change in pressure which is the pressure drop across the porous medium with length (L)

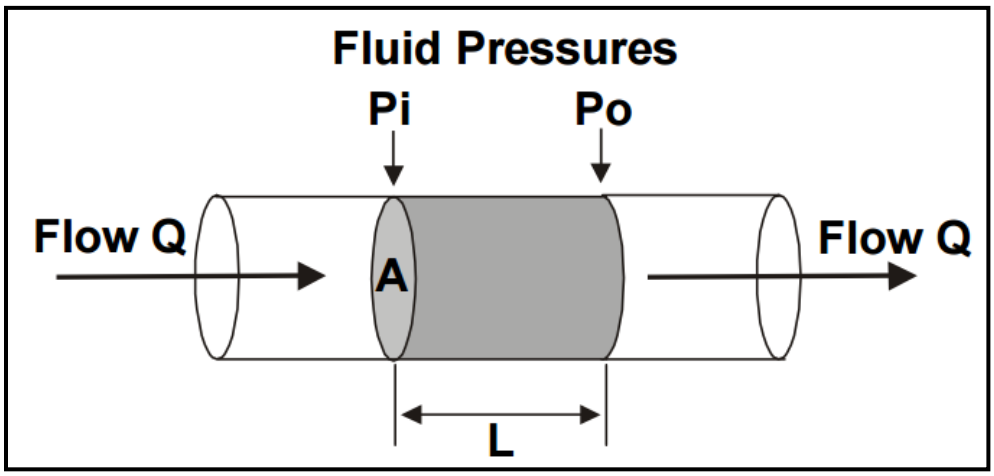

Figure 13: Fluid flow in a porous media and permeability definition (Glover, 2011)

The permeability values of sedimentary rocks range from Nano- Darcy to tens of Darcy and classification of reservoir rocks based on permeability is given in ***Table 7.***

Table 7: Permeability classification of reservoir rocks (modified after Glover, 2011)

Permeability Value (mD)	Classification
<10	Fair
10-100	High
100-1000	Very High
>1000	Exceptional

Permeability Determination

Permeability can be determined from different sources like from lab testing on cores, well testing or from well logs. In this study, different permeability values were provided in a core report

(Horizontal permeability, Vertical permeability, measured permeability (Kg), Klinkenberg corrected gas permeability (KL)), NMR log permeability (MPRM) and the permeability derived from the regression analysis of core porosity versus permeability plot (PoroPerm cross plot). In addition to these given permeability values, it can be also estimated in the log analysis software Techlog using the following two methods:

Wyllie-Rose method[3]

$$K = Kw * \frac{PHIT^d}{Swirr^e}$$

Where:

Swirr = Irreducible water saturation, v/v

Kw = constant

Table 8: Input parameters of Wyllie Rose method (taken from Techlog software 2016 version 2)

Wyllie-Rose coefficients	Wyllie Rose fluid	Swirr	D	E	Kw
Timur	Oil	0.2	4.4	2	3400
	Gas	0.2	4.4	2	340
Morris-Biggs	Oil	0.2	6	2	62500
	Gas	0.2	6	2	6500

Coates Method[4]

For clean zones:

$$K = Kc * PHIE^4 * \left(\frac{1 - Swirr}{Swirr}\right)^2$$

Else:

$$K = Kc * PHIE^4 * \left(\frac{PHIT - PHIE * Swirr}{PHIE * Swirr}\right)^2$$

[3] *The formula of Wyllie Rose method is taken from Techlog software, 2016 version 2*

[4] *The formula of Coates method is taken from Techlog software, 2016 version 2*

Where:

PHIE = Calculated effective porosity

PHIT = Calculated total porosity

Kc = Constant

The methods given in the software works best for the data where the default values are generated but in this paper, the methods were not applied in the estimation of permeability. This is because they have more than two unknowns to be determined. However, the NMR permeability (MPRM) given in the log suite is similar with Coates method. In addition to MPRM, Porosity-permeability relationship was used to estimate the permeability of the target reservoirs based on the data from core report results. This relationship was done in Techlog software using cross plot of logarithm scale of permeability in the Y-axis and the linear scale of porosity in the X-axis. Core Klinkenberg corrected gas permeability and core porosity from well 6406/12-3S and 6406/12-3B was used in this analysis. Regression of the data points gives linear relationship and the permeability of the formations in terms of porosity was given in the form of $\log K_{Core} = A*\phi_{Core}+B$.

2.9. Water Saturation

Fluid saturation is the fraction of the pore space in the rock occupied with a certain fluid and can be expressed in a formula as:

$$\text{Saturation of fluid} = \frac{V_{fluid}}{V_P} = \frac{\text{total volume of the fluid occupying the pore spaces}}{\text{total pore spaces in the rock (pore volume)}}$$

The percentage of the oil, gas and water saturation in the pore spaces is given as:

$$S_{oil} = \frac{\text{Volume of oil}}{\text{Pore Volume}} \text{x } 100$$

$$S_{gas} = \frac{\text{Volume of gas}}{\text{Pore Volume}} \text{x} 100$$

$$S_{water} = \frac{\text{Voluume of water}}{\text{Pore Volume}} \text{x} 100$$

The water saturation can be classified as total water saturation and effective water saturation, and this can be expressed in a formula:

$$Sw_{total} = \frac{V_{wt}}{\emptyset_t} = \frac{V_{CBW}+V_{CAP}+V_{FW}}{\emptyset_t} \quad [16]$$

$$S_{we} = \frac{V_{wt}-V_{CBW}}{\emptyset_e} \quad [17]$$

Where:

V_{CBW} = Volume of clay bound water

V_{CAP} = Volume of capillary bound water (irreducible volume of water)

V_{FW} = Volume of free water

The total saturation of the fluids present in the reservoir sum up to 100% and it could be oil and water only, gas and water or reservoir containing three fluids (gas, water and oil).

$$S_w + S_o + S_g = 1$$

Water saturation estimation

Water saturation is one of the important inputs in the volumetric calculation of hydrocarbon in place of the oil and gas fields. In the estimation and analysis of water saturation of reservoir rocks, researchers have developed different theoretical and experimental approaches. This can be determined from different data inputs like capillary pressure measurements, core data, Wireline Logs and Drill stem test from well testing. However, not all these data are provided in this thesis work and the emphasis of the analysis and interpretation will be on log-derived saturations of different models. The models used in a log analysis of water saturation depends on the type of the formation and they are grouped as clean sand models for shale free formations and shaly-sand models for shale/clay containing reservoirs. The rock model of the two methods including the rock and fluid constituents are given in ***Fig.14.*** The figure illustrates the rock model considered in the Archie model is the matrix and the pore space that contains the irreducible water saturation (capillary bound water) and the free fluid (hydrocarbon and water). The shaly sand rock model includes the clay mineral in addition to the Archie rock model. However, the detail classifications of water are beyond the scope of this paper and they are not going to be

discussed. In this study generally the clay bound water; irreducible water and the free water are considered.

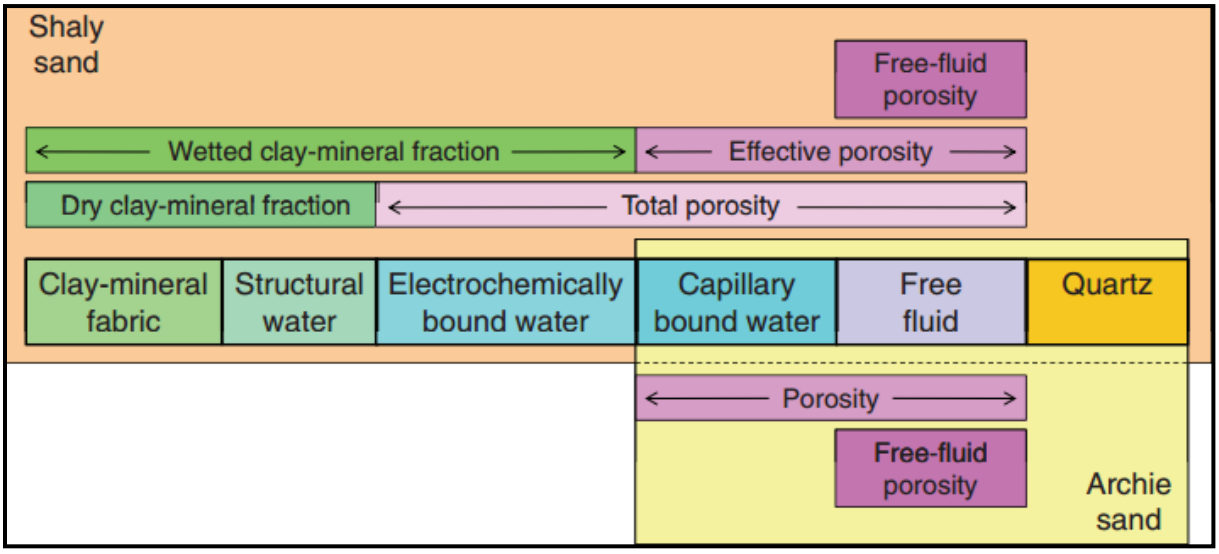

Figure 14: Rock model of clean sand Archie model and shaly sand model (Worthington, 2011)

2.9.1. Clean Sand Water Saturation model (Archie Model)

Archie (1942) was the first author that established clean sand formation water saturation equation based on the principle of saline water in the pore spaces is the entire contributor of the conductivity of the formation. This principle creates a difficulty with rocks containing thin beds between sand layers(formations with clay mineral and silt), rocks with variable mineralogy and texture, rocks with different porosity types (like micro porosity, fractures, fissures and vugs), and oil wet formations. The criteria for accurate estimation of porosity and saturation from Archie equation are clean sand formations with single rock type, intergranular porosity, water wet formation, and homogenous in mineralogy and texture (Worthington, 2011).

Archie has developed first law and second law equations to solve the water saturation of clean sand from resistivity and formation resistivity factor from porosity (Archie, 1942). The equations are given as follow:

The first law: $$F = \frac{R_o}{R_w}$$

Alternatively, F can be expressed also as $F = \frac{a}{\emptyset^m}$

Second law: $I_r = \frac{R_t}{R_o} = S_w{}^{-n}$

Combining the first and second laws of Archie gives the water saturation as:

$$S_w = \sqrt[n]{\frac{a.R_w}{\emptyset^m.R_t}} \qquad [18]$$

Where:

F = Formation resistivity factor

R_w = Formation water resistivity, Ωm

R_o = Resistivity of fully brine saturated rock, Ωm

R_t = True formation resistivity (Resistivity of partially brine-saturated rock), Ωm

I_r = Resistivity Index, fraction

m = cementation exponent (Porosity exponent)

n = saturation exponent

a = tortuosity factor

S_w = water saturation, fraction

In this study, Archie water saturation was used for comparison to the shaly sand models and to see the effect of shale in the reservoir. In the absence of any lab-derived data, the constants **a, m**, and **n** were taken as **1, 2**, **and 2**, respectively in all calculations of the water saturations both in the clean sand and shaly sand models.

Input parameters in the log analysis of clean sand Sw

In the calculation of water saturation, the deep resistivity log (RDEP) was taken as true formation resistivity (R_t) assuming that it is corrected for invasion, thin bed and bore hole effects. The other input parameter formation water resistivity (Rw) was not available in the given raw data of the composite log. To get this resistivity apparent formation water resistivity (Rwa) was estimated by Archie equation from precomputation part of the software using the deep

resistivity and porosity as input parameters. Vertical base line was inserted to the estimated Rwa curve and the Rw was taken in the clean sand water zone where the Archie water equation gives Rwa=Rw=$\emptyset^2 * R_t$. However, selecting the Rw from the Rwa curve increases the uncertainty in the calculation of water saturation, and this is because of the variation in the value of Rw in the clean sand zone. The value of Rw lies in a range of 0.08-0.12 Ωm and using the lower or the higher value gives different result in the calculation of water saturation and finally in the calculation of the hydrocarbon in place in the reservoir. To minimize the error an average value of 0.1 Ωm was taken in the estimation of the water saturation. In addition to this method, another method was tried to get the formation water resistivity by extrapolating brine conductivity given at surface condition from core analysis report of well 6406/12-3S.The formation resistivity given at surface condition should be corrected to formation temperature. The formula used to get the Rw at formation temperature (in degree Celsius) was as follow:

$$R_2 = R_1 \frac{(T1+21.5)}{(T2+21.5)} \quad [19]$$

Where:

R_2 = The Formation water resistivity (Rw) at formation temperature, Ωm

R_1= The Formation water resistivity (Rw) at surface temperature and for well 6406/12-3S it was given 0.225Ωm

T_1 = the surface temperature where in this study brine conductivity was taken at 20^0C

T_2 = Formation temperature in this study in the log data it is given as WTBH

For the two wells the formation water resistivity was derived only from Archie method derived Rw.

2.9.2. Shaly sand water saturation models

The presence of clays (Shales) in a reservoir formation complicates the log interpretation and estimation of water saturation. This is due to the conductive nature of the clay minerals that creates extra conductivity in the formation. Archie model fails to include the clay conductivity because it considers that, the only electrically conductive material in the formation is the formation saline water. Therefore, Archie equation for shaly sand formations water saturation results in an erroneous and misleading output. The overestimated water saturation of Archie

equation makes the petroleum industry professionals and the company to be pessimistic for looking oil and gas finally bad reserve estimation. To address this problem petrophysicists develop theoretical and experimental models that includes the conductivity caused by the presence of shale in the reservoir. The Archie equation is used as a basis to develop the shaly sand equations and they include the clay conductivity in terms of CEC, BQV, Qv, and resistivity of shale (Doveton, 2002). The equations can be expressed as Archie +X (Cs) which is given in the following form:

$$\frac{1}{R_t} = \frac{{S_w}^2}{F.R_w} + C_s \qquad [20]$$

Where: Cs term sometimes X term is used as general term as shown in ***Fig.15***. The different shaly sand conductivity models use different terms to accommodate the effect of shale on the formation conductivity, i.e. some of them use volume of shale and others the double layer effect of clay (the cation exchange capacity) on the surface of the clay.

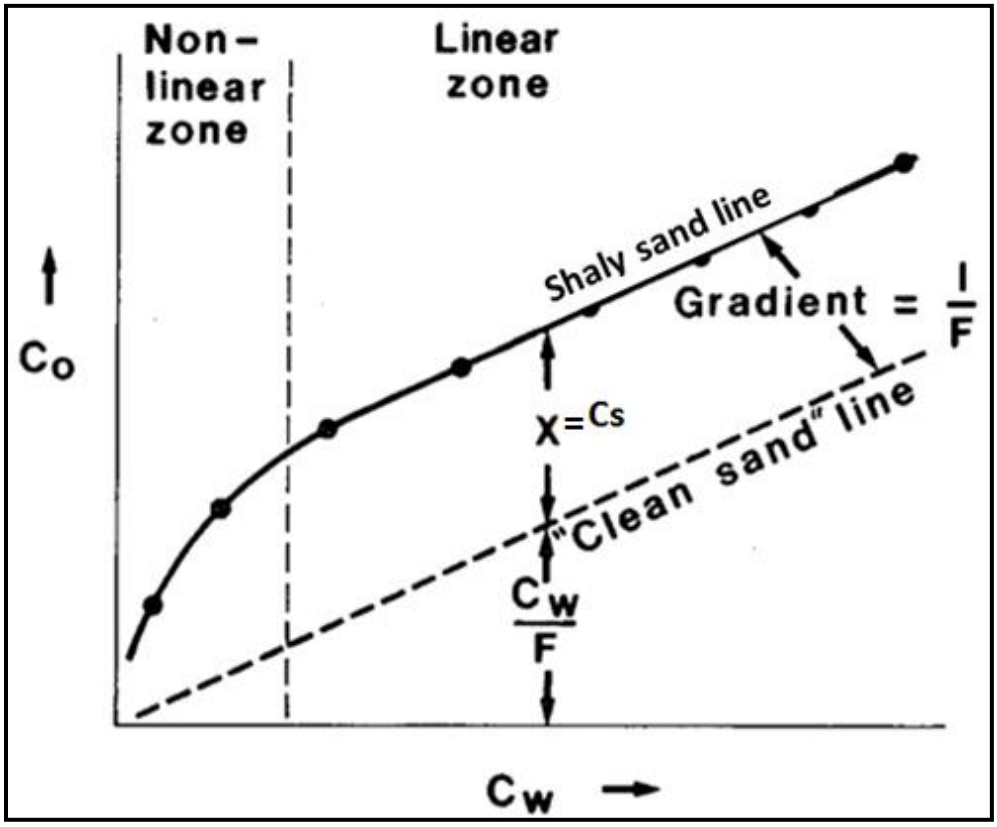

Figure 15: Variation of fully brine saturated rock conductivity (Co) with changing formation water conductivity (Cw) in shaly sand (Worthington, 1985)

Shaly sand models are categorized into two groups based on their applications and input parameters (Worthington, 1985). These are:

I. Shale Volume (V_{sh}) based models: These models use volume of shale as input in the water saturation estimation and they are applicable in logging data without calibrating with core data input parameters. Some of the models are:

- Poupon-Leveaux (Indonesia) model
- Simandoux model
- Modified Simandoux model

The type of porosity used in these modes is the effective porosity and the estimated water saturation is the effective water saturation (S_{we}). In Techlog software, these methods are found under the category of the effective water saturation.

II. Cation Exchange Capacity (CEC) or Conductivity based models: The input parameters used in this model are the total porosity and electrical properties. Shale volume is not used in these models as input parameter and in log analysis; the shale related values are correlated with core-derived values. Some of the models are:

- Dual-water model
- Waxman-Smits and modified Waxman-Smits model
- Juhasz model

The shaly sand models are effective in certain conditions but if that condition fails, they will be no longer effective. Therefore, none of these models are perfect in solving the shaly sand water saturation universally using one equation in all conditions (Doveton, 2002).

In this study, the core-derived input parameters (e.g. CEC, BQV) were not provided but still in Techlog, it is possible to calculate water saturation based on the conductivity based models. The problem is the uncertainty in input variables will lead to erroneous results because garbage in will lead to garbage out. To minimize this error two volume of shale-based models (Indonesia and Simandoux) were applied to estimate the shaly sand water saturation.

Indonesia Model

Poupon and Leveaux developed this model in 1971 based on field data from Indonesia the place where the name of the model got. This model is developed for laminated shale distribution, low salinity formation water, and high shale volume reservoir (Poupon and Leveaux, 1971).

Based on the logging responses and core photograph images of lithology distribution, the shale in the sandstone layers of Pil and Bue fields are distributed in laminated mode. Therefore, the following formula of Indonesian equation was applied in the determination of the shaly sand water saturation.

$$\frac{1}{R_t} = \frac{{S_w}^2}{F.R_w} + \sqrt[2]{\frac{{V_{sh}}^{2-Vsh}}{F.R_w R_{sh}}}{S_w}^2 + \frac{{V_{sh}}^{2-Vsh}{S_w}^2}{R_{sh}} \quad [21]$$

Where:

R_{sh} = Resistivity of shale, which is obtained from the deep resistivity log in a shale zone

V_{sh} = Shale volume, v/v

The Poupon-Leveaux is generally regarded as effective water saturation model that uses effective porosity as input parameter. However, the paper itself is not specific whether effective or total porosity was used in their formula but in (Worthington, 1985) paper it is explained that the water saturation is related to the total interconnected pore spaces of clean sand streaks. In this study, the input parameters used in Techlog are summarized in **Table 9**.

Table 9: Input Variables for Indonesia water saturation model

Input Variable	Unit	Description	Value
Formation resistivity (Rt)	Ohm.m	Rdeep log reading in zone of interest	Variable
Effective porosity	v/v	Calculated effective porosity	variable
Shale volume	v/v	Calculated shale volume	variable
Tortuosity Factor (a)	--	Constant	1
Cement Exponent (m)	--	Constant	2
Saturation Exponent (n)	--	Constant	2
Resistivity of Shale (Rsh)	Ohm.m	Rdeep log reading in the shale zone	4
Formation water resistivity (Rw)	Ohm.m	From Rwa in clean sand water zone	0.1

Simandoux Model

This model was developed to estimate core conductivity on homogeneous mixtures of sand and Montmorillonite clay mineral based on experimental work (Simandoux, 1963). This model adds

resistivity of shale and shale volume to the Archie water saturation model to accommodate the extra conductivity induced by the presence of clay and clay minerals. In the Techlog software, the water saturation was estimated based on the following formula:

$$\frac{\emptyset_e{}^m}{a * R_w} * S_W{}^n + \frac{V_{sh}}{R_{sh}} * S_w - \frac{1}{R_t} = 0$$

Generally, the water saturation models use different principles and working conditions and in this work, the results of the three models will be compared in the next chapter. The comparison of the clean sand water saturation and shaly-sand water saturation was done based on bulk water volume because the input parameters (e.g. Porosity) used in the methods are different and the output is different. The bulk volume of water (BVW) can be classified as effective BVW (BVW_E) and total BVW (BVW_T), and it is expressed using the following formula.

$$BVW_{total} = \emptyset_{total} * Sw_{total}$$

$$BVW_{effective} = \emptyset_{effective} * Sw_{effective}$$

However, comparing using BVW for the three models is expected to be different and what should be comparable are the bulk hydrocarbon volume (BVHC). In this study, the focus is the comparison of the water saturation values of the models and discusses the results. Therefore, the BVW for each model was used to see how much the pore spaces of the reservoir are occupied with water. The Bulk volume of hydrocarbon is given as:

$$BVWC = PHI * (1 - Sw)$$

Chapter Three: Result

In this chapter, the results of the petrophysical analysis from well log data, formation pressure data, and from core analysis report will be illustrated and presented in terms of figures and tables. The results of the estimated parameters to be illustrated and presented are:

- Lithology determination for each well
- Shale volume for each well
- Fluid type and fluid contact determination for each well
- Porosity comparison for each well
- Porosity-permeability relationship for well 3S and well 3B
- Finally comparison of the clean sand and shaly sand water saturations of each well

3.1 Lithology determination

Well 6406/12-3 S

The identification of lithology in well log analysis is done based on logging responses in the depth intervals. The logs used in the identification of lithology are mostly gamma ray, density log, and combination of Density-Neutron logs. There are depth intervals with uniform or similar responses of the logging measurements but in this study, the whole interval of the well is subdivided into five zones as shown in ***Fig.16*** mainly based on lithology and fluid content. However, in the reservoir section it is mainly based on fluid content and to be consistent the same zonation is applied to the lithology zonation. All the depth interval measurements are given in m, MD (Measured Depth).

Zone 1 [3505-3514 m] – this zone is identified as Marl lithology and marked with high gamma ray, high neutron and high-density readings in the top part from 3505-3509 m, and the rest 5 meters show low gamma ray, low neutron and higher density log responses.

The reservoir interval of this well was identified from 3514-3912 m in Intra-Melke sandstone formation and it contains **Zone 2**, **Zone 3** and **Zone 4.**

The dominant lithology in the given reservoir interval of this well is sandstone. However, the top part of the reservoir interval 3514-3516 m and the bottom part mostly from 3775-3912 m are dominated by shale. In the shale containing depth intervals, the response of gamma ray and neutron log is higher than the sand containing intervals. Based on lithology distribution in the

reservoir section of zone 3 and zone 4 up to 3775 m are similar but the general zonation takes in to account the fluid content that is going to be illustrated in the next sections of this paper as shown in ***Appendix A1.***

Zone 4 [3912-3977 m] – This interval is identified as Shale containing zone and the gamma ray, neutron and density logs give higher value comparing to the other zones.

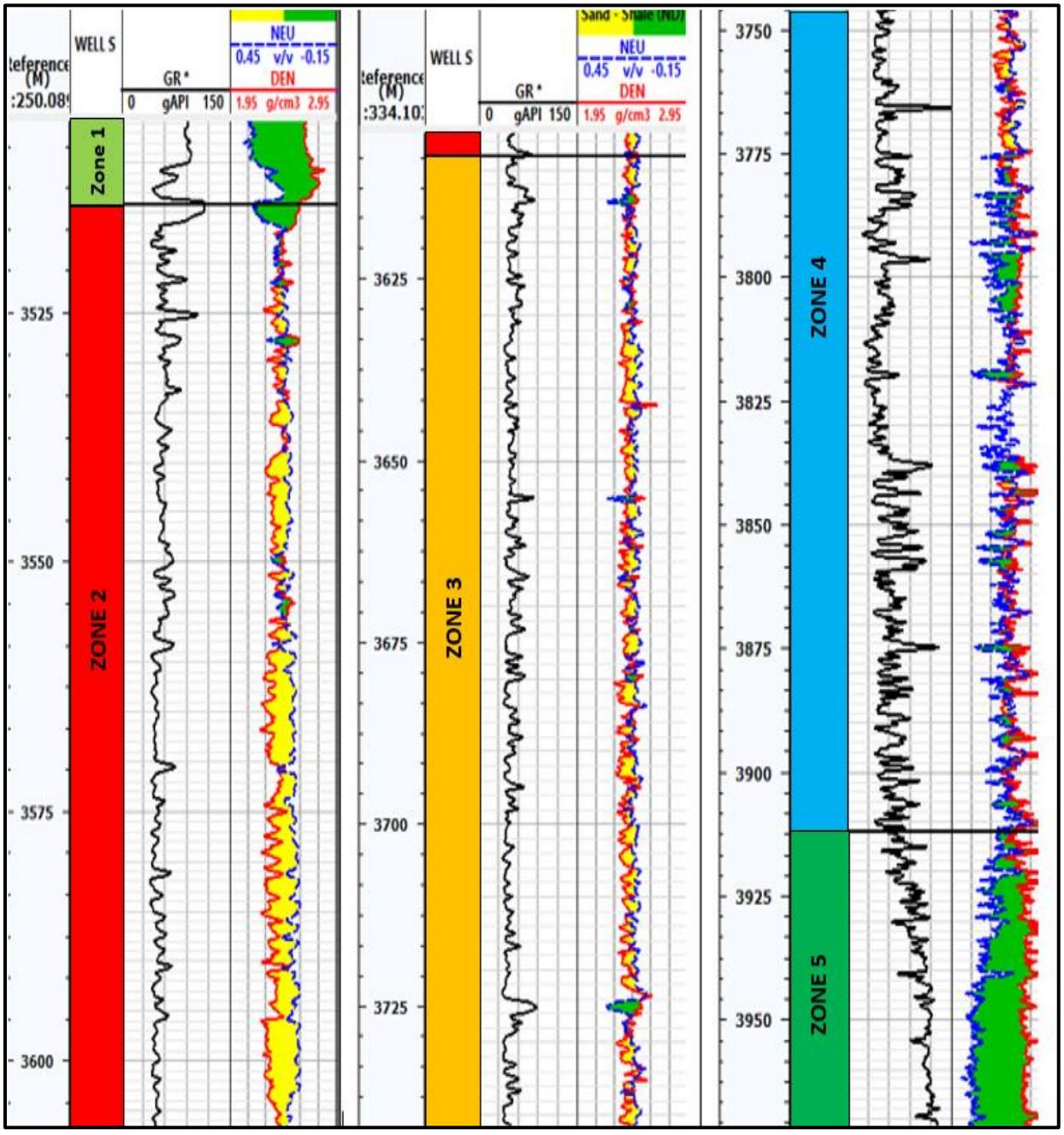

Figure 16: GR response and Density-Neutron crossover of the whole interval of well 6406/12-3S

In the gamma ray response, there are depth intervals with exaggerated low and high reading streaks. The maximum and minimum gamma ray recorded in the whole interval of this well were 163 gAPI and 21gAPI respectively and the maximum and minimum readings in the depth intervals of this well are given in ***Table 10*.**

Table 10: Maximum and minimum gamma rays in the depth interval of well 6406/12-3S

Depth interval	Gamma Ray		
MD [m]	**Min**	**Max**	**Average**
3514-3608	38	116	55
3608-3745	35	89	49
3745-3912	21	163	58
3912-4001	50	141	107

In addition to GR and Density-Neutron cross over responses, the Density-Neutron cross plot of the reservoir interval [3514-3912 m] is given in ***Fig.17,*** which illustrates the distribution of the data points. The bulk density response in the depth interval is given in y-axis and the neutron porosity in the x-axis with color scale of Gamma Ray (GR). Based on the distribution of the data points Shale, clean sand and shaly sand lithologies were identified. The detailed distribution of the data points in zones (2, 3 and 4) of the well are given in ***Appendix A2, 3 and 4*.**

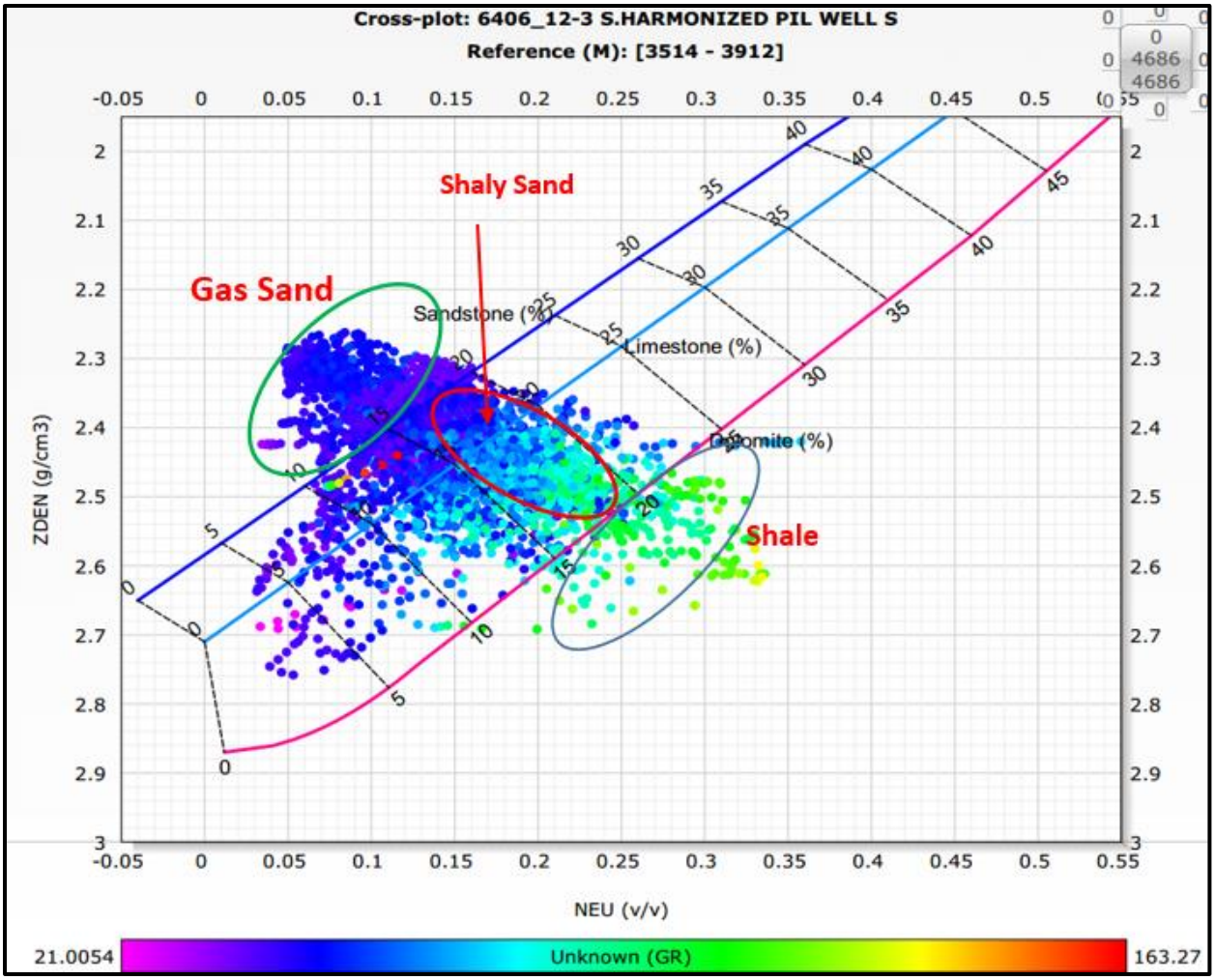

Figure 17: Density-Neutron Cross plot of the reservoir interval of well 6406/12-3S

In addition to the presence of shale in the lithology determination, the presence of other minerals distributed in the sandstone and clay type of the reservoir interval of [3514-3745 m] was identified as shown in ***Fig. 18*** from Thorium (in the y-axis) and Potassium (in the x-axis) cross plot. As shown in the plot, much of the data points lie in the Illite, Micas and Glauconite minerals.

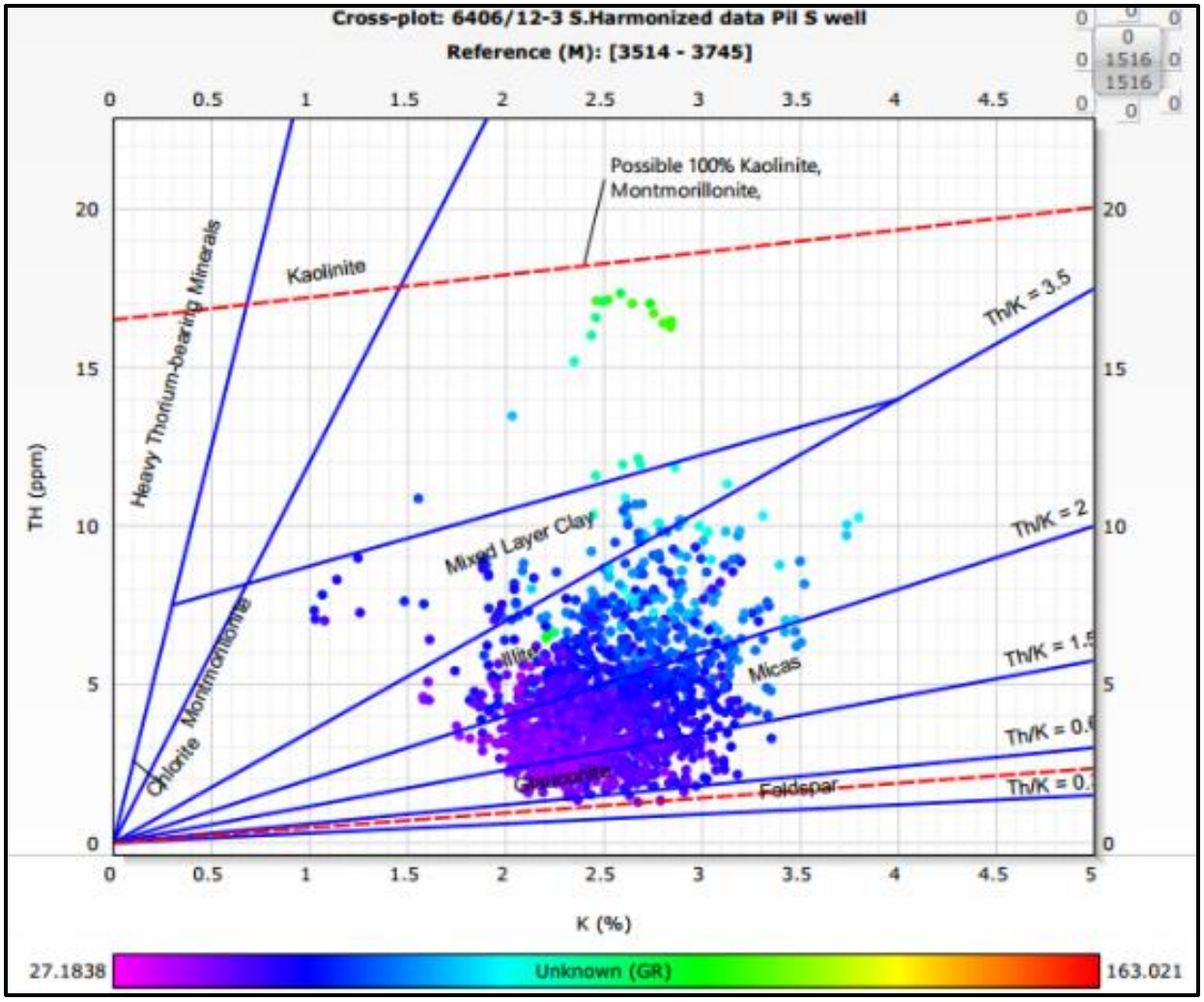

Figure 18: Thorium - Potassium Cross plot of reservoir interval [3514-3745 m]

Well 6406/12-3B: Lithology

The reservoir interval of this well is from 3761-4264 m (Measured depth), and the top (**Zone 1**) and bottom (Zone 4) of the reservoir formation are Spekk and Melke shale formations. The depth interval 3761-3846 m of the reservoir section is highly dominated with sand containing very thin laminae of shale in between. However, the lower part of the reservoir from 3896 m to 4264 m is highly dominated with shale and the thicknesses of the sand layers are very thin. Therefore, the top part of the reservoir is characterized as dominantly clean sand section and the lower part is dominantly shaly-sand. As described above the fluid content zonation is applied in this well also but above and below the reservoir section the lithology is different. Therefore, the same zonation is used through the well in estimation and determination of all parameters.

The gamma ray response and Density-Neutron crossover (separation) in the top, bottom and reservoir section of this well is given in ***Fig.19.***

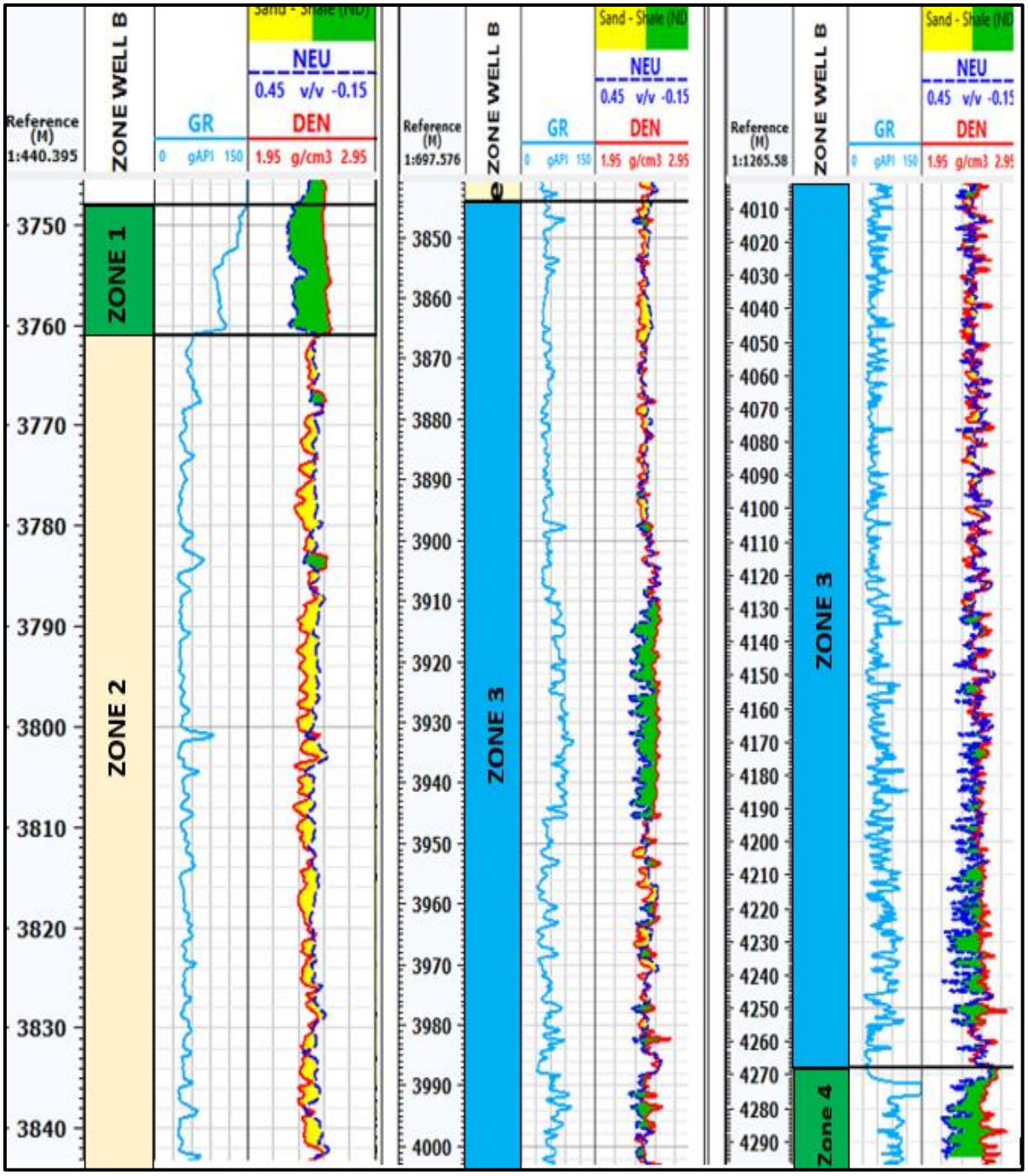

Figure 19: Gamma ray response and Density-Neutron crossover of well 6406/12-3B

The reservoir interval Density-Neutron cross plot of this well is given in ***Fig.20***. As shown in the figure, the maximum crowds of the data points lie between sandstone and limestone line. The

color scale shows the gamma ray response and the high gamma ray data points tends to move away from the sandstone line towards the right hand direction. The low gamma ray data points lie in the sandstone line and between the sandstone and limestone lines.

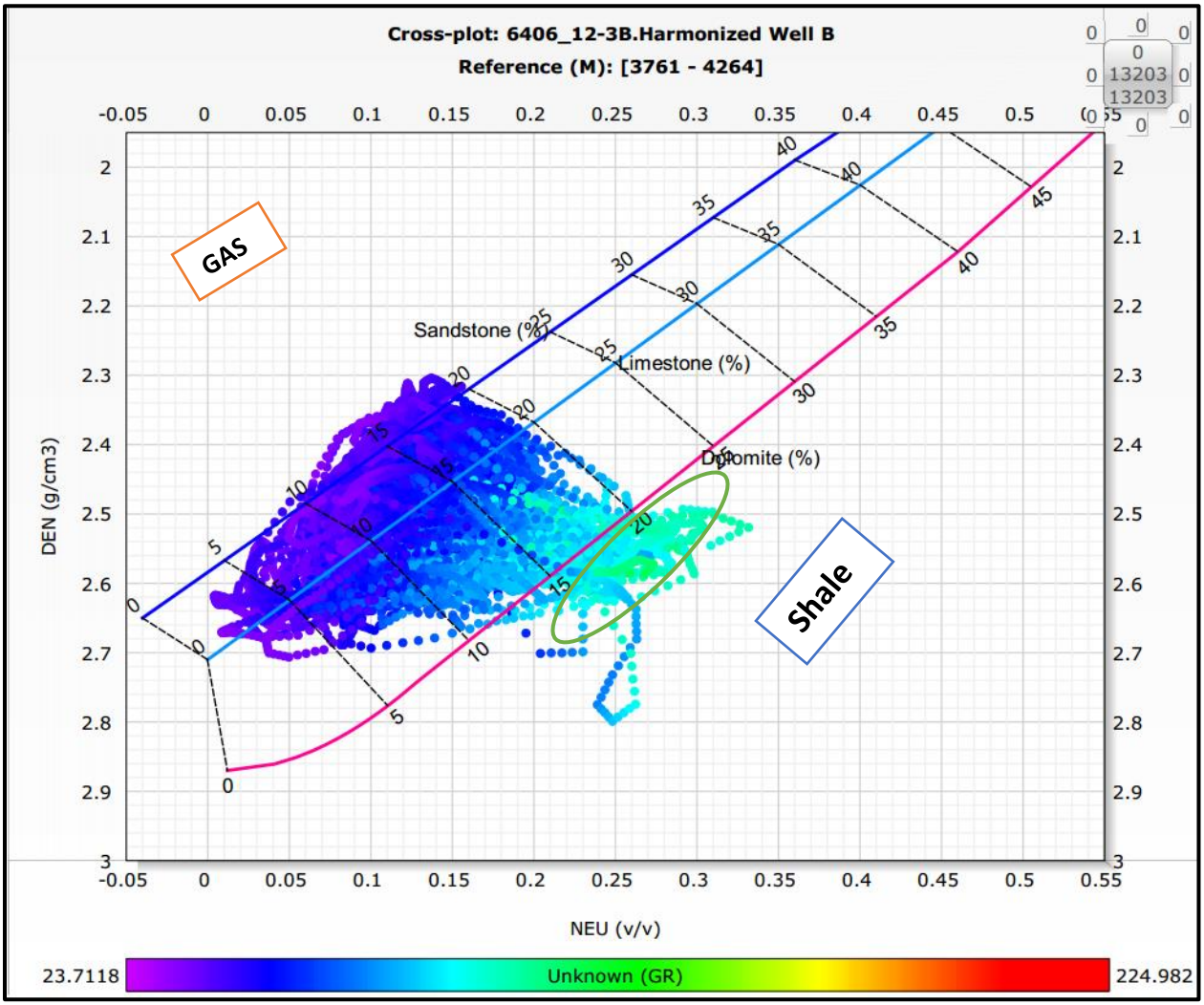

Figure 20: Density-Neutron cross plot of the reservoir interval of well 6406/12-3B

Well 6406/12-3A: Lithology

The reservoir section of this well is given from 4053-4114 m and the same zonation criteria was used as in well 6406/12-3S and 3S.

Zone_1 and zone_5 of this well is dominated by shale and the reservoir interval is dominated lithology with sandstone. However, the top part of the reservoir zone_2 (4053-4065m) is dominated by shale as shown in ***Fig.21***.

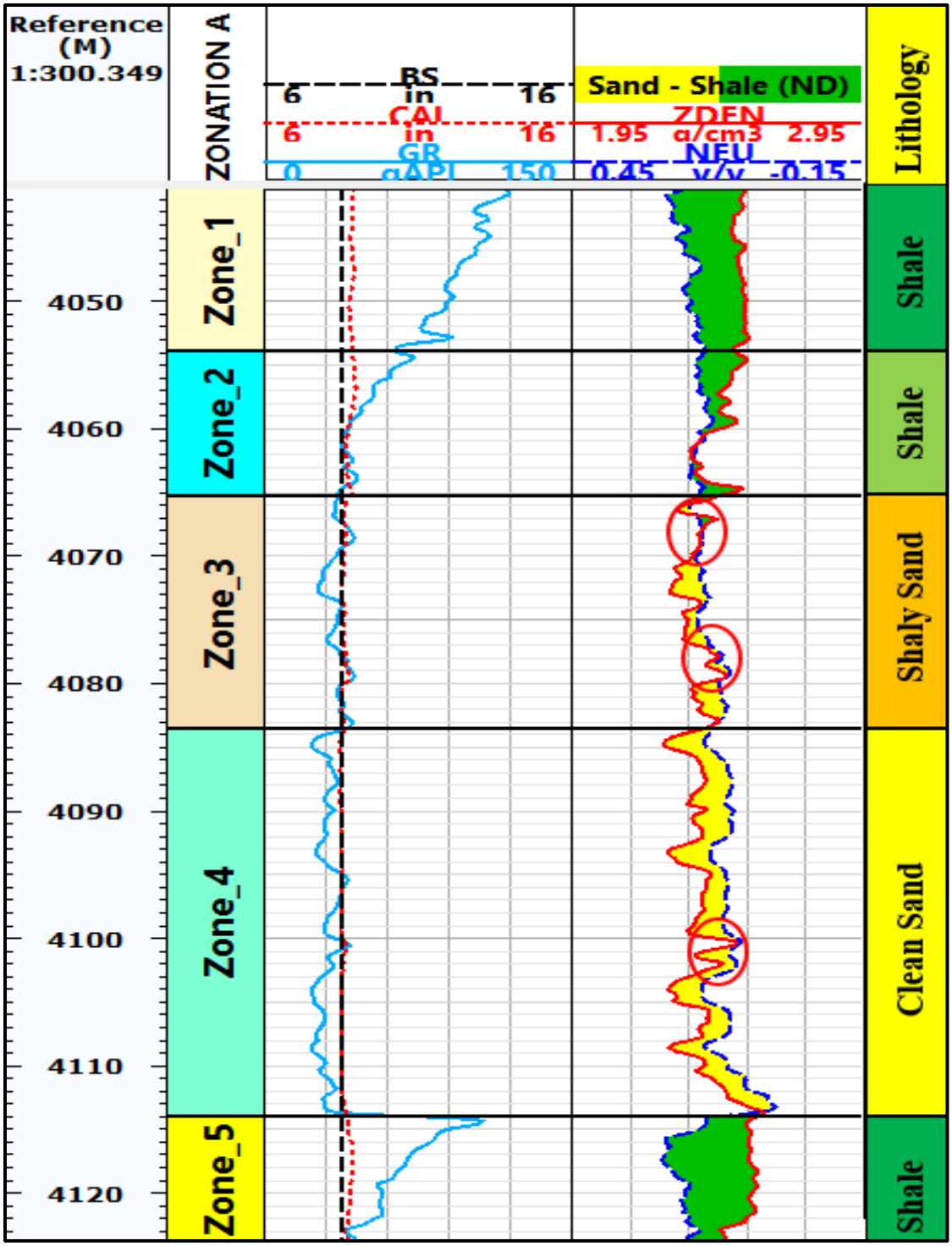

Figure 21: The gamma ray response and Density -Neutron crossover of Well A in the depth interval 4041-4124 m

Density-Neutron cross plot of this well shows much crowd of the points lie in the sandstone line and limestone line as shown in ***Fig.22.***

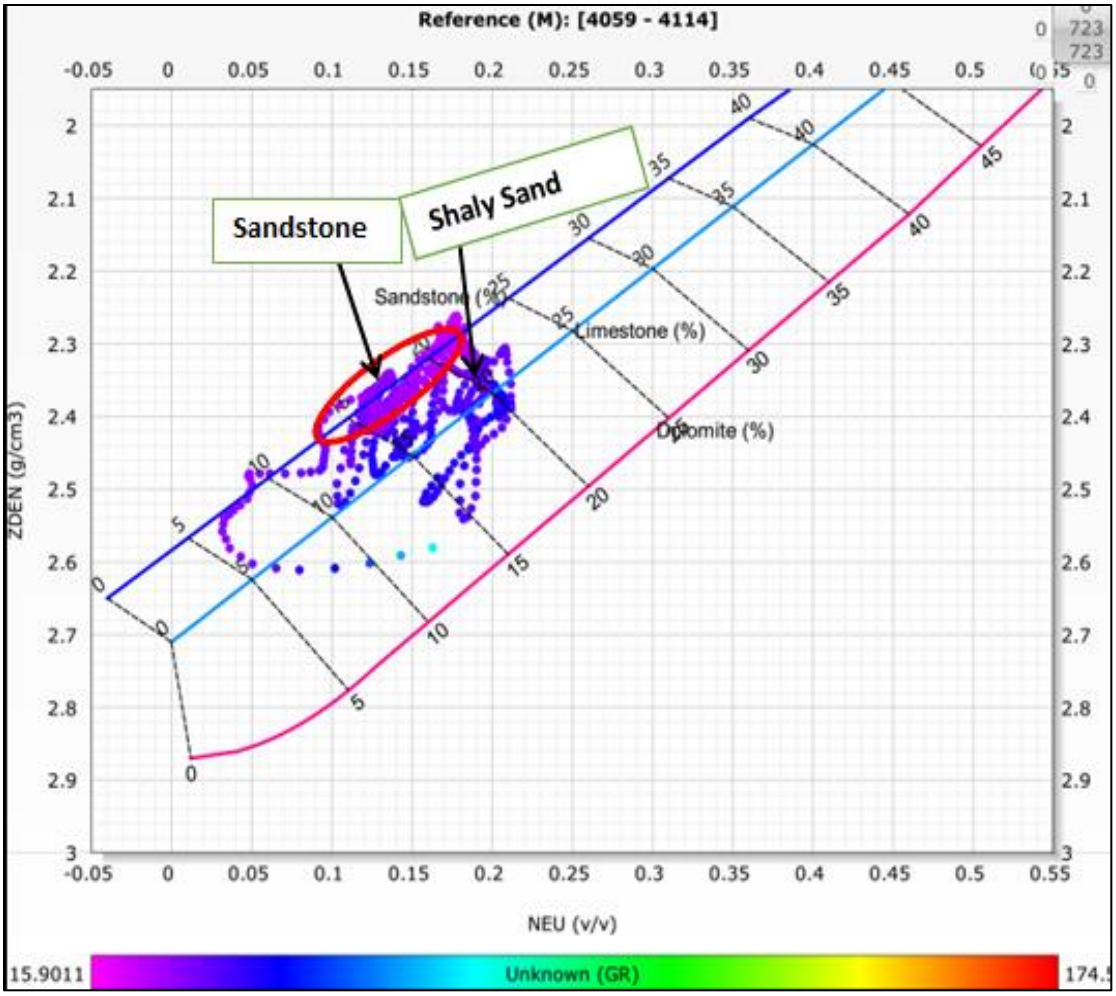

Figure 22: Density-Neutron cross plot of the reservoir interval of well 6406/12-3A

3.2. Volume of shale

The volume of shale was calculated based on the linear method of gamma ray and the results of the three wells are presented in terms of logging plots to show the reading at each depth interval and in terms of histogram distribution to show the percentage of shale volume in the given depth interval.

Well 6406/12-3S: Vsh

The maximum GR of this well were chosen from the thick shale in the Melke formation ***Fig.16*** above and the calculated shale volume from GR log of the reservoir interval is given both in the log and Histogram distribution ***Fig.23.*** The shale volume in the top of the reservoir (2-3 m) and the bottom of the reservoir is higher than the rest of the reservoir. The maximum percentage of the shale volume in the reservoir interval lies below 20% but there are depth intervals that reach 100% though they are not enough to create full deflection.

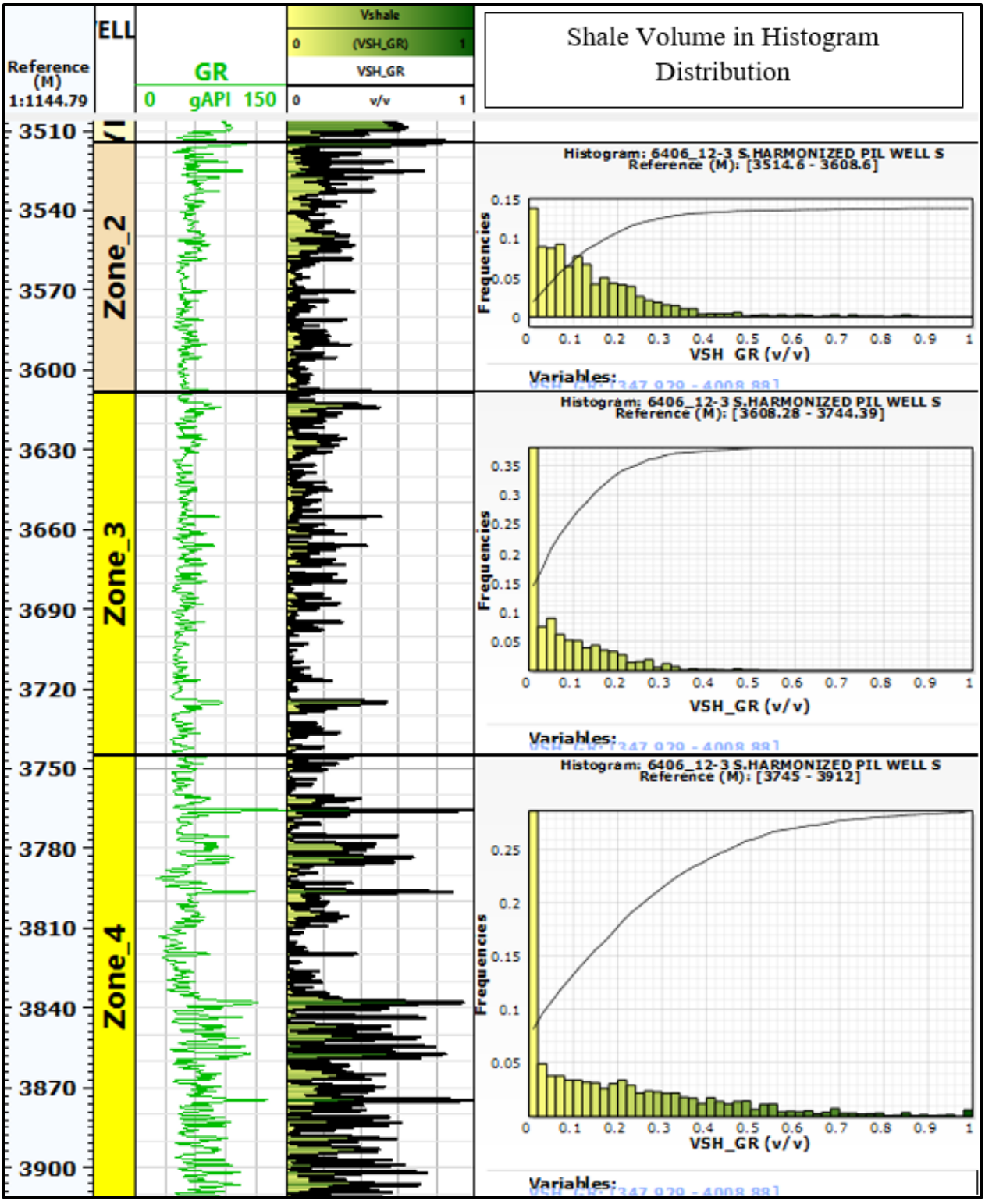

Figure 23: Shale Volume of well 6406/12-3S in the reservoir interval

Well 6406/12-3B: Volume of Shale (Vsh)

The shale volume in the reservoir section of this well is given in ***Fig.24*** from 3761-3844 m and in ***Fig.25*** from 3844-4267**.** The maximum concentration of the shale volume in the top part of the reservoir is less than 30% and in some part of the depth intervals, though their thickness is in centimeters but the Vsh reaches up to 90% as shown in the figure. With increasing depth in the reservoir section, the shale volume increases and the thickness of the shale zones increase, which is more shaly sand in the bottom of the reservoir as shown in ***Fig.25***.

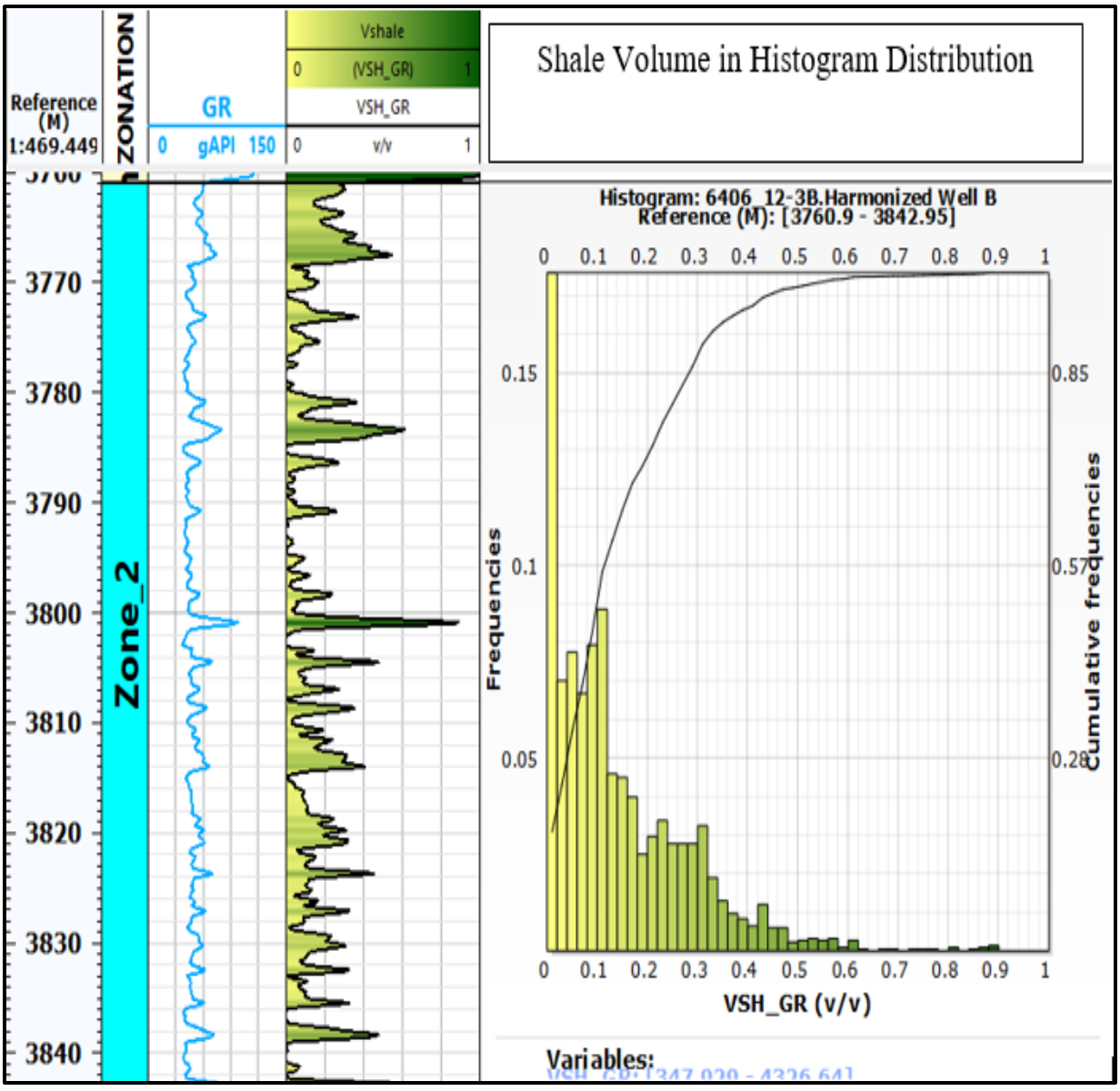

Figure 24: Shale Volume of well 6406/12-3B in the depth interval of 3761-3843

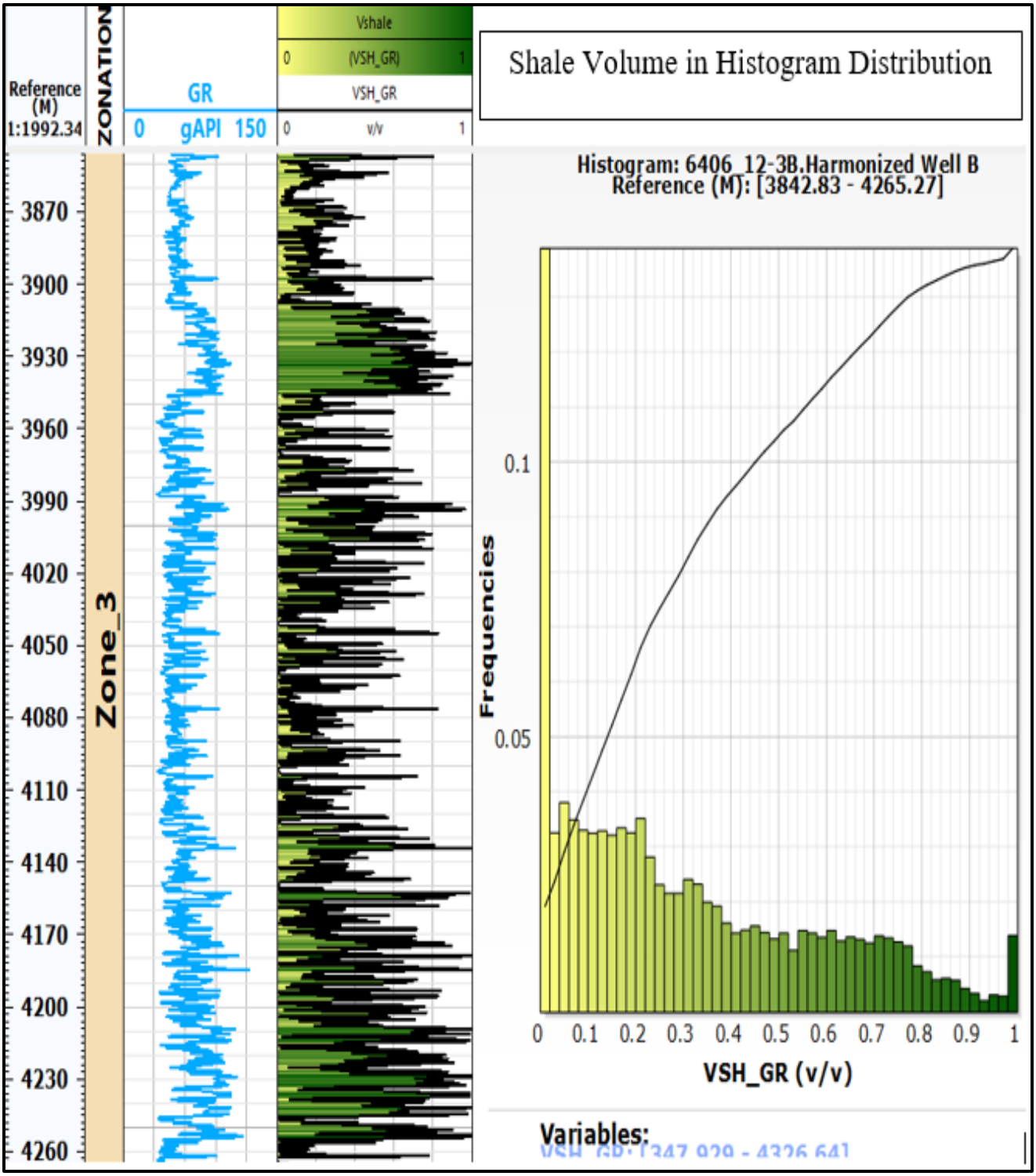

Figure 25: Shale volume of reservoir interval from 3844 to 4267 m of well 6406/12-3B

Well 6406/12-3 A: Shale Volume

The shale volume in the reservoir interval of this well is very low comparing to Intra-Melke sandstone formation of well 6406/12-3S and 3B. As shown in the Histogram and log plot ***Fig.26***

the maximum percentage of the shale volume distribution is less than 10% and the maximum concentration lies in the depth interval 4053-4059 m. The lower part of the reservoir has almost zero shale volume.

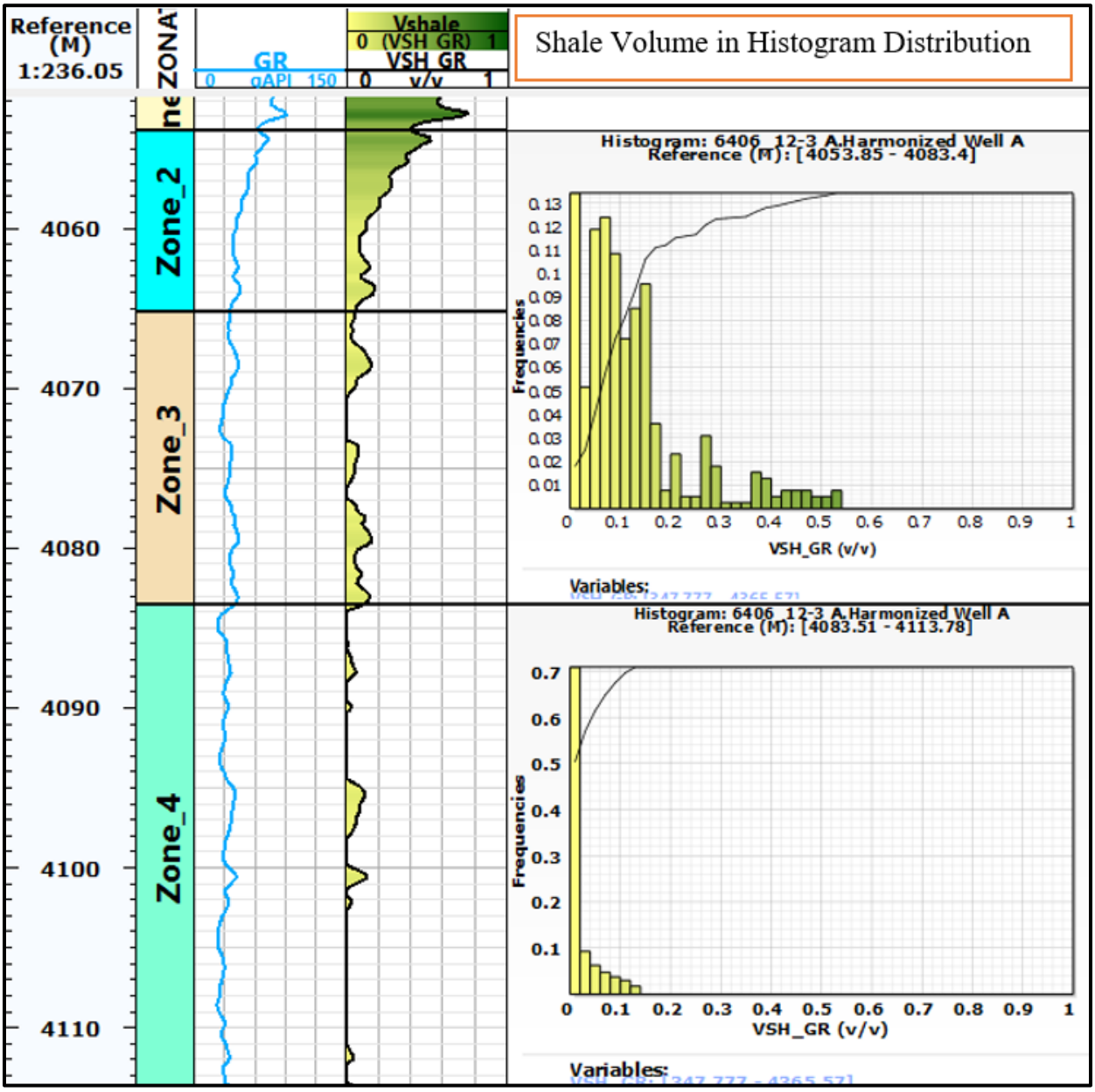

Figure 26: Shale volume of the reservoir interval of well 6406/12-3A

3.3 Fluid type and fluid contact determination

The fluid types and fluid contacts are determined and identified from logging responses in the three wells and wells 6406/12-3S and 6406/12-3B they are supported with formation pressure analysis results.

Well 6406/12-3S

The fluid types and fluid contacts from logging response of Density-Neutron separation and resistivity log of this well are given in ***Fig. 27*** and the detail zonation is given in ***Appendix A1***. The gas oil contact (GOC) was identified at depth of 3608 m and the Oil water contact (OWC) at 3745m. As shown in the figure, the gap between the density log and neutron porosity log in the gas zone is higher than the oil and water zone. In addition, the resistivity reading log response is higher especially in the depth interval of 3560-3608 m.

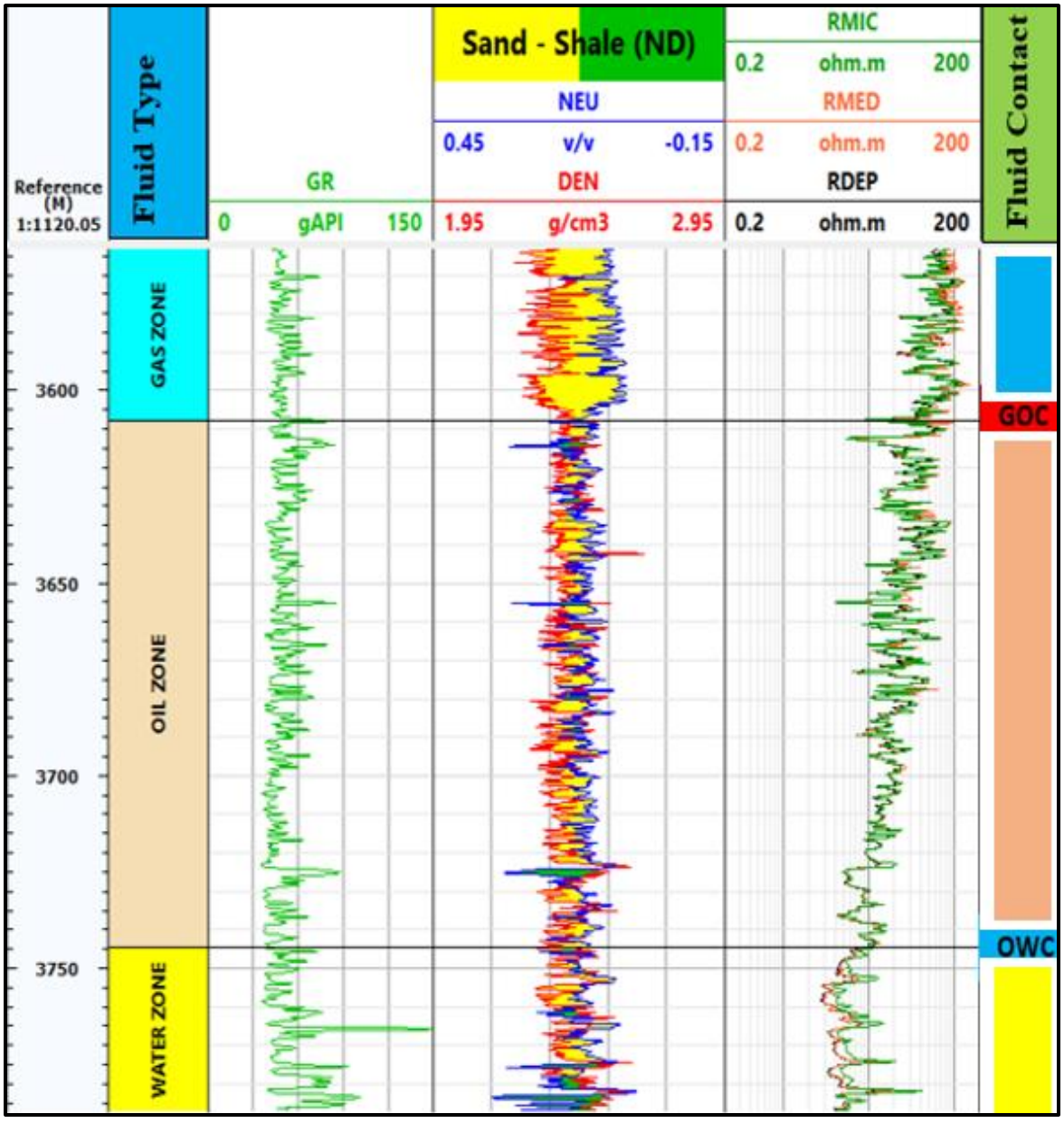

Figure 27: Fluid types and fluid contacts based on logging responses of well 6406/12-3S

In addition to logging responses, the fluid type and fluid contacts from pressure gradient analysis of depth intervals 3285.9-3539.3 m (TVD) or 3523.6-3777.04 m (measured depth) are given in ***Fig.28.*** From the given plot of true vertical depth versus formation pressure, density of fluids, pressure gradient is calculated as shown in ***Table 11.*** The regression coefficient (R^2) of the pressure trend lines is approximately one.

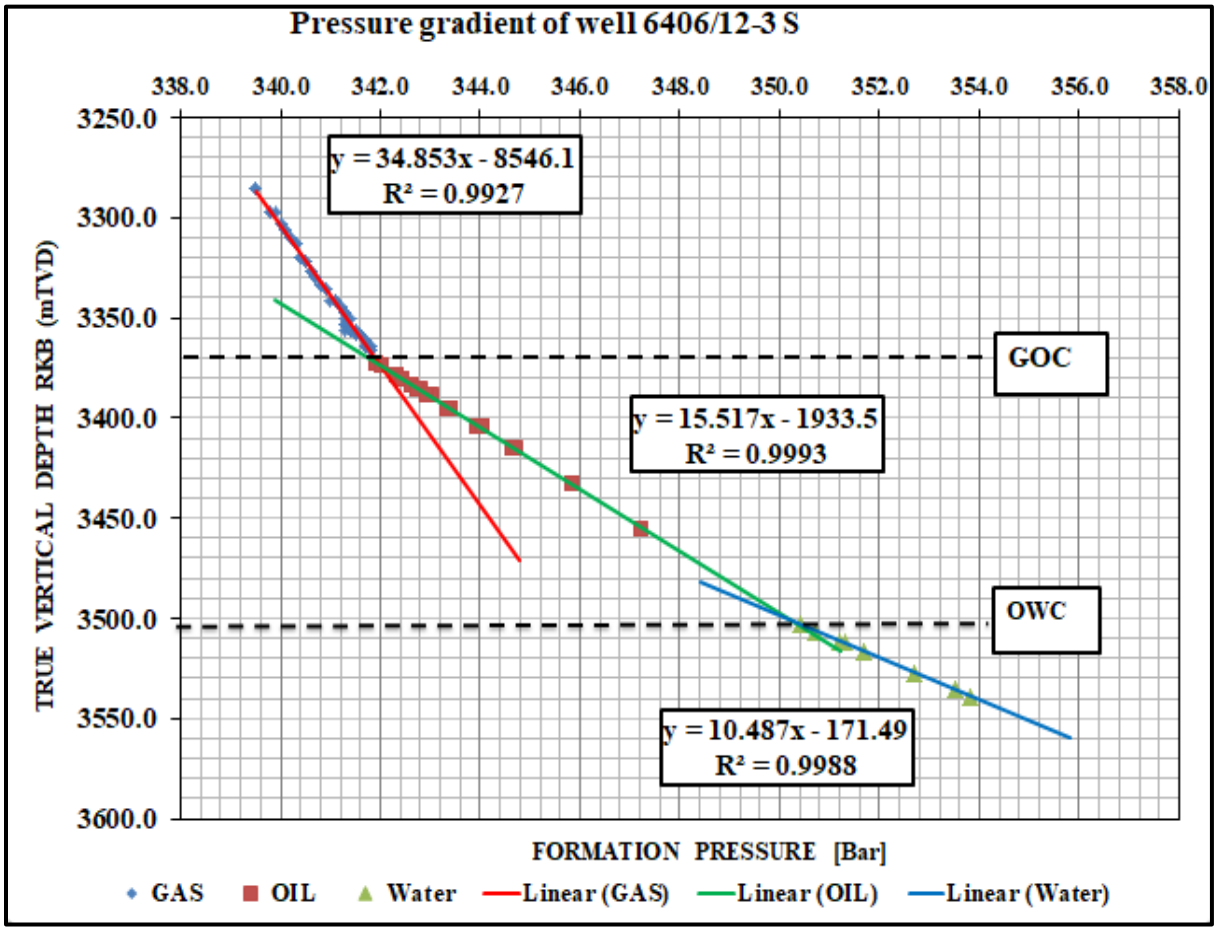

Figure 28: Fluid type and fluid contacts determination from formation pressure Vs TVD of Well 6406/12-3 S

The derived values of density (RHO) and pressure gradient from the plot are given in ***Table 11***. Based on the results three fluids are identified that confirms the results of the logging responses

Table 11: Computed values of pressure gradient, fluid density and identified fluid type of well 6406/12-3S

Depth Interval		dp/dz	dp/dz	1/g	RHO	RHO	Fluid type
M, MD RKB	M, TVD RKB	[bar/m]	[Pas/m]	[Kg/N]	[kg/m3]	[g/cc]	
3523.6-3603.57	3285.9-3365.9	0.0288	2880	0.102	293.6	0.294	Gas
3609.96-3692	3372.2-3454.3	0.064	6400	0.102	652.4	0.65	Oil
3740.49-3777.04	3502.7-3539.30	0.0955	9550	0.102	973.5	0.97	Water

Well 6406/12-3B: Fluid types and fluid contacts

Contacts from logging responses of Density-Neutron separation and resistivity log is given in ***Fig.29***.

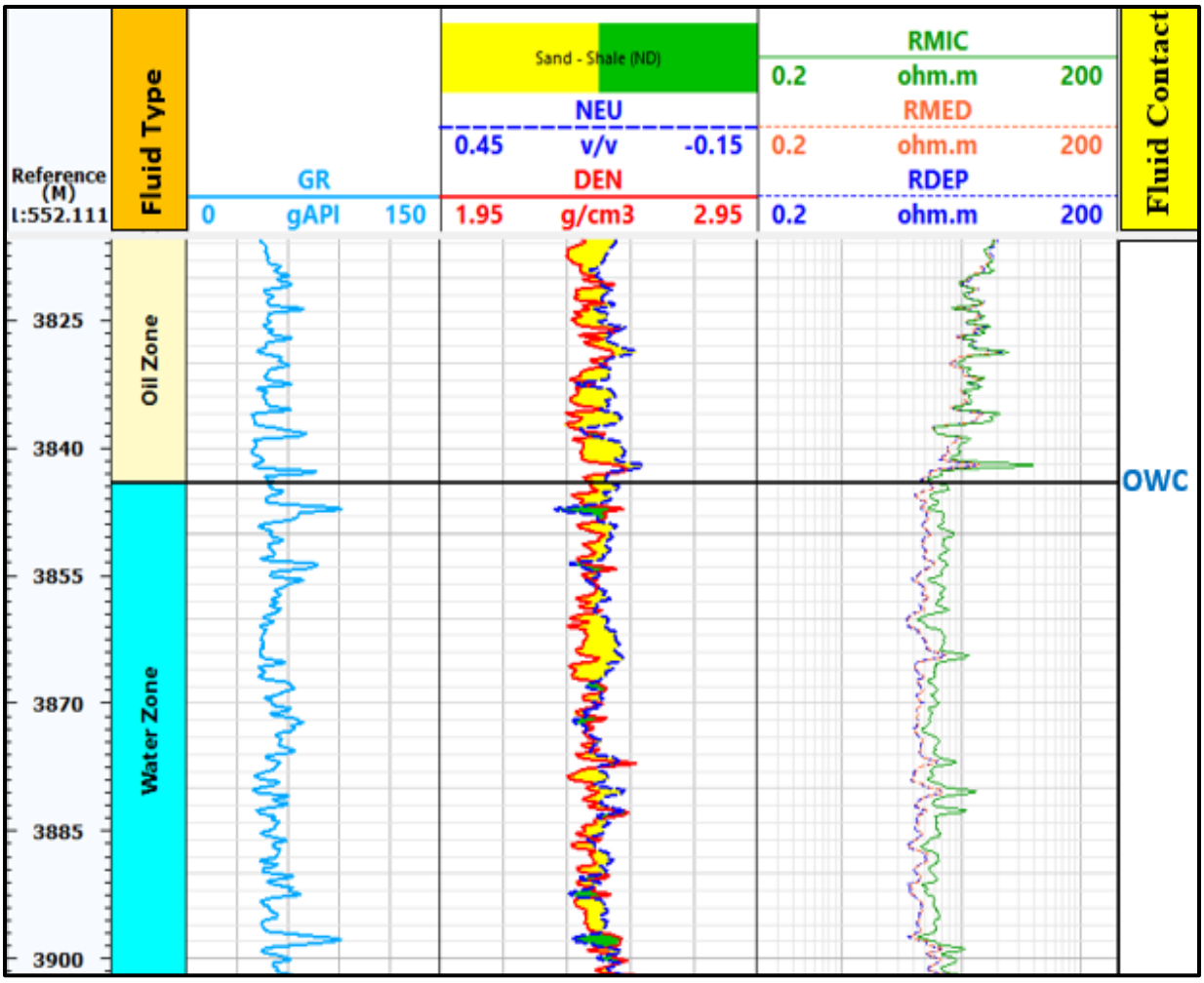

Figure 29: Fluid types and fluid contacts of well 6406/12-3B from logging response

Fluid types and fluid contacts from pressure gradient

Pressure gradient of the formation pressure data is given for depth interval of 3761.69-4035.19m (MD) or 3440.8- 3714 m (TVD) as shown in ***Fig.30***, and the identification of the fluid types, contacts and density fluid calculation is done based on these data points. The calculated density of fluids, the pressure gradient and identified type of fluids are summarized in ***Table 12.*** The intersection of the pressure trend line is the depth of the fluid contacts. The regression coefficient (R^2) is approximately one in the three pressure trend lines, which shows perfect matching (fitting) of the data points. The fluid contacts are identified at 3806 m [MD] (3485 m, TVD), and 3849 m, MD (3528 m, TVD).

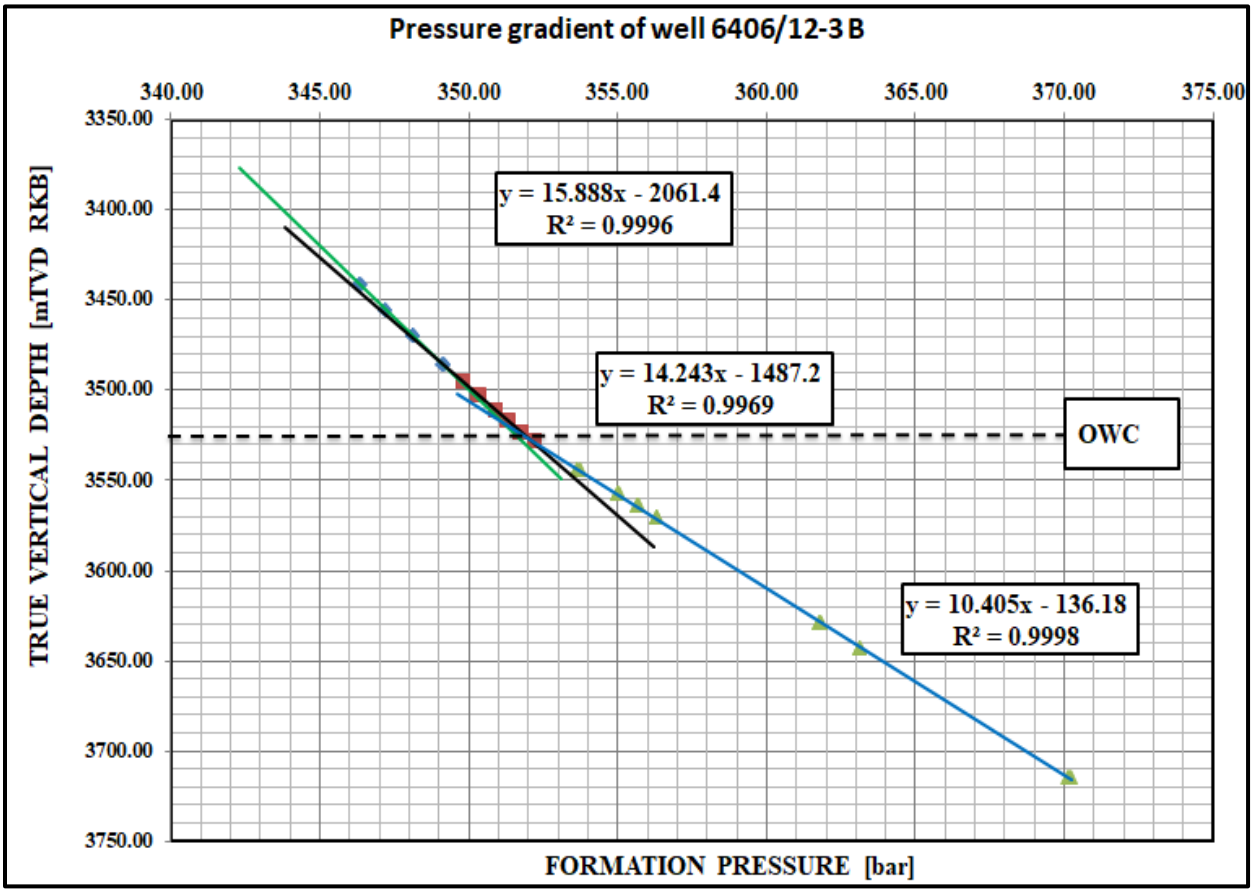

Figure 30: Fluid type and fluid contacts determination from formation pressure Vs TVD of well 6406/12-3B

The fluid densities calculated from the pressure gradient of the data points are given in ***table 12*** and the depth intervals are given in measured depth and true vertical depth.

Table 12: Computed values of pressure gradient, fluid densities and fluid types of well 6406/12-3B

Depth Interval		dp/dz	dp/dz	1/g	RHO	RHO	Fluid
M, MD	M, TVD	[bar/m]	[Pas/m]	[Kg/N]	[kg/m3]	[g/cc]	type
3761.69 -3806	3440.8 -3485.1	0.0635	6350	0.102	647.3	0.65	Light Oil
3815.40 -3849.2	3494.5 -3528.3	0.0696	6960	0.102	709.5	0.71	Oil
3863.99 -4035.2	3543.1 -3714	0.0957	9570	0.102	975.5	0.98	Water

Well 6406/12-3 A: Fluid Types and Fluid contacts

The fluid type and fluid contact of this well is given only from logging response as shown in ***Fig.31***. No gas was identified in the reservoir and the reservoir contains oil and water only. Therefore, the only contact will be the oil water contact.

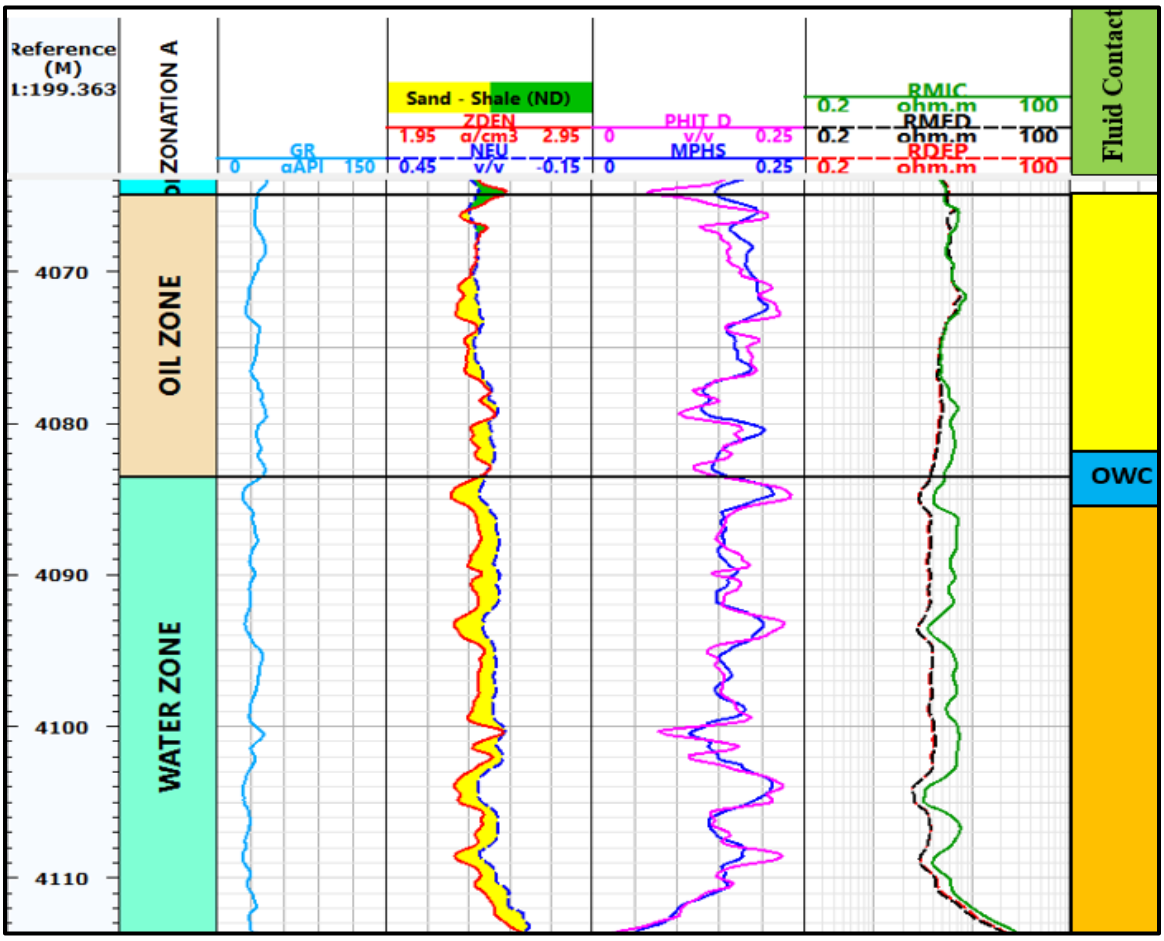

Figure 31: Fluid types and fluid contacts of well 6406/12-3A from logging responses

The summary of the fluid contacts in terms of measured depth and true vertical depth [TVD] of the three wells are given in ***Table 13.***

Table 13: Summary of fluid contacts from logging response and pressure gradient

Well	**Fluid contacts from logging response**				Contacts from pressure gradient			
	GOC		OWC		GOC		OWC	
	MD	TVD	MD	TVD	MD	TVD	MD	TVD
6406/12-3S	3608	3370	3745	3504	3607	3370	3740	3502
6406/12-3B	No gas		3843	3521/22	No gas		3849	3528
6406/12-3A	No gas		4083	3444	No gas		-	-

3.4 Porosity comparisons

The estimated Porosity comparisons of each well are given in terms of log plots and summarized tables of the average values. For simplicity and clear understanding of the porosity differences in the gas zone, oil zone and water zone, it is given in separate plots for each well.

Well 6406/12-3 S

The porosity comparison of this well involves comparing the results of the estimated Density log total porosity, DMRP, effective porosity and PHIT_D_gradient, and the given core porosity for each fluid types of the reservoir section.

Comparison of porosities in the gas zone:

Fig.32, 33 and ***34*** of track 3 shows the comparison of the estimated total density porosity using the density of fluid 1 g/cc, and density of matrix 2.65 g/cc (PHIT_D), the gas corrected Density-Magnetic Resonance porosity (DMRP), Core porosity (Core_PHI), and the NMR porosity given in the log suite (TCMR/MPHS) of the gas zone.

Track 4 shows the comparison of DMRP and the total density porosity (PHIT_D_gradient) calculated using the fluid density from the pressure gradient analysis (0.29 g/cc for gas zone, 0.65 g/cc for oil zone and 1 g/cc for water zone) keeping the same the matrix density (2.65g/cc). As shown in the plot, the PHIT_D_gradient porosity is lower in the gas zone and it has better much with DMRP values comparing to PHIT_D as could be expected.

Track 5 also shows the effective density porosity (PHIE_D) calculated using ***equation [9]*** taking the density of the fluid 1 g/cc and density of matrix 2.65 g/cc.

The density porosity and DMRP they are low in the depth intervals of high gamma ray and this decrease in porosity is not much observed in the nuclear magnetic resonance (MPHS).

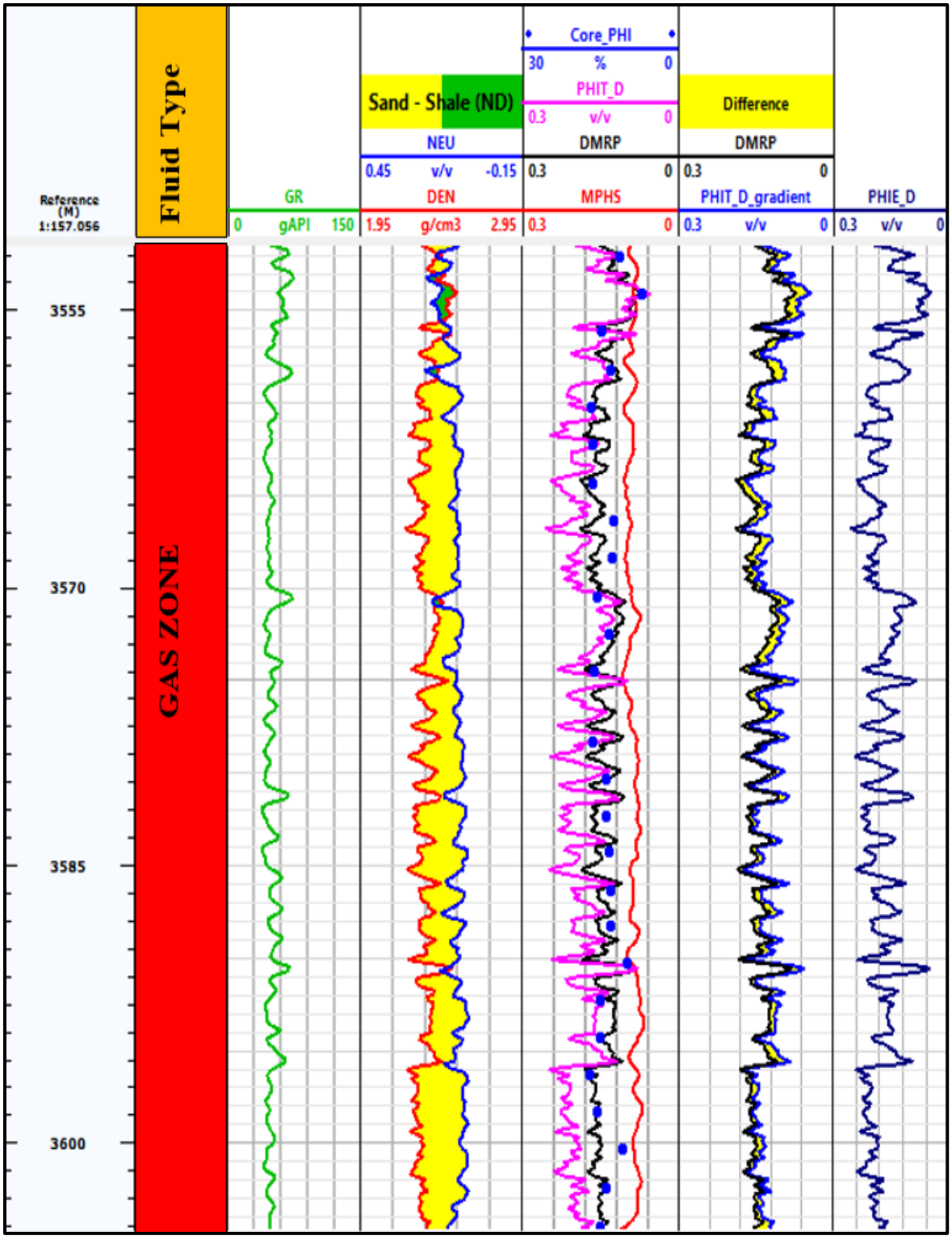

Figure 32: Porosity Comparisons in the gas zone of well 6406/12-3S

Comparison of porosities in the oil zone:

The response of the above porosity types in the oil zone are given in ***Fig.33*** and as shown in the figure the gap between the density porosity and DMRP reduces and in some depth intervals, they overlay to each other.

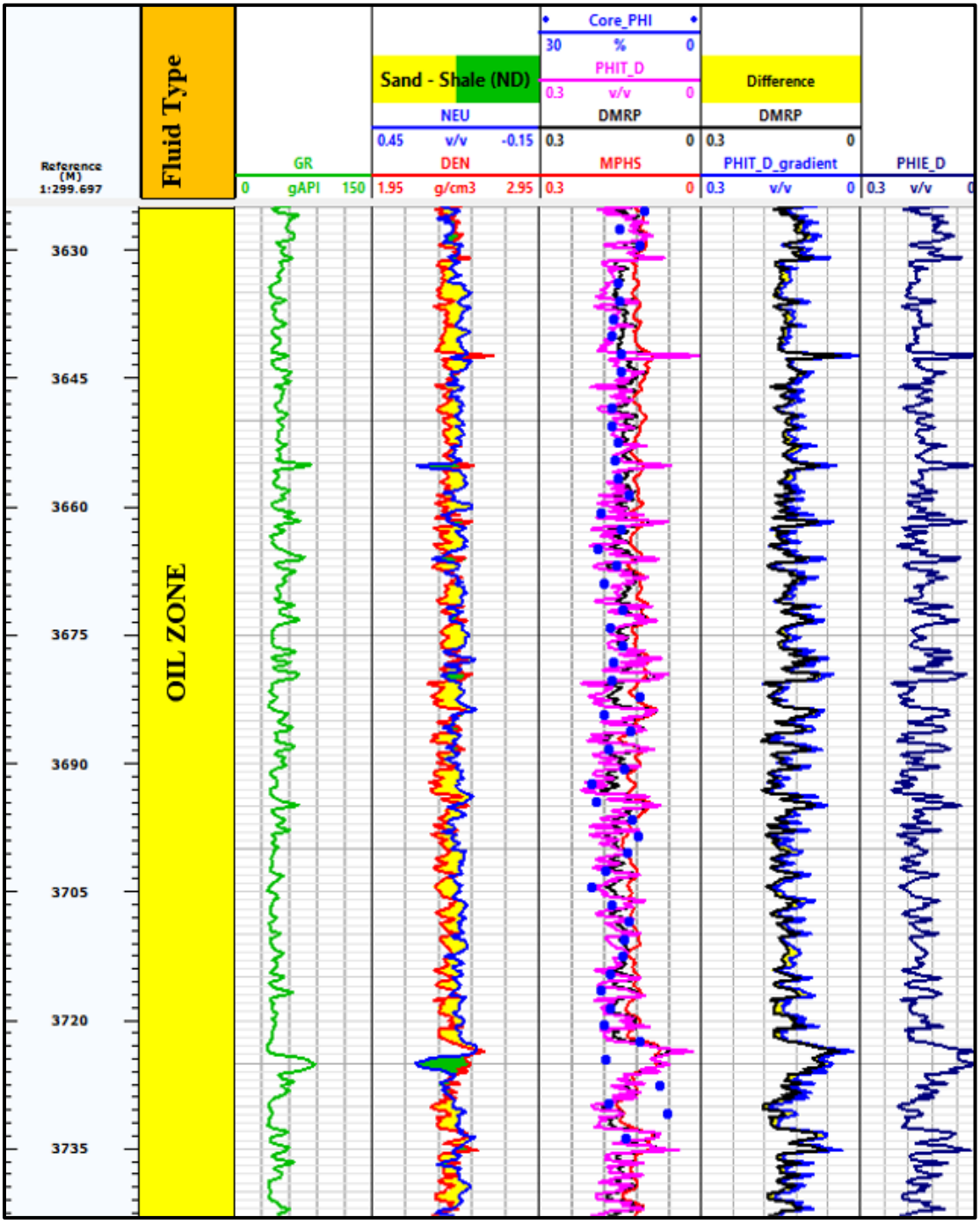

Figure 33: Comparison of DMRP, PHIT_D and PHIT_from pressure gradient porosities of the oil zone of well 6406/12-3S

Comparison of porosities in the Water Zone:

In the water bearing depth interval, core porosity is not available but the other porosity types are given in ***Fig.34.*** As shown in the figure, the gap between the porosities decrease further comparing to the oil zone and almost all they overlap to each other. The porosity distribution of all the porosity types in the top part of the water zone gives high porosity value but from 3773-3806 m gives lower value that reaches up to zero. However, there are missing data of NMR porosity from 3806-3836 m, density porosity from 3822-3836 m, and DMRP is missing from 3806- 3836 since it is derived from NMR and density porosities.

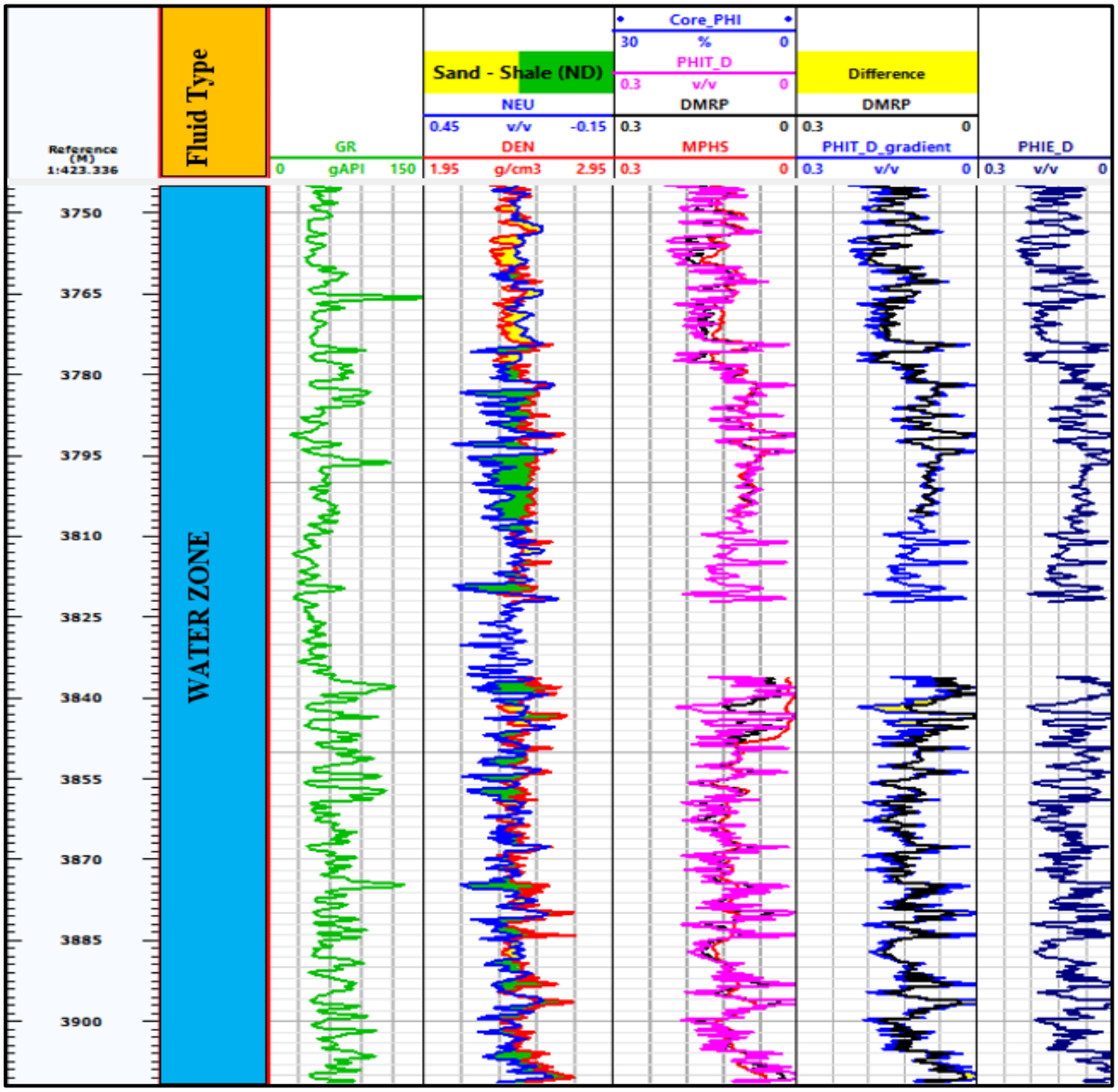

Figure 34: Comparison of DMRP, PHIT_D and MPHS in the water zone of well 6406/12-3S

The minimum, maximum and average estimated porosities including the shale volume in the reservoir intervals of this well are summarized in ***Table 13***.

Table 14: Summary of computed porosities in the reservoir interval of well 6406/12-3S

Depth [m]	PHIT_D [%]			MPHS [%]			Vsh [%]			PHIE_D [%]		
	Min	Max	Ave	Min	Max	Ave	Min	Max	Ave	Min	Max	Ave.
3514-3516	2	14	5	5	12	7	16	85	55	0	0.06	**0.02**
3517-3608	3	25	17	6	13	9	0	51	13	3	23	16
3609-3745	0	22	15	7	16	12	0	46	9	4	20	14
3746-3912	0	21	11	0	16	9	0	100	20	0	21	9

Depth Interval	DMRP [%]			Core_PHI [%]			
	Min	Max	Ave	Cored depth, [m]	Min	Max	Ave
3514-3516	0	0.06	0.02				
3517-3608	3	23	16	3524-3607.9	4.5	20	14
3609-3745	4	20	14	3610-3732	7.7	20	15
3746-3912	0	21	9	**…….No core data…….**			

Well 6406/12-3 B

The comparison of porosity in this well includes core porosity, density porosity and NMR porosity. Since there is no gas cap (gas bearing) depth interval, the DMRP porosity is not included. The NMR porosity responds consistently in the depth interval but the density porosity responds in alternate high and low values of zigzag response and the reason is going to be discussed in the next chapter.

The porosity display given in track three shows the comparison of core porosity, NMR porosity and density porosity. As shown in the figure the core porosity has best much with density porosity and the NMR porosity has higher values in the depth intervals of high gamma ray reading and positive Density-Neutron separation. For example in the depth interval 3767-3769 m of ***Fig.35*** the NMR porosity reads 12 % and the density porosity reads 6 % which is 6 % difference between them.

Porosity Comparison in the oil zone:

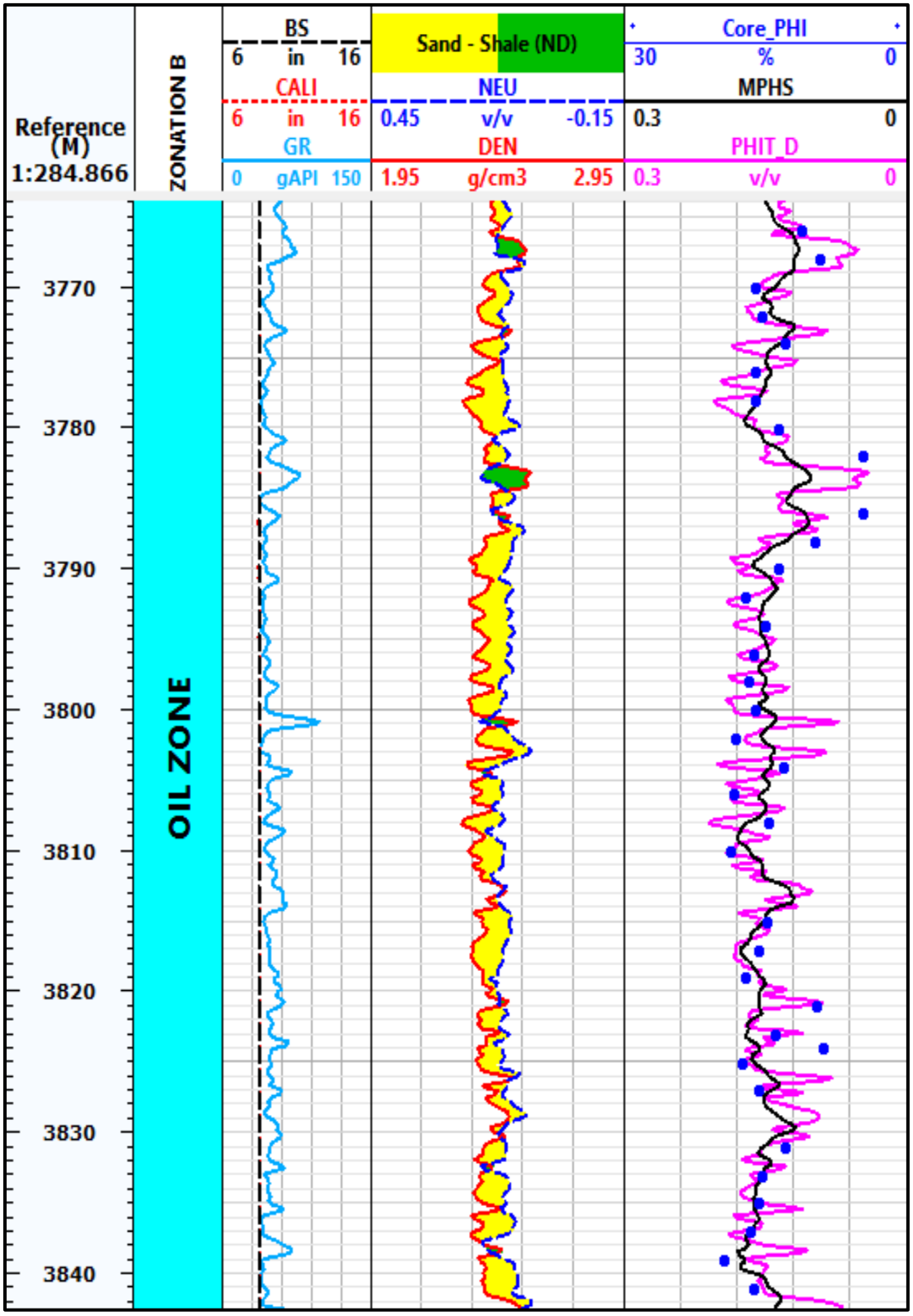

Figure 35: Comparison of PHIT_D and MPHS porosities in the oil zone of well 6406/12-3B

Porosity comparison in the water zone of well B:

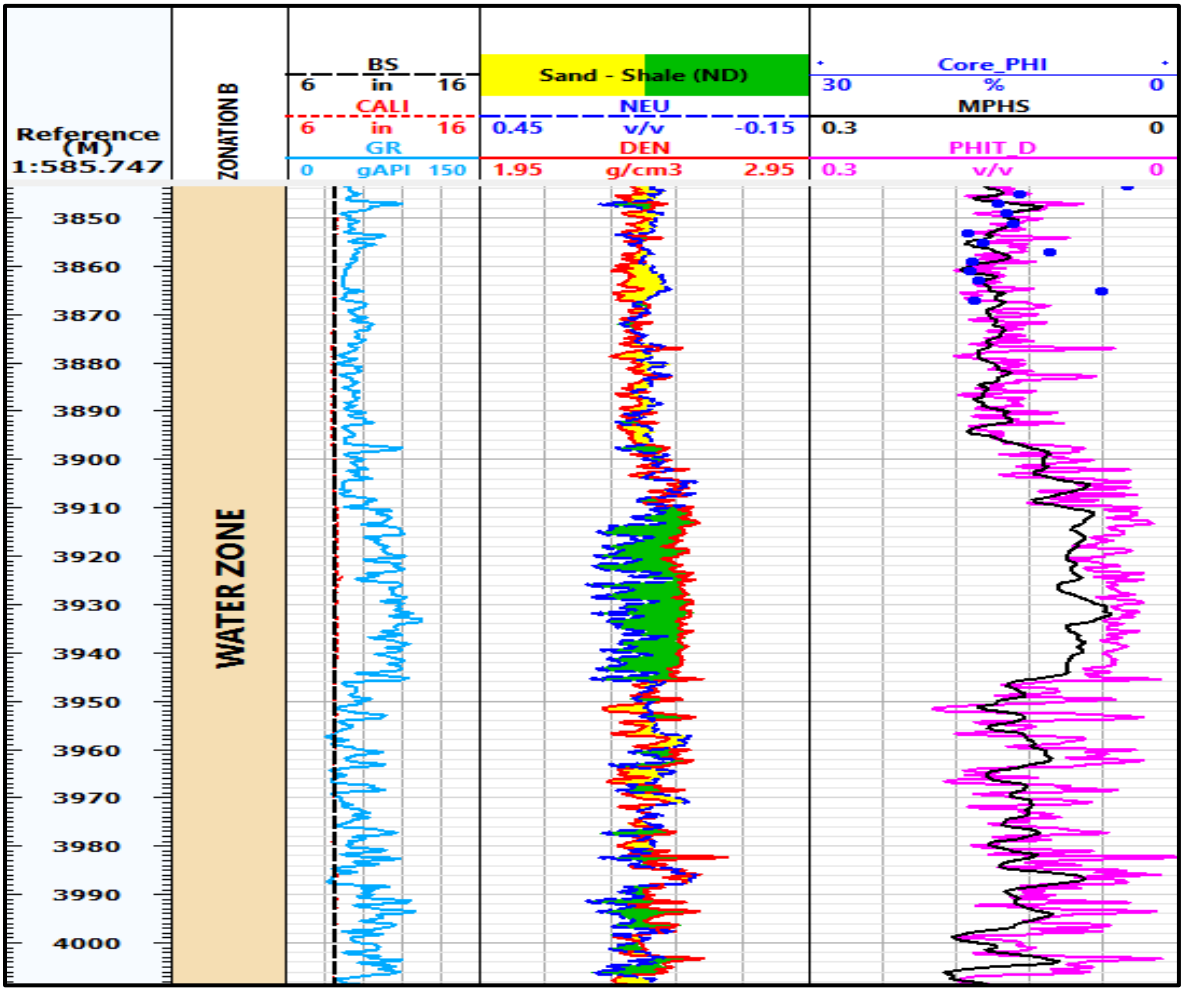

Figure 36: Comparison of PHIT_D and MPHS porosities in the water zone of well 6406/12-3B

The minimum value, maximum value and average porosity responses in the reservoir depth interval of well B is summarized as follow:

Table 15: Summary of computed porosities in the reservoir interval of well 6406/12-3B

Depth Interval [m]	**PHIT_D[%]**			**MPHS [%]**			**Vsh [%]**			**PHIE_D [%]**		
	Min	Max	Ave.	Min	Max	Ave.	Min	Max	Ave	Min	Max	Ave.
3761-3844	5	19.4	14.5	10.3	17.5	14.7	0	52.3	14.5	1.3	19	13.2
3844-4264	0	19.3	9.3	4.3	18.6	11.4	0	96	31	0	19.4	6.7

Cored depth [m]	Core_PHI [%]		
	Min	Max	Ave.
3728 – 3867	4.1	19.3	**13**

Well 6406/12-3 A:

In this well, since no gas cap is identified the DMR porosity is not included but the NMR porosity (MPHS/TCMR) has good match with the calculated density porosity as shown in ***Fig. 37*** of the reservoir interval of the well. However, in the top part of the reservoir the density porosity is higher and the gap between them decreases towards the lower part of the reservoir best fit in the water zone.

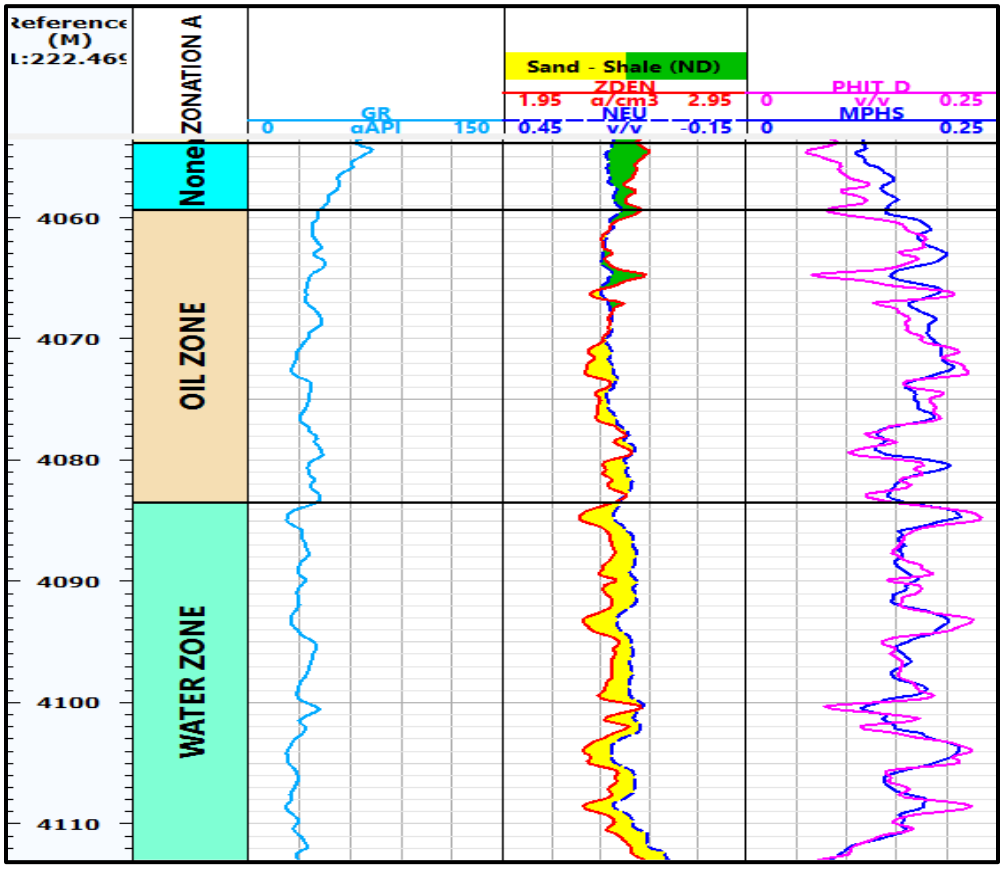

Figure 37: Comparison of PHIT_D and MPHS porosities in the reservoir interval of Well 6406/12-3A

Table 16: Summary of computed porosities in the reservoir interval of well 6406/12-3A

Depth Interval [m]	PHIT_D [%]			MPHS [%]			Vsh [%]			PHIE_D [%]		
	Min	Max	Ave	Min	Max	Ave.	Min	Max	Ave	Min	Max	Ave.
4053-4059	6.5	11.4	9	11	15	14	12	72	33	1.3	12	8
4059-4065	10	17.2	15	15	19	17.5	5	15	11	7	19	15
4065-4083	12	22	17	13.5	20	17	0	15	7	10	23	17
4083-4114	4	23	15.4	6	21	15	0	95	5	0	24	16

3.5. Water saturation

Well 6406/12-3 S: Comparison of Archie, Indonesia and Simandoux water saturations

The water saturation is given for the reservoir interval of the well and for clear display of the log readings; it is given in three zones (gas zone, oil zone and water zone) as shown in ***Fig.38***, ***39*** and ***40.***

Track 2- shows Sw comparisons using the Rw obtained from the Archie method i.e. using Rw=0.1

Track 3-shows the comparison of Sw generated from the temperature corrected formation water resistivity where the Rw is variable in the depth intervals (Sw_T corrected) and Sw_AR.

Track 4- shows the comparison of the temperature corrected Rw based Archie, Indonesia and Simandoux Sw

In the gas zone**,** the top part with high shale volume interval from 3516-3555 m the water saturation is higher comparing to the lower part of 3556-3608 m. It starts to rise in the oil zone starting from 3615 and continues increasing in the bottom section of this zone. As shown in the plots the Indonesian and Simandoux Sw**,** they almost overly to each other and their difference are very small. Generally, the Sw values generated from the temperature corrected Rw are lower than the values generated from Rw =0.1.

The summarized average water saturations of the three models in the depth interval of the reservoir section are given in ***Table 17*****.**

Comparison of water saturations in the gas zone:

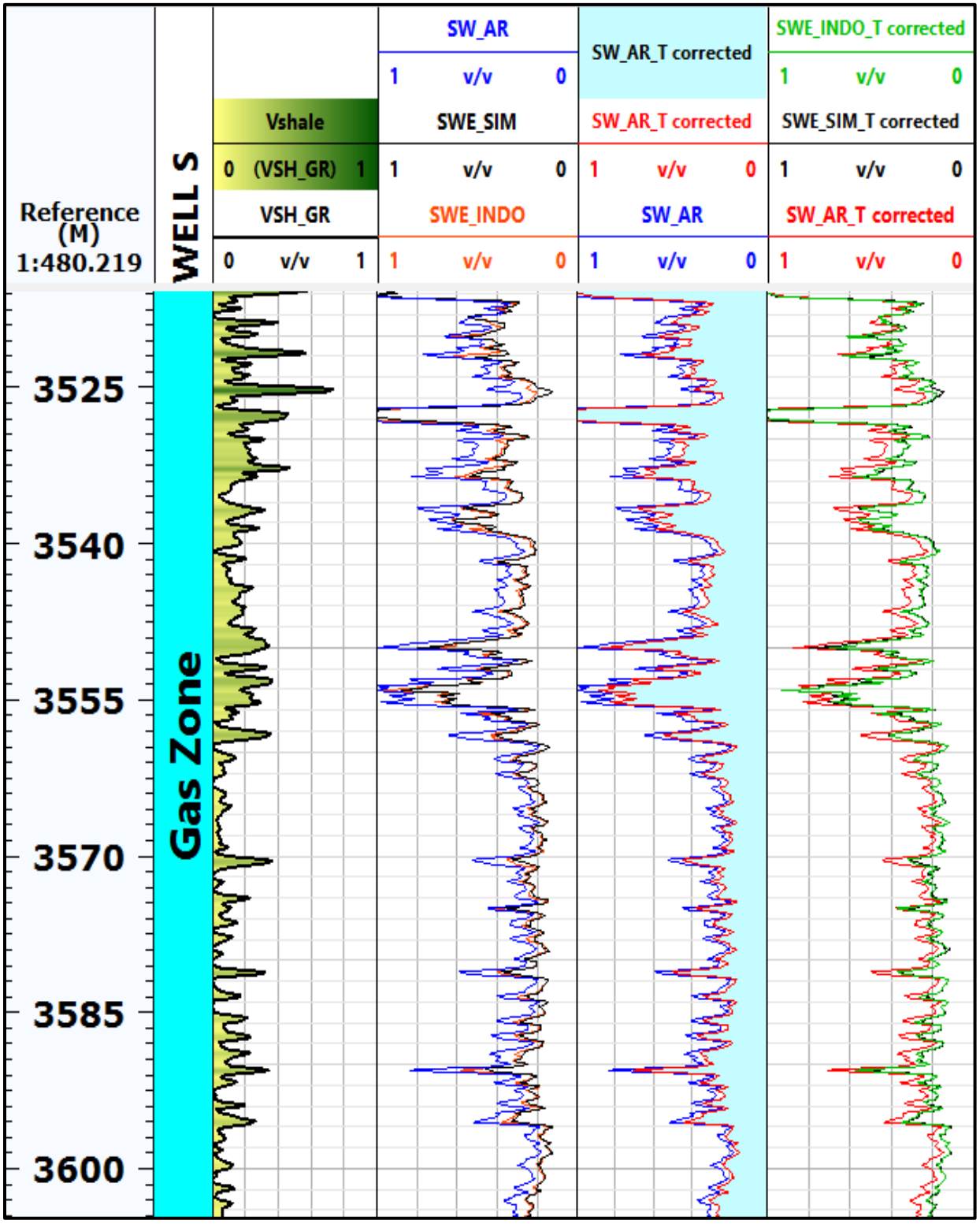

Figure 38: Water saturation (Archie, Indonesia and Simandoux) in the gas zone of well 6406/12-3S

Oil Zone water saturation comparisons:

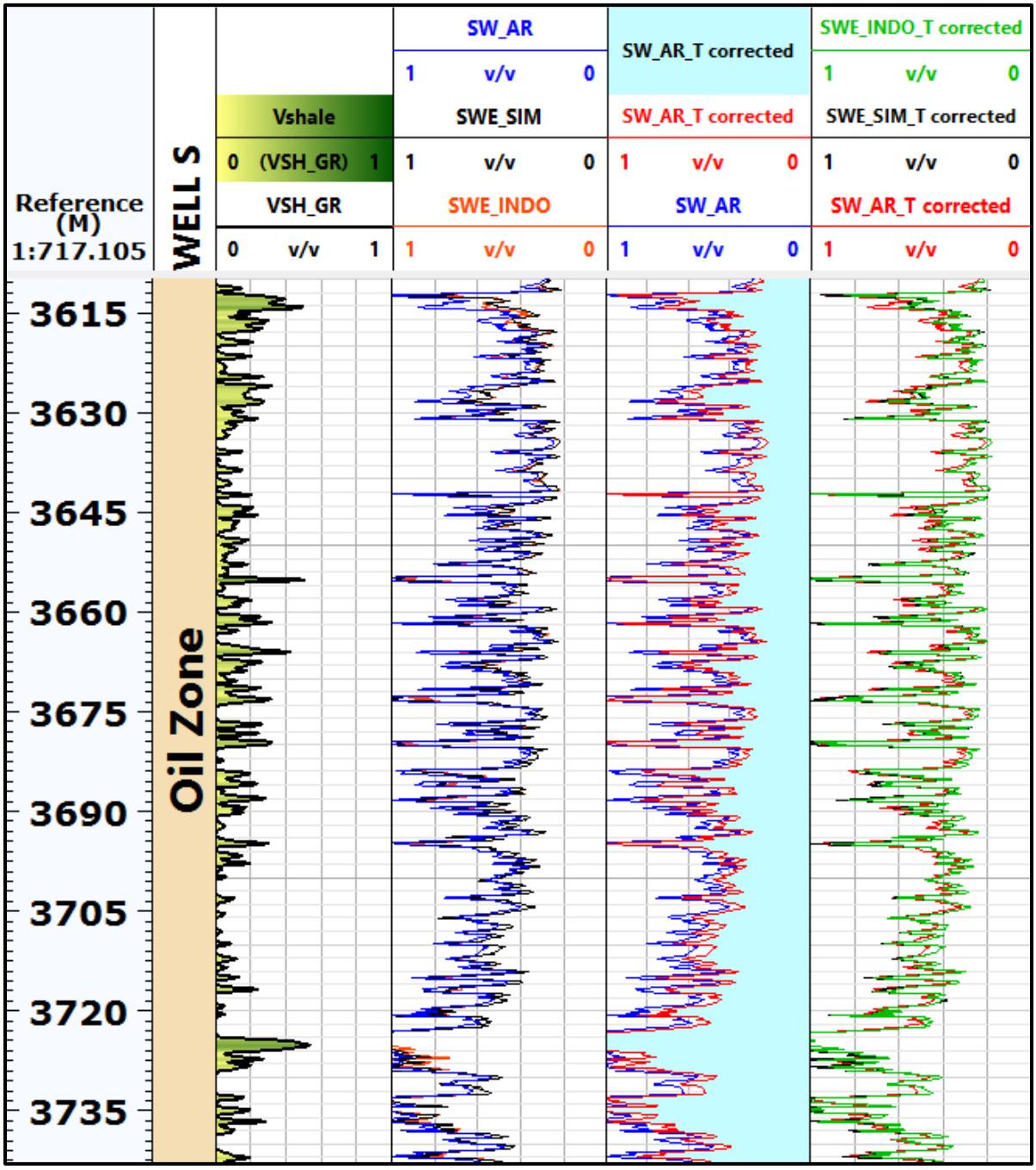

Figure 39: Water Saturation in the oil zone of well 6406/12-3S

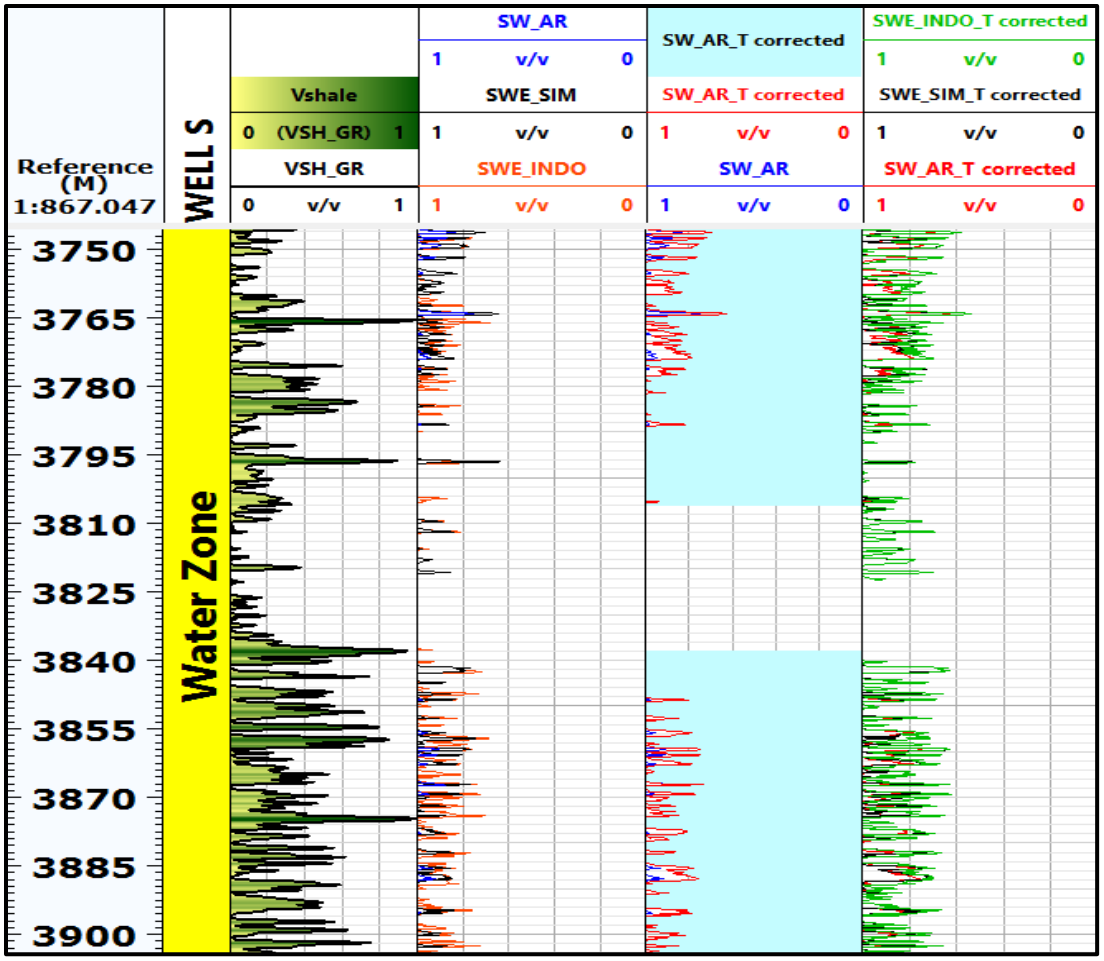

Figure 40: comparison of water Saturation in the water zone of 6406/12-3S

The average water saturations in the reservoir interval of both the Rw=1 derived and variable Rw (Temperature corrected, SW_T) derived values including the average shale volume in the interval are summarized in ***Table 17***.

Table 17: Summary of computed average water saturations in the reservoir interval of well 6406/12-3S

Depth Interval [m]	**Vsh [v/v]**	**SW using Rw= 0.1 [v/v]**			**Sw_T_Corrected [v/v]**		
		AR	INDO	SIM	AR	INDO	SIM
3514-3516	0.55	0.94	0.93	0.92	0.92	0.92	0.92
3517-3608	0.13	0.4	0.31	0.29	0.34	0.28	0.27
3609-3745	0.09	0.58	0.52	0.52	0.5	0.45	0.46
3746-3912	0.2	0.99	0.95	0.98	0.96	0.9	0.93

Well 6406/12-3B

Track 3 of this well shows the comparison of water saturations estimated based on the formation water resistivity derived from the apparent formation water resistivity in the clean sand water zone. As shown in the figure the Archie Sw is higher than both Indonesia and Simandoux Sw throughout the reservoir. The Sw values of Indonesian and Simandoux models are almost overlaid to each other in the oil zone and in the water zone they give similar values with Archie model. In the depth interval of 3761-3819 m the average value of water saturation lies in the 40% but from 3820 m the water saturation starts to increase to an average value of more than 60 % and finally reaches 100 % at 3843 m.

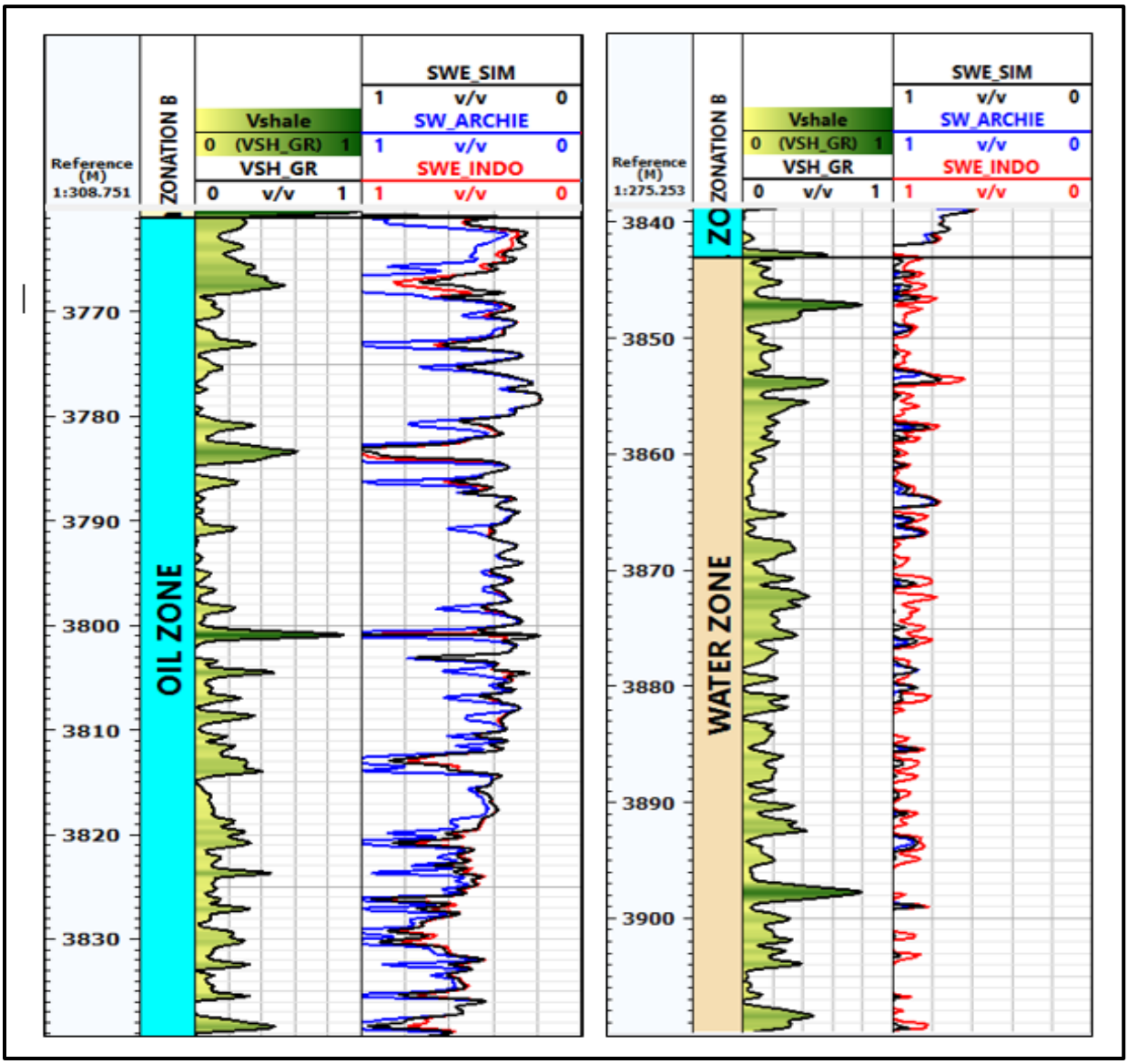

Figure 41: Comparison of water saturation in the oil zone and water zone of well 6406/12-3B

Table 18: Summary of computed water saturations in the reservoir interval of well 6406/12-3B

Depth Interval	Ave. Vsh	Ave. Sw_AR	Ave.Swe_INDO	Ave.Swe_SIM
m	v/v	v/v	v/v	v/v
3761-3844	0.15	0.59	0.494	0.492
3844-4264	0.32	0.98	0.93	0.91

Well 6406/12-3A: Water saturation

The water saturation in the oil zone of the three models is very high where the maximum percentage lies above 75 %. The shaly-sand models (Indonesia and Simandoux) do not have much difference with Archie results as shown in ***Fig.42*****.** The summarized values of the average Sw of the three models in the reservoir interval of this well is given in ***Table 19.*** As shown in the table and figure the water saturation in the oil zone gives suspiciously high but there is no problem with the input parameters. Therefore, the result is taken as reasonable value in this well.

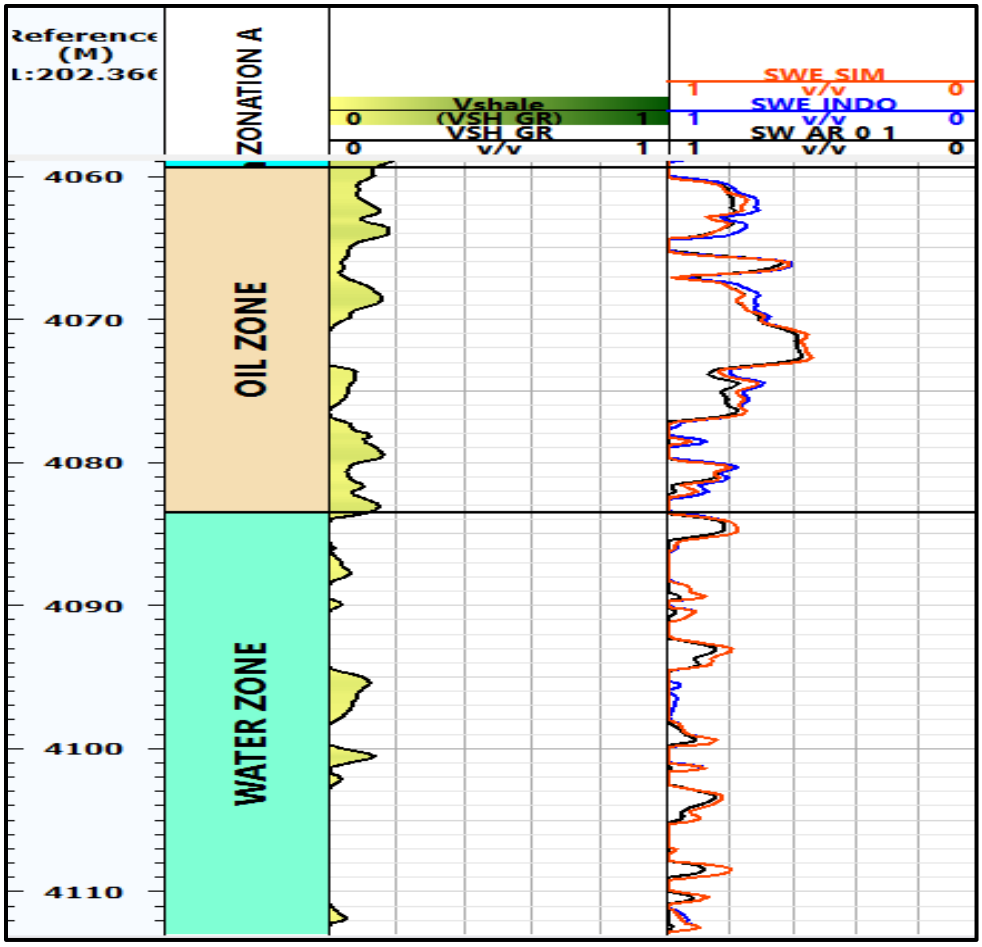

Figure 42: Comparison of water saturation in the oil zone and water zone of well 6406/12-3A

Table 19: Summary of computed water saturations in the reservoir interval of well 6406/12-3A

Depth Interval	Ave. Vsh	Ave. Sw_AR	Ave. Swe_INDO	Ave. Sw_SIM
M	v/v	v/v	v/v	v/v
4053-4059	0.33	1	0.99	1
4060-4065	0.11	0.85	0.82	0.85
4066-4083	0.07	0.82	0.79	0.81
4084-4114	0.05	0.97	0.94	0.94

3.6. Permeability and Porosity-Permeability relationship

Well 6406/12-3S

The permeability calculation across the reservoir section of this well is given in track 3 of ***Fig.43.***

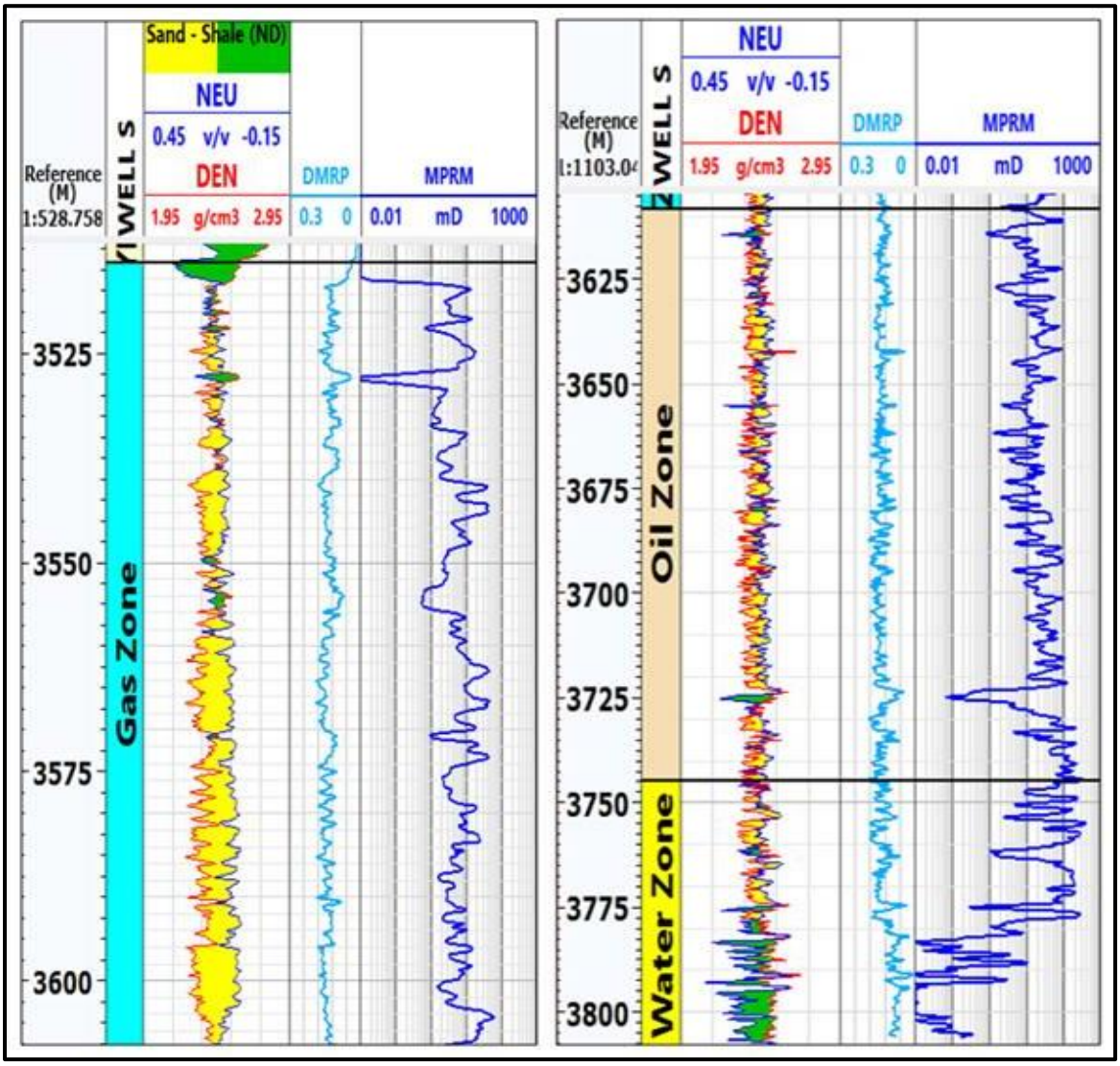

Figure 43: Permeability distribution in well 6406/12-3S

As shown in the figure above, the permeability is high in the depth intervals with high porosity. The logarithmic reading steps of the vertical grid lines are 0.01, 1, 10, 100, and 1000. In the gas zone, the permeability is very low comparing to oil zone and water zone, where maximum of the values lie below 10 mD. However, in the oil zone and water then the maximum reading of the permeability values lie below 40 mD.

Porosity-Permeability relationship

In addition to the NMR Permeability, permeability equation is generated from core data values of porosity-permeability relationship. The Porosity- Permeability relationship (PoroPerm cross plot) of this well in a depth interval of 3524.05-3732.35 m is given in ***Fig.44***. The relationship shows linear regression of Klinkenberg gas corrected permeability given in the Y-axis in a logarithmic scale and the core porosity in the X-axis with linear scale. The regression equation developed from the relationship is given as:

$$\text{Log k} = 0.2543347 * \text{Core Porsity} - 2.132018$$

The regression coefficient (R^2) which is the matching of the data points of this relationship, gives 0.82. As shown in the figure the crowd of points with high porosity has high permeability.

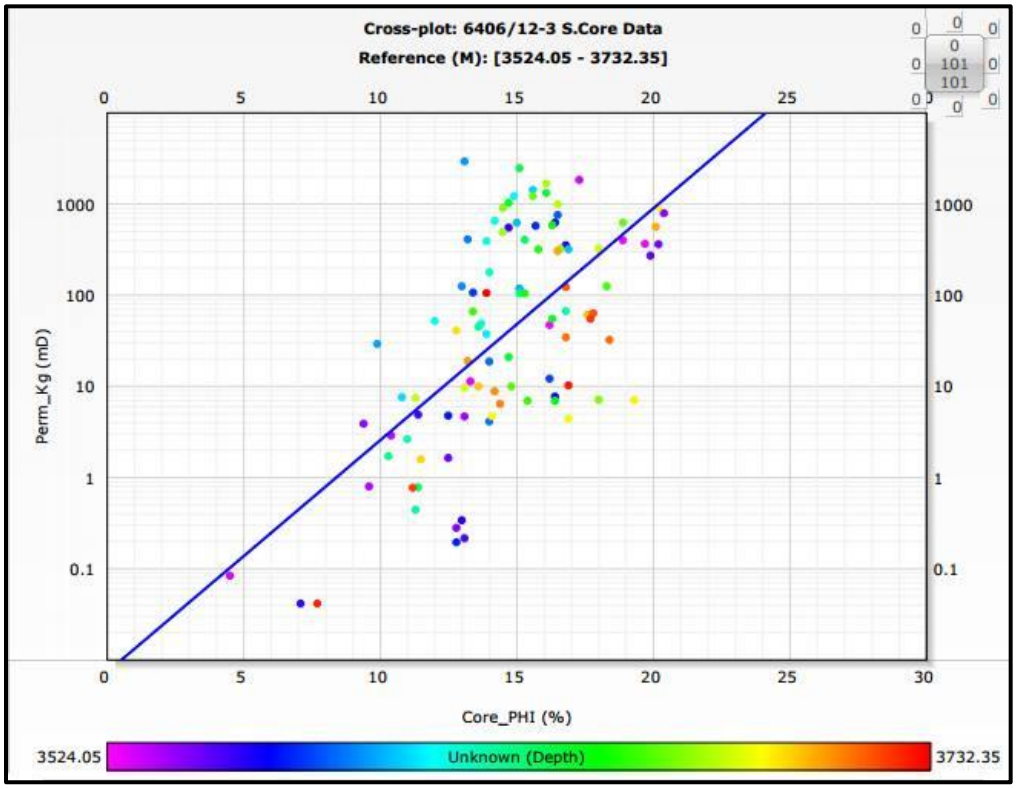

Figure 44: PoroPerm relationship of core permeability and core porosity of well 6406/12-3S

Well 6406/12-3B:

The Permeability distribution in this well is given in track 3 of ***Fig.45*** and as shown in the figure the permeability in the depth intervals of 3761-3843m (oil zone) and 3844 till the end (water zone) gives higher value comparing to permeability distribution of well S. However, shale containing depth intervals have low permeability that reaches up to zero for example in depth interval 3922-3945 m and from 4125 till the end. In zones of high porosity the permeability is high and in zones of low porosity the permeability is low.

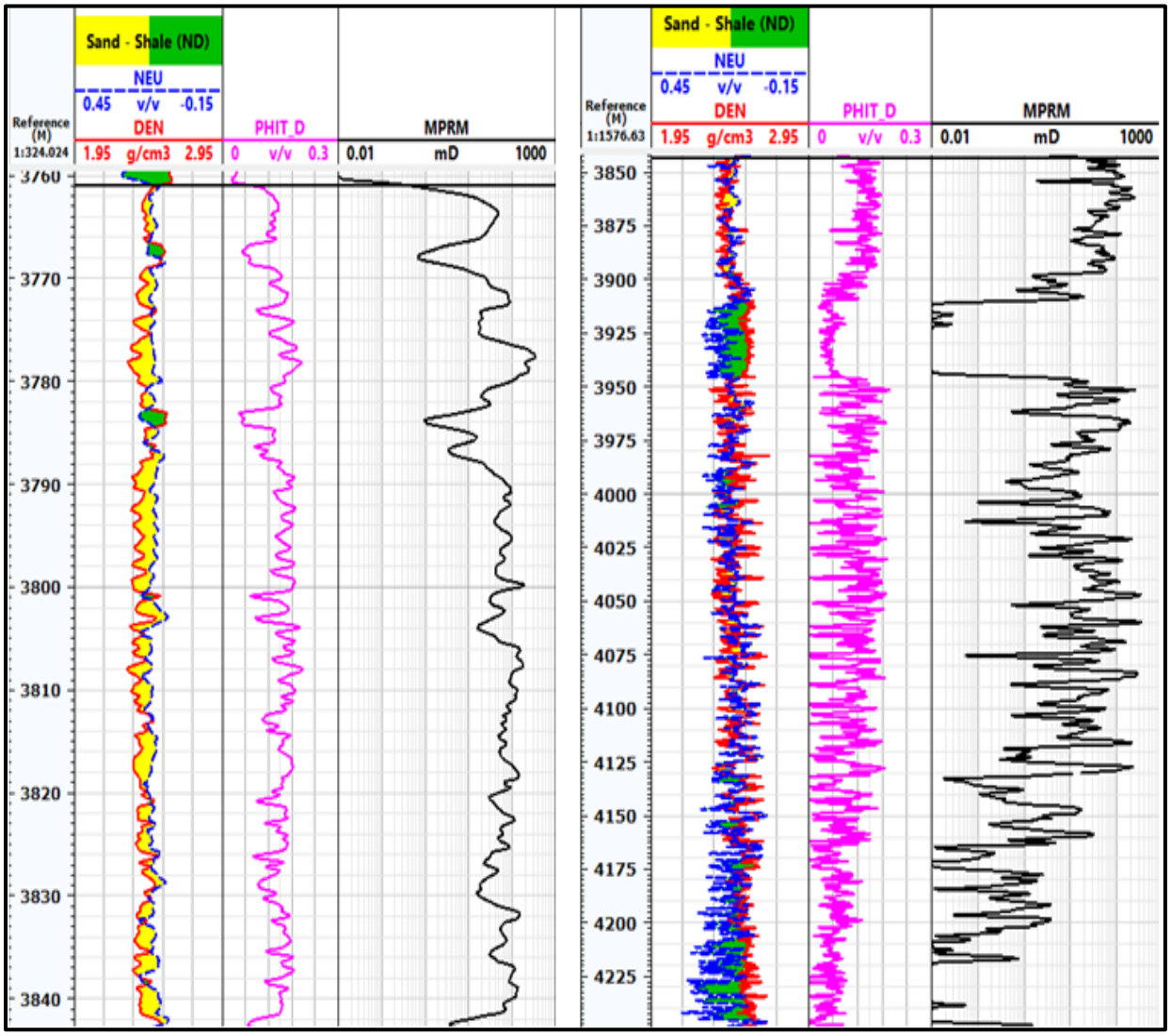

Figure 45: Permeability Distribution in well 6406/12-3B

Porosity-Permeability relationship:

The relationship in this well is done in the depth interval of the reservoir section from 3728.08 to 3867.1 m as shown in ***Fig.46.*** The depth intervals with lowest porosity 5-10 % the permeability

lies below 1 mD and the depth intervals with high porosity have high permeability that reaches greater than 700 mD. The regression equation of this well is given as:

$$\text{Log k} = 0.3709482 * \text{Core Porsity} - 4.110014$$

The regression coefficient (R^2) of the data points is given as 0.8421, which is better match than well S.

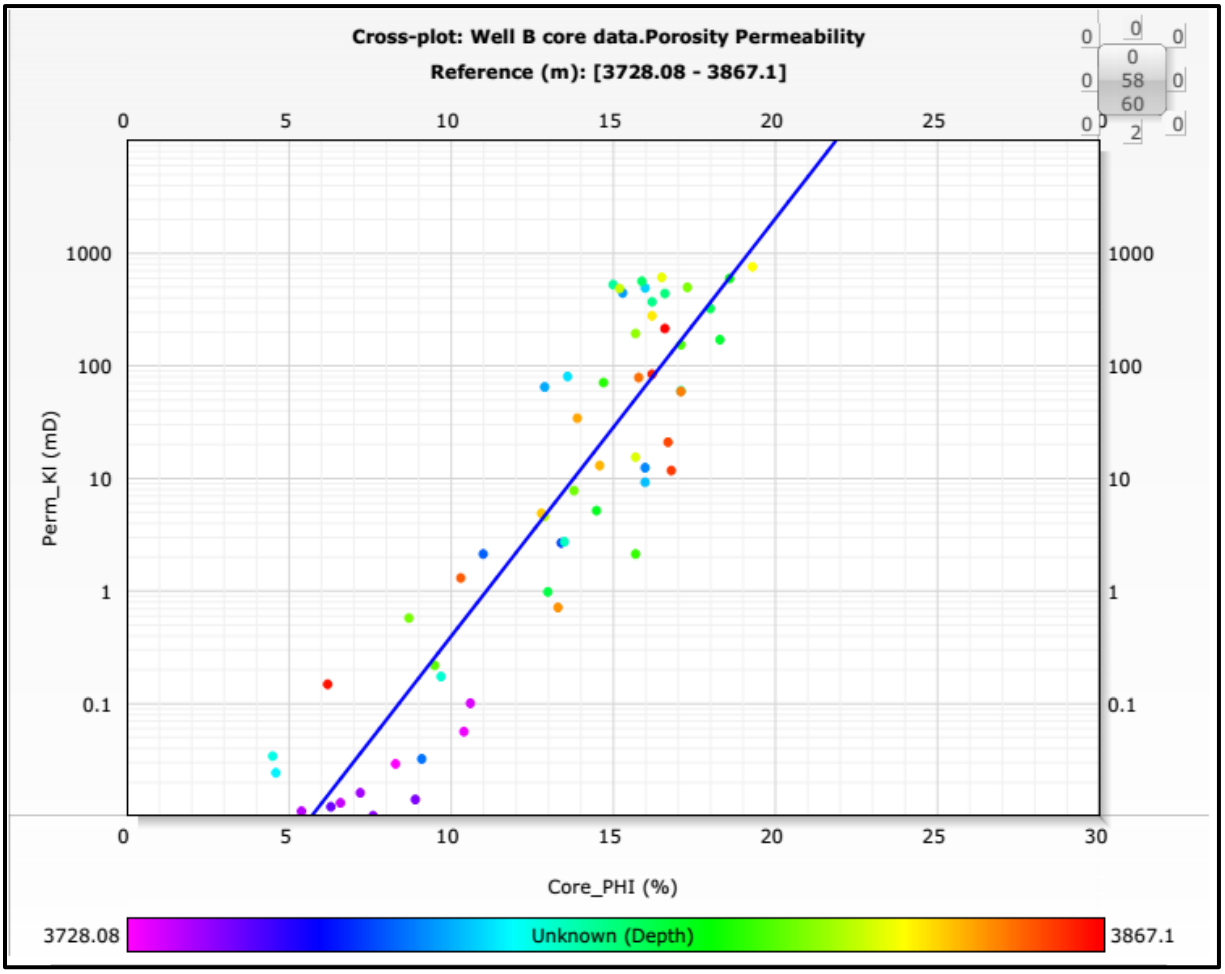

Figure 46: PoroPerm relation of core permeability and core porosity of well 6406/12-3B

Well 6406/12-3A: Permeability

The permeability distribution of this well is given in track 3 of ***Fig.47*** and as shown in the figure the permeability of the reservoir is higher in the water zone comparing to the oil zone. The permeability values are high in the depth intervals of high porosity but in low porosity depth intervals it is low that reaches up to zero like in the depth interval 4099-4102 m.

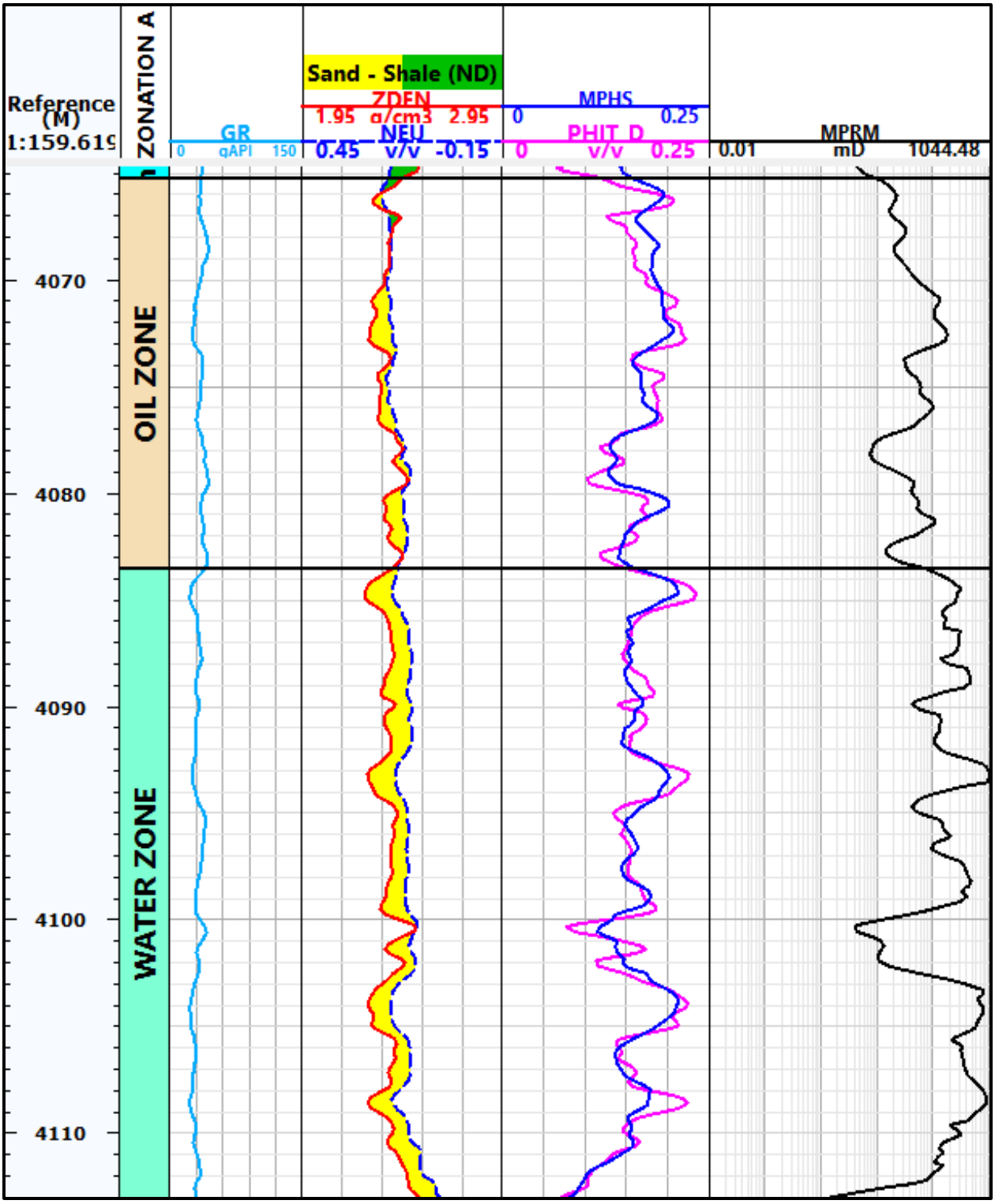

Figure 47: Permeability Distribution in well 6406/12-3A

The minimum, maximum and average permeability values recorded from the NMR and core permeability of the three wells are summarized in ***Table 20***.

Table 20: Summary of permeability distribution in the reservoirs of Pil and Bue wells

Well	Depth Interval	MPRM			Cored Interval	Core Permeability		
		Min	Max	Ave.		Min	Max	Average
6406/12-3S	3517-3608	0.005	65.96	8.77	3524-3608	0.023	2800	314.7
	3609-3745	0.06	318.6	31.95	3609-3732	0.023	2374	290.8377
	3746-3912	6.68E-16	395.5	27.87	---------	**Not cored**		
6406/12-3B	3761-3844	0.47	353.7	61.7	3728-3843	0.003	749	149.5
	3845-4264	1.85E-06	363.4	26.7	3845-3867	0.148	212	46.7
6406/12-3A	4065-4083	7.5	181.7	54.6	**No Core data**			
	4084-4114	1.3	1044.5	293.3				

Core permeability-log Permeability

Fig. 48-shows the comparison of the log permeability and core permeability in the cored depth intervals of well 6406/12-3S and as shown in the figure the core permeability values are much higher than the log permeability at the gas zone. However, in the oil zone they have much better much.

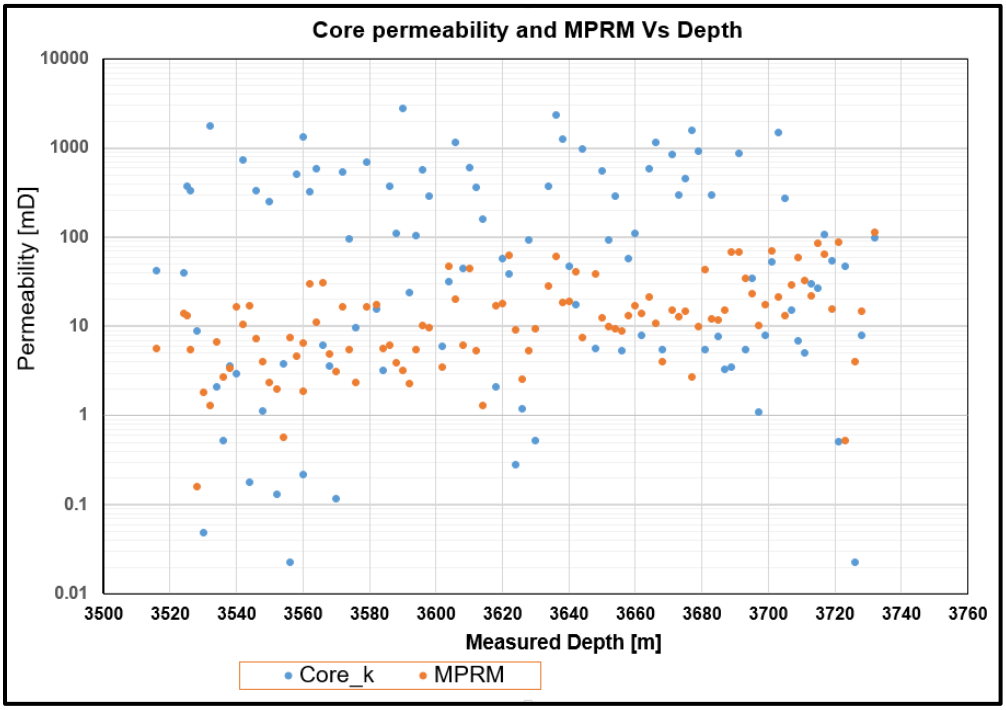

Figure 48: Core Permeability and Log permeability comparison of well 6406/12-3S

Chapter Four: Discussion

Lithology determination of the target reservoirs

Lithology determination and interpretation is very important input in reservoir characterization because wrong lithology interpretation will lead to erroneous results of the other steps such as porosity and water saturation estimation. Lithology interpretation of the target reservoirs of the three wells of this study was performed using log analysis based on the response of gamma ray log, density log, resistivity log, neutron porosity and density log in combination with neutron log. Depth intervals with high gamma ray reading, low resistivity response, high neutron reading, low density, and positive separation of Density-Neutron porosity was identified as shale zones (clay containing layers). Zones with low gamma ray, high resistivity, negative Density-Neutron cross over, and low neutron reading separation were identified as sand containing intervals. This interpretation was supported with the lithology description given in the core analysis report of the two wells in the field.

Fig.16 of well 6406/12-3S and ***Fig. 19*** of well 6406/12-3B shows the gamma ray response with high streaks/picks in between the low gamma ray response of the depth intervals and Density-Neutron porosity crossovers showing positive and negative separation. In the zone of high gamma ray response, the Density-Neutron crossover shows positive separation (both neutron log and density log reads towards high value) and this is because of the shale effect in between the sand layers.

According to (Ellis and Singer, 2007) the gamma ray reading in the shale gives high value due to the presence of radioactive elements like Thorium (Th), Potassium (K) incorporated with clay minerals. However, the crowd of the data points in the Th-K cross plot ***Fig.18*** lies in the Mica zone and this could be suspected for the presence of heavy minerals in the sandstone that makes the gamma ray to give higher value. The other indicator of shale presence in the reservoir is the high response of neutron log reading in the streaks of gamma ray reading and this is due to the presence of hydroxyl (OH^-) group in the clay minerals that increases the hydrogen index of the formation.

Fig. 17 shows the distribution of the data points of the reservoir interval of the well where the maximum cloud of the points lie in the sandstone line and limestone line. However, the cloud of points in the limestone, dolomite line and the points indicating away from the sandstone line are

due to the effect of gas that pulls up from the sandstone line and the shale effect pulling down towards the right hand corner direction. Therefore, the data points in the limestone line are not showing the limestone lithology because if it was limestone the response of the gamma ray would become lower and the Density-Neutron porosity cross over will overlay each other. The same thing happens in well 6406/12-3B as shown in ***Fig.20₂*** where the cloud of the points lies in the clean sandstone line and towards the limestone and dolomite lines. However, no gas effect is observed in the cross-plot because the data points pulling up from the sandstone line like in well 6406/12-3S are not observed in this well. Generally, the overall lithology characterization of the Intra-Melke formation in both wells is determined as shaly sand reservoir.

The lithology distribution of well 6406/12-3A as shown in ***Fig.21*** is highly dominated by clean sand that is because the gamma ray response is very low throughout the reservoir and Density-Neutron crossover shows negative separation except the top part of the reservoir. There are tiny separations and the GR is a bit higher in the reservoir interval with circles in the figure, and this is due to shale effect. Therefore, the quality of the Rogn formation reservoir is better than the Intra-Melke sandstone formation because the shale distribution in the reservoir is very low.

Shale volume

For accurate water saturation and effective porosity estimation, correct determination of shale volume is critical. Wrong selection of the two extreme points (the maximum shale zone reading and the minimum clean zone reading) leads to exaggerated values of the petrophysical parameters especially in the estimation of the effective porosity and shaly sand water saturation. Hence, the estimated hydrocarbon in place of the area will be misleading to the decision of the company that makes them to expect more or less than the actual value. In this study, to minimize the uncertainty related to choosing the maximum and minimum reading of the gamma ray log an average high value in the 100% shale zone and an average minimum value in the 100% clean sand zone was taken. The reason why this mechanism was performed is that as shown in ***Fig.16*** and ***Table 9*** there are exaggerated pick values in both the low reading and high reading values but they do not give full deflection and even their thickness is in centimeters. Taking these pick points as minimum and maximum results in an exaggerated shale volume even in the clean sand zone may result in high shale volume. The other source of Uncertainty is the representativeness of the shale type selected in defining the maximum reading for the calculation. The maximum reading of the shale zone was not taken from shale in between the sand layers rather it was taken

from the shale formations above and below the target reservoirs. This is because the shale in between the sand layers will be influenced by the response of sand from above and below or the shale itself my contain sand in it since they are deposited in the same area. The other thing to be considered is that when choosing the shale far from the reservoir it is assumed to have the same properties like the adjacent shale zones.

The shale volume estimated in the three wells of this study shows high shale volume in the thin laminae of the shale layers in the sandstone formations and low value that reaches up to zero in the clean sand interval. Getting high shale volume at any time does not mean that the only mineral in the sand layers is clay because the presence of heavy minerals like mica and feldspar makes the gamma ray log to give high values, which results the shale volume calculated from the gamma ray to give high values. However, according to (Bhuyan and Passey, 1994) in their paper they explain two assumptions are commonly made in a calculation of shale volume from gamma ray. These assumptions are 1). The composition of shale is 100% clay 2). The increase of the gamma ray response (counts) from clean sand to shale is due to the increase of the clay content only. In this study, these assumptions are applied in the interpretation of the shale volume estimated and the type of lithology determination in the three wells.

The shale volume of Intra-Melke formation of the reservoir section of well 6406/12-3B is more shaly sand with an average range of 14.5 -31% as shown in ***Table 15*** and the average shale volume of well 6406/12-3S lies in a range of 9-20% except the 2 m top section of the reservoir as shown in ***Table 14.*** The 11% difference will bring great effect in the estimation and interpretation of the petrophysical parameters comparing to well S. In well 6406/12-3A, the middle and bottom part of the reservoir the shale volume is much lower than the other wells but in the top part, it is highly dominated with shale. However, there is uncertainty in some depth intervals of this well where the gamma ray and density log reading increases but the neutron log decreases. This problem should be suspected that the response might not be from the clay mineral in the sandstone layers rather it could be from the presence of other heavy minerals. However, to be specific to the overall reservoir interval it does not have an effect since it is observed in centimeters thickness.

Fluid types and contacts from pressure gradient and log responses:

Determination of fluid type and fluid contacts in a reservoir is critical for determination of the hydrocarbon in place (STOOIP), and for detailed and accurate petrophysical analysis. For

accurate porosity estimation, the reservoir should be subdivided in to zones based on fluid type and fluid contacts because if the fluid type and its depth limit is known, correct fluid density will be applied. Fluids in a reservoir are aligned one over the other due to gravity segregation where the denser will go below the less dense fluid and in most reservoirs gas lies on top of oil and oil on top of water. In a logging analysis, the response of the fluids to different logging measurements is different. Therefore, in this study as described in the result and methodology part the focus of discussion is the response of resistivity log, density log and neutron porosity log and support these results with the pressure gradient analysis result.

Well 6406/12-3S:

The reservoir interval of this well was subdivided into five (5) zones based on the logs uniform responses in the depth intervals as shown in ***Appendix A1.***

Zone_1 [3505-3514 m] - the density-Porosity crossover shows a big positive separation and low resistivity reading and no fluid was identified.

Zone_2 [3514-3608 m] - shows higher resistivity reading than the adjacent shale and big negative Density-Neutron separation, which is an indication of hydrocarbon gas bearing interval. This is because the presence of gas in the pores causes the neutron log to give too low porosity due to its lower concentration of hydrogen atoms than water or oil and low-density reading since it is lighter than oil and water. In addition to these characteristics, the other indicators of gas in that zone was the crowd of data points that lied above the sandstone line of the Density-Neutron cross plot as shown in ***Fig.18.*** Large deficit (gap) between nuclear magnetic resonance porosity and density log total porosity also confirms the presence of gas in the given depth interval.

According to the pressure gradient analysis of ***Fig.28*** and ***Table10***, it confirms the logging response result, where the calculated density lies in range of [0.1-0.55] approximately 0.3 g/cc. Therefore, based on the density estimation it is a low-density gas and the detail classification of gas type is not the aim of the study.

Zone_3 (3608-3745 m) - this depth interval is identified as oil-bearing interval based on the responses because both the hydrogen index of oil and the density of oil are higher than the gas phase that narrows the gap between the density and neutron log. The resistivity still remains higher to certain depth in this zone and starts to decrease from 3725 – 3745 m, which is an indication of the decrease in oil saturation that tends to be mixed with underneath water zone.

The formation pressure test data points taken in this interval confirms as it is oil-bearing interval where the calculated density lies in a range of [0.65-0.85] g/cc.

Zone_4 [3745-3912 m] - the resistivity log starts to decrease from 3745m, which is due to the salinity of the water that increases the conductivity, and the negative separation of Density-Neutron crossover decreases from above zone but not that much. This is due to the hydrogen index of water and oil does not have much difference but it gives a bit higher neutron porosity reading in the water zone. The other thing is the density of water is a bit higher than the density of oil except in heavy oils and the gap between the density log and neutron porosity log becomes narrower than the oil zone. In general, the mechanism of identifying hydrocarbon bearing zones from water bearing zones is, the value of resistivity log reads high value in the hydrocarbon zone and decreases when it comes to water zone. Therefore, zone_4 was identified as water zone. In addition to these logging responses, the formation pressure test gradient analysis on this interval confirms the presence of water and the density calculated 0.97 g/cc lies in a range of [0.95-1.05].

Zone_5 has almost the same properties as **zone_1** where the resistivity log reads lower values and the Density-Neutron cross over with positive separation, which is an indication of shale zone without fluid indications.

The overlying of the resistivity logs (deep, medium and micro) is due to the oil based mud drilling fluid therefore the contrast in resistivity will be very low.

The fluid contacts are identified based on the response of the resistivity reading accompanied with the Density-Neutron separation. The fluid contacts as indicated in the log response the oil water contact is identified at a depth of 3745m but in the Norwegian Petroleum Directorate website the OWC was given at a depth of 3742 m. This is because the resistivity log responds uniform in the transition zone but after 3745 m, it starts to decrease. However, the OWC from pressures gradient analysis the intersection of the oil pressure line and the water pressure line lies at 3740m, which is 5 m up from the logging response contact. This could be the effect of the oil saturation reduction and the pore spaces are starting to be occupied with water in the transition zone.

Well 6406/12-3B:- This well is subdivided into four zones based on the above criteria of logging responses as shown in ***Appendix B1*** and supported from the results of pressure gradient analysis.

Zone_1 of this well shows low resistivity and big positive separation of Density-Neutron cross over which does not show fluid indication.

Zone_2 (3761-3843 m) - the resistivity log shows high reading value and the density- neutron cross over shows negative separation. The only fluid indicated in this zone was the oil zone. However, in the Norwegian Petroleum directorate website of Pil and Bue wells, this well was categorized as oil and gas discovery well but there were no indications of gas presence from the overall display of the logs. In addition to this the Density-Neutron cross plot of the well also does not show the gas trend data points from the sandstone line.

The calculated density from the pressure gradient analysis in this depth interval as shown in ***Table 11*** is not the same throughout. In addition to this, the pressure line of the data points does not lie at the same trend line as shown in ***Fig.30***. Based on the estimated density the reservoir contains the same fluid with different densities. Therefore, the top part of the reservoir almost half of the reservoir (40 m thickness) contains light oil and the rest interval from 3815-3843 m is a bit denser oil but still the reservoir is oil bearing reservoir. There are crowd of points that pulled apart a bit from the sandstone line in the Density-Neutron cross plot but this is due to the effect of light oil in the reservoir. The light oil section of this well has the same density with the oil discovered in well 6406/12-3S. Therefore, the oil discovery in the Intra-Melke sandstone formation of Pil field contains light oil and heavy oil.

Zone_3 (3844-4264) indicates clear decrease in the resistivity log reading and small decrease in the Density-Neutron cross over which is an indication of water zone. The rest of the well **Zone_4** was showing the same properties as **Zone_1** logging responses, which is shale zone without fluid indication.

The fluid contact based on logging response and pressure gradient analysis has big difference because **5** m difference in volumetric hydrocarbon calculation brings a great effect. Therefore, as mentioned in well 6406/12-3S this could be due to the pressure of water in the transition zone and the fluid contacts from logging response were taken in the estimation of the petrophysical parameters.

Well 6406/12-3A:

In this well as expressed in chapter two, the fluid type and fluid contact analysis will be discussed based on logging response as shown in ***Fig.31*** and it is subdivided in to five zones as shown in ***Appendix C1.***

Zone_1 - is the section of the well above the reservoir interval that shows low resistivity and positive separation between the density log and neutron porosity log without fluid indication.

Zone_2 (4053-4065 m) –this zone is the top part of the reservoir where the response of the neutron log and density log response is high with positive separation in between. This is an indication of no fluid depth interval. However, starting from 4065m of **zone_3** the resistivity log starts to increase and the Density-Neutron crossover starts to show clear negative separation, which an indication of hydrocarbon and continues up to 4083 m.

Zone_4 (4083-4114 m) – this zone is differentiated from the above zone based on resistivity log because it is difficult to say it is oil or water based on the Density-Neutron crossover. Therefore, at a depth of 4083 m, the deep resistivity log starts to decrease and this zone is identified as water bearing section of the reservoir.

Zone_5- it has the same responses as zone_1 and it is identified as no fluid zone.

Porosity of the Reservoirs (PHI)

Well 6406/12-3 S:

Fig.15, ***16***, and ***17*** compares the estimated porosities in the gas, oil and water zone. All the porosity types show lowest values in the first 2-3 meters of the reservoir interval from 3514-3516m. This is due to high shale volume of the depth interval, which is much higher with an average shale volume of 55% comparing with low shale volume of 7-23% of the rest reservoir interval, and the effective porosity in that interval is almost zero. Based on the comparison, the density log derived porosity gives higher value in the gas zone with an average porosity of 17% as shown in ***Table 14***. The NMR porosity in this zone underestimates the porosity to an average porosity of 9% almost half of the density porosity.

According to Breda et.al, 2000, in their conference paper explained that the deviation of NMR porosity and density porosity in the gas phase from the real porosity estimations is caused due to three factors. These factors are low hydrogen index and partial polarization of gas, which reduces

the NMR porosity, and the low gas density that increases the density porosity. The partial polarization (incomplete polarization) of gas is caused by its long polarization time (a function of its density) (Ellis and Singer, 2007). To compensate the effects an accurate porosity has been obtained by the gas corrected DMR porosity method that can be used to improve log-based estimates of gas reserves and formation permeability. The average porosity from core porosity and the average porosity from DMRP give the same result of 14% in the gas zone and they have good match in the log display as shown in ***Fig. 32.*** The other porosity estimated was the density porosity based on the density of fluid from the pressure gradient analysis and this porosity best match with the DMR porosity. However, the density of fluid is expected to be higher in the invaded zone due to the presence of mud filtrate and the density of gas, oil or water is expected to be higher than the pressure gradient analysis density calculation. Therefore, the DMR porosity is still preferred for this study.

In the oil and water zone, the gap between the density porosity and NMR porosity is minimized and in some depth intervals overly to each other but still, they do not give the same value. As shown in ***Table 14*** the average porosity of density porosity is higher than the NMR porosity with 3% difference in the oil zone but the percentage gap decreases in the water zone 2% difference.

According to Allen et al., 1998, it is common for both porosities to agree well in the oil zone and water zone since the NMR response depends on the total hydrogen content of the formation. However, the small gap may be created due to matrix density and fluid density effects on the density porosity in the oil zone and only matrix density effect in the water zone since correct density of fluid is used for the water zone. The porosity derived from density log mostly depends on the choice of matrix density, which varies with lithology, but the NMR porosity is independent of the matrix mineralogy.

Based on the estimated porosities in the reservoir interval of the well, the porosity distribution of the Intra-Melke sandstone formation has good porosity, which is enough to hold hydrocarbons. The porosity decreases with depth in both the log-derived porosities and the core-derived porosity and this is due to the compaction effect and shale distribution. As shown in ***Fig.34*** from 3773- 3806 m the shale effect is clearly seen where all the porosity values are very low and in some depths with zero porosity. This affects the quality of the reservoir by filling the pore spaces with shale, blocking the fluid flow by blocking the vertical permeability of the pore spaces, and

further it complicates the estimation of water saturation though it is not in the hydrocarbon-bearing interval.

Well 6406/12-3B:

In this well gas bearing zone was not identified based on the logging responses and the porosity estimated from density porosity and the given NMR porosity (MPHS/TCMR) almost matches to each other as shown in ***Fig. 35,*** and ***36.*** The small gap between these porosities in the log display and the small difference in porosity ranges as given in ***Table 15*** could be due the grain size effect. As explained above in Well 6406/12-3S the NMR porosity is not dependent in the matrix density and this could be one reason, and the other reason is the density of fluid used in the estimation of the density porosity is still the density of water even in the oil zone. However, this value does not bring huge difference in the result of the reserve estimation.

The porosity value of the Intra-Melke formation of this well decreases with depth in the reservoir interval, which is due to the increase in shale distribution in the reservoir especially in the water zone and due to compaction effect on the pores. However, the range of the average porosity of this formation in both wells (6406/12-3S and 3B**)** is almost similar.

Well 6406/12-3A:

In this well, the top part of the reservoir the first 6 m is characterized with low porosity due to its shale domination as shown in ***Fig*.26** and the grain size effect creates gap between NMR porosity and density porosity**.** Both the NMR porosity and the density total porosity almost overly in the oil zone and water zone and the average porosity from 4065-4083 m and from 4083-4114 m is the same as shown in ***Table 16***. For oil and water bearing reservoirs of well 6406/12-3B and A, the NMR porosity is more preferable than the total density porosity. This is because as explained above the NMR porosity is not dependent in the mineralogy of the matrix but to be consistent the density log derived porosity was applied in the water saturation estimation of the three wells.

Effective Porosity

The other type of porosity estimated from the total density porosity and the shale volume was the effective porosity. This porosity type includes the pore spaces in the reservoir, which contains the hydrocarbon, and formation water without the clay bound water. In the depth intervals of clean sand or zones with zero shale volume the effective porosity and total porosity results are

the same as shown in ***Fig.34, 35 and 37*** of the three wells. Based on the average effective porosity of the reservoir interval of Intra-Melke sandstone formation in both wells, it is higher in well 6406/12-3S than well 6406/12-3B as shown in ***Table 14*** and ***15***. This is an indicator of high shale distribution in the sands of well 6406/12-3B, which reduces the interconnected porosity. In the case of well 6406/12-3A, the shale content of Rogn sandstone formation is small and this is indicated in the estimated total porosity and effective porosity. As shown in ***Table 16,*** the estimated average total porosity ranges 9-17% and the effective porosity ranges 8-17 %. The other observations in the display of total density porosity in the shale containing depth intervals give some porosity values but the effective porosity gives almost zero value in that interval. As shown in ***Table 13*** of well 6406/12-3S in the depth interval of 3514-3516m the average total porosity is 5% and maximum value 14% but the effective porosity gives an average value of 0.02 %. This could be due the clay bound water (CBW) that appears as porosity in most porosity logs. There are uncertainties to be considered in the estimation of the effective porosity and they are related to volume and bulk density of shale. For well 6406/12-3S and 3B, grain densities were given in the core report lithology description but the density of mudstone/shale given in the report contains pyrite mineral. The presence of this mineral increase the density of shale and the values given in the report were not taken as input density rather it was selected from the shale zone reading of the density log. However, the values were not taken from the shale streaks in the sandstone layers, this because as explained above in the selection of the maximum gamma ray reading it was preferred to be selected from the thick shale zone. This was done to get representative and reasonable shale reading because the thin laminae of shales distributed in the sandstone do not give full deflection for the analysis.

Water Saturation

Estimation of water saturation is the important parameter and the basis for economic production decision of hydrocarbon reserve of the target reservoirs. Overestimating or under estimating of this value leads to high or low hydrocarbon saturation since oil or gas saturation is given as **1-Sw.** If the water saturation is high, the hydrocarbon saturation will be low which makes to be less interested in the field. In this study, comparison of clean sand Archie water saturation, Indonesia and Simandoux effective water saturation are the models to be discussed. In the comparison, the Archie results are used as reference to see the changes or the effect of shale in the estimation of Sw.

Well 6406/12-3S:

Water saturation estimated in the first top three meters of the Intra-Melke sandstone formation penetrated by this well gives very high value both in the clean sand and shaly sand models as shown in ***Table 17*** and ***Fig.38*****.** This is due to the low porosity, high shale volume, and the fine-grained effect. In addition, in the depth intervals of shale streaks the water saturation is still higher than the clean sand zones, which shows the effect of clay or shale. The other effect observed in the estimation of Sw is the change in Rw brings 2-8% changes in the result. Therefore, accuracy of the input parameter is the matter for accurate water saturation.

Well 6406/12-3B:

Fig.41 and ***Table 18*** of this well shows high water saturation in the hydrocarbon bearing interval of 3761-3844 m with an average value of 59% using Archie and the shaly sands models give the same value that is 49%. As shown in the figure, the water saturation is higher in the depth intervals of high shale volume and this is due to the extra conductivity of clay that reduces the formation resistivity which is translated to high water saturation. The shale distribution in this well is much higher than well 6406/12-3S and fine-grained particles hold much water that makes the water saturation of the well to be higher.

Well 6406/12-3A:

The water saturation estimated in this well gives high value comparing to the two wells drilled in the Pil prospect and only less than 20% of the pore spaces of this well are occupied by hydrocarbons as shown in ***Table 19.*** The water saturation in the oil zone of this well gives suspiciously high water saturation and it was tried using different assumptions like changing fluid density in the porosity calculation and changing the formation water resistivity (Rw) as shown in ***Appendix C2***. However, the values give high water saturation in all assumptions and this may be due to the well trajectory that might target the transition zone (the zone near the water zone and bottom of the oil zone) in the Rogn formation. This reason is given because the aim of the well 6406/12-3A was drilled to check the continuity of the reservoir encountered in well 6406/12-3S and 3B unfortunately the well targets different reservoir with 18 m hydrocarbon column. In addition, the values of the three models show small difference and this is because of the good quality of the reservoir with minimum shale volume.

Generally, the value from Archie model of the three wells gives high water saturation relatively to the shaly sand Indonesian and Simandoux models. This is because the water saturation estimation is a function of porosity, formation resistivity and formation water resistivity and these properties are affected by shale presence in the formation. The shale distribution in the sandstone layers of the reservoir suppress the formation resistivity that causes an error directly translated to the over estimation of the water saturation. This effect was clearly observed in the estimated water saturation of the hydrocarbon-bearing zone with the shale streaks. The reason for this case is the water left bound in the clay minerals (CBW), and the capillary bound water (Irreducible water saturation) in the reservoir from the displacement of oil migration. When hydrocarbon migrates from source rock to reservoirs, it displaces the water previously saturating the pore spaces but it is obvious to have irreducible water saturation left.

Based on the different literature reviews, it is assumed that shaly sand models give lower water saturation comparing to Archie and the result of Indonesian and Simandoux water saturations in the three wells of this study are as expected. However, in comparing both saturations it should be based on the Bulk volume of water (BVW) because the Indonesian equation and Simandoux equation uses the effective porosity that tends to minimize the porosity contribution whereas the Archie uses the total porosity. In the Indonesian equation, there are some uncertainties to be expected because (Poupon and Leveaux, 1971) in their paper explained that the Indonesia equation can give higher water saturation for shale volume of less than 40% and this model is effective for 40-90% shale volume. In every calculation of the petrophysical parameters, there are uncertainties related to the input parameters and the results are associated with errors. However, it is obvious that errors are an inevitable and it is common to tolerate and live with some uncertainties in scientific calculations. These errors can be minimized by selecting proper input parameters based on scientific reasons. In this study, the results estimated are still reasonable and satisfactory because the input parameters used were chosen in a proper zone with a proper lithology of the target formations. However, this does not mean that the results are free of uncertainties and in the estimation of water saturation; there were some uncertainties of the input parameters that contribute to the result. These are related to:

- Shale volume (Vsh) and bulk density of shale (RHOB_shale) - in calculating the effective porosity inaccurate estimation of these input parameters leads to wrong results. Using this

wrong value will result in overestimated or underestimated effective water saturation of the Indonesian and Simandoux model.

- Formation water resistivity (Rw) - since it was not given in the log suite it was estimated from Archie method in the water zone of clean sand. However, the value was not exactly 0.1 Ohm.m but it ranges from 0.08 to 0.12 even in the clean sand water zone. As shown in ***Table 17*** the water saturation using the temperature corrected Rw gives lower Sw comparing to Rw derived from the clean sand Archie method water zone. Therefore, this change may contribute for pessimistic or optimistic decision on the target field. The other uncertainty related to Rw is, the Indonesian method works best in high Rw, and Simandoux in low Rw but in this study the same Rw was applied for all models.
- Cementation exponent (m) and saturation exponent (n) - because the accuracy of water saturation strongly depends on the uncertainty of these exponents. In this work, the default values of the software were taken as an input in the estimation. However, cementation exponent (m) values vary with rock type and the saturation exponent (n) varies depending on the wettability of the rock. Strongly water wet rocks can give **2** or lower value but oil wet rocks give higher value (Lewis et al., 1988).
- Total porosity - because in the estimation of the porosity, the density of fluid used was taken 1.0 g/cc and this result is high porosity in the gas zone. To minimize the error DMRP was used in the estimation of Archie Sw but in the calculation of Indonesian equation, the input parameter for the calculation of the effective porosity was the total density porosity. This happens the software does not allow importing the DMRP directly in the estimation.
- The other uncertainty was the estimated resistivity of shale since the value was taken in the shale zone far away from the sandstone formation and the shale may not be the same with the shale distributed in between the sand layers. In addition to this, the shale resistivity varies from **2** Ohm.m-6 Ohm.m in the shale zone.

For detail Uncertainty analysis of petrophysical analysis and error calculations in a petrophysical calculation it is recommended to read the paper **(Stalheim, 2016).** In the paper, the errors associated with petrophysical parameters are clearly stated but in this thesis it is not the objective of the study to deal with the errors and error calculations.

Permeability of the reservoirs

For hydrocarbon bearing reservoirs and economically viable reserves to be produced the communicability of the pore spaces (hydraulic conductivity) is needed. That means we should have fluid flow through the pore spaces. The NMR permeability (MPRM) and the permeability generated from the porosity-permeability relationship are going to be discussed. In a log analysis the sign of permeability of the formation can be indicated by the porosity of the reservoir because most probably if it is porous it could be permeable, mud cake indicated by caliper and separation on the resistivity log curves. However, the resistivity logs almost overly to each other with minimum resistivity contrast since the drilling mud is oil based mud.

The average permeability distribution in well 6406/12-3S lies in range of 8.77-31.95 mD but the permeability distribution in the gas zone is lower than the oil and water zone. This is because the effect of gas on the NMR permeability. In addition the permeability is low in the depth intervals containing shale because clays have the ability to fill the pore spaces that impede the communicability and blocks the fluid movement among the pore spaces.

The regression coefficient (R^2) values of 82% and 84 % of the wells 6406/12-3S and 6406/12-3B, shows that matching (fitting) of the data points and this is an indication of good relationship between porosity and permeability.

According to (Glover, 2011), the permeability range 10-100 and 100-1000 is classified as high to very high based on this range the permeability of the three wells is classified as high to very high as shown in ***Table 20***.

Chapter Five: Conclusion

The petrophysical interpretation of the three wells in Pil and Bue prospects confirmed that the target reservoirs have good to very good quality. Based on gamma ray, Density-Neutron crossover and cross plot log responses the lithology of the reservoirs contains dominantly sand with thin shale laminae distributions. The shale content in the wells drilled in to the Intra-Melke sandstone formation has lower value in the hydrocarbon bearing section than the water bearing zones and in both wells of this formation the shale volume increases with depth. However, the shale distribution in the Rogn formation reservoir is very low comparing to Intra-Melke sandstone formation. In addition to this the reservoir quality increases with depth and the water zone has better quality than the hydrocarbon bearing section. Comparison of the different porosity calculations also shows best match in the oil zone and water zone. However, in the gas bearing reservoir of well 6406/12-3S the density porosity gives higher value and NMR porosity gives lower value. This is due to the nature of gas that makes the responses different and the problem in the gas zone was solved using DMR porosity that gives best values comparing to density and NMR porosities.

Uncertainties are common in scientific calculations and there are uncertainties related to density of fluid in total density porosity and bulk density of shale in effective porosity calculations. Therefore, using these values to estimate water saturation may result in erroneous values of hydrocarbon in place reserve estimation of the fields.

From the water saturation results of the three wells in low shale volume depth intervals, the clean sand water saturation (Archie) and the shaly sand water saturations (Indonesia and Simandoux) give almost similar values. Therefore, in these zones the Archie model can be used to estimate Sw but 10% difference brings significant effect in the calculation of in place hydrocarbon of the reservoirs. In the three wells, the water saturation is very high, in well 6406/12-3A though the reservoir quality is very good, less than 20 % of the pore spaces are occupied with hydrocarbons.

In the estimation of water saturations there are different things to be considered in the accuracy of the generated results and these are related to the input parameters and working condition of the models. In this study, the same input parameters (like n, a, m and Rw) were applied in the estimation of both the clean sand and the shaly sand models. However, even the input parameters are effective or designed to certain conditions (like water wet reservoir, oil wet reservoir and

other conditions). The challenge of shaly sand water saturation models, they are effective at certain conditions if that condition fails to match the estimated water saturation will be wrong. In this study, since the hydrocarbon bearing section of the reservoirs has less shale content the effect of shale on the logging measurements may not have exaggerated effect.

REFERENCES

Abouzaid, A., Thern, H., Said, M., ElSaqqa, M., Elbastawesy, M. and Ghozlan, S., 2016. Nuclear Logging While Drilling in Complex Lithology-Solution for a Glauconitic Sandstone Reservoir, SPE/AAPG Africa Energy and Technology Conference. Society of Petroleum Engineers.

Alexander, T., Baihly, J., Boyer, C., Clark, B., Waters, G., Jochen, V., Le Calvez, J., Lewis, R., Miller, C.K. and Thaeler, J., 2011. Shale Gas Revolution. Oilfield Review, 23(3).

Allen, D., Crary, S. and Freedman, B., 1998. How to use borehole nuclear magnetic resonance. Oceanographic Literature Review, 3(45): 586-587.

Amyx, J.W., Bass, D.M. and Whiting, R.L., 1960. Petroleum reservoir engineering: physical properties, 1. McGraw-Hill College.

Archie, G.E., 1942. The electrical resistivity log as an aid in determining some reservoir characteristics. Transactions of the AIME, 146(01): 54-62.

Bardon, C. and Pied, B., 1969. Formation water saturation in shaly sands, SPWLA 10th Annual Logging Symposium. Society of Petrophysicists and Well-Log Analysts.

Bassiouni, Z. and Bassiouni, Z., 1994. Theory, measurement, and interpretation of well logs.

Bhuyan, K. and Passey, Q., 1994. Clay estimation from GR and neutron-density porosity logs, SPWLA 35th Annual Logging Symposium. Society of Petrophysicists and Well-Log Analysts.

Bøe, R., Fossen, H. and Smelror, M., 2010. Mesozoic sediments and structures onshore Norway and in the coastal zone. Norges geologiske undersøkelse Bulletin, 450: 15-32.

Breda, E., Silveira, A., Homovc, J. and Minetto, C., 2000. Quick Look Methodology for Gas Detection Using NMR and Density Porosity, SPE Asia Pacific Oil and Gas Conference and Exhibition. Society of Petroleum Engineers.

Bugge, T., Knarud, R. and Mørk, A., 1984. Bedrock geology on the mid-Norwegian continental shelf, Petroleum geology of the North European margin. Springer, pp. 271-283.

Dalland, A., Worsley, D. and Ofstad, K., 1988. A Lithostratigraphic Scheme for the Mesozoic and Cenozoic and Succession Offshore Mid-and Northern Norway. Oljedirektoratet.

Doveton, J., 2002. All models are wrong, but some models are useful:“solving” the Simandoux equation. Kansas Geological Survey, Kansas USA.

Ellenor, D. and Mozetic, A., 1986. The Draugen oil discovery. Habitat of Hydrocarbons on the Norwegian Continental Shelf. Norwegian Petroleum Society, Graham & Trotman, London: 313-316.

Ellis, D.V. and Singer, J.M., 2007. Well logging for earth scientists. Springer Science & Business Media.

Freedman, R., Minh, C.C., Gubelin, G., Freeman, J., McGinness, T., Terry, B. and Rawlence, D., 1998. Combining NMR and density logs for petrophysical analysis in gas-bearing formations, SPWLA 39th Annual Logging Symposium. Society of Petrophysicists and Well-Log Analysts.

Gaymard, R. and Poupon, A., 1968. Response of neutron and formation density logs in hydrocarbon bearing formations. The Log Analyst, 9(05).

Glover, P., 2011. Petrophysics MSc course notes. Clay/Shale Effects on Porosity and Resistivity Logs.

Heum, O., Dalland, A. and Meisingset, K., 1986. Habitat of hydrocarbons at Haltenbanken (PVT-modelling as a predictive tool in hydrocarbon exploration). Habitat of hydrocarbons on the Norwegian continental shelf: 259-274.

Jackson, R., Carnegie, A. and Dubost, F., 2007. Pressure Measurement and Pressure Gradient Analysis: How Reliable for Determining Fluid Density and Compositional Gradients?, Nigeria Annual International Conference and Exhibition. Society of Petroleum Engineers.

Jenkins, R.J., 1966. Accuracy of porosity determinations. The Log Analyst, 7(02).

Jongkittinarukorn, K. and Tiab, D., 1997. Identification of flow units in shaly sand reservoirs. Journal of Petroleum Science and Engineering, 17(3-4): 237-246.

Lacentre, P.E. and Carrica, P.M., 2003. A Method To Estimate Permeability on Uncored Wells Based on Well Logs and Core Data, SPE Latin American and Caribbean Petroleum Engineering Conference. Society of Petroleum Engineers.

Lewis, M.G., Sharma, M.M. and Dunlap, H.F., 1988. Wettability and stress effects on saturation and cementation exponents, SPWLA 29th Annual Logging Symposium. Society of Petrophysicists and Well-Log Analysts.

Logan, W., 1989. Bridging the gap between core permeability and log-derived permeability, SPWLA 30th Annual Logging Symposium. Society of Petrophysicists and Well-Log Analysts.

NPD, 2017. NPD fact page. http://factpages.npd.no/factpages/ , visited: 03/2017.

Poupon, A. and Leveaux, J., 1971. Evaluation of water saturation in shaly formations, SPWLA 12th Annual Logging Symposium. Society of Petrophysicists and Well-Log Analysts.

Rider, M.H., 1986. The geological interpretation of well logs.

Shanmugam, G., 1985. Types of porosity in sandstones and their significance in interpreting provenance, Provenance of arenites. Springer, pp. 115-137.

Simandoux, P., 1963. Dielectric measurements on porous media, application to the measurements of water saturation: study of behavior of argillaceous formations. Revue de L'institut Francais du Petrole, 18(S1): 193-215.

Stalheim, S.O., 2016. On Error Calculation and Use of First-Order Error Propagation as Integral Part of Petrophysical Calculation. Petrophysics, 57(05): 465-478.

Thomas, E. and Stieber, S., 1975. The distribution of shale in sandstones and its effect upon porosity, SPWLA 16th annual logging symposium. Society of Petrophysicists and Well-Log Analysts.

Vernay, P., Mathieu, J.P., Leduc, J.P., Martinez, L., Bastien-Dubes, A. and Fourmentraux, P., 2009. Fast track lithological interpretations applied to detailed evaluation of Norwegian Sea basin, International Petroleum Technology Conference. International Petroleum Technology Conference.

Worthington, P.F., 1985. The evolution of shaly-sand concepts in reservoir evaluation. The Log Analyst, 26(01).

Worthington, P.F., 2011. The petrophysics of problematic reservoirs. Journal of Petroleum Technology, 63(12): 88-97.

Xiaoquan, K. and Yongjie, X., 2009. An improved plot for wireline pressure data gradient interpretation. Petrophysics, 50(03).

Zhou, L. and Mardambek, J.O., 2008. Reservoir Fluid Evaluation from Real Time Pressure Gradient Analysis: Discussions on Principles, Workflow, Applications and Limitations, SPE Asia Pacific Oil and Gas Conference and Exhibition. Society of Petroleum Engineers.

Appendix A: Well 6406/12-3S

A1: The whole interval display of the logging measurements and zonation of well 6406/12-3S

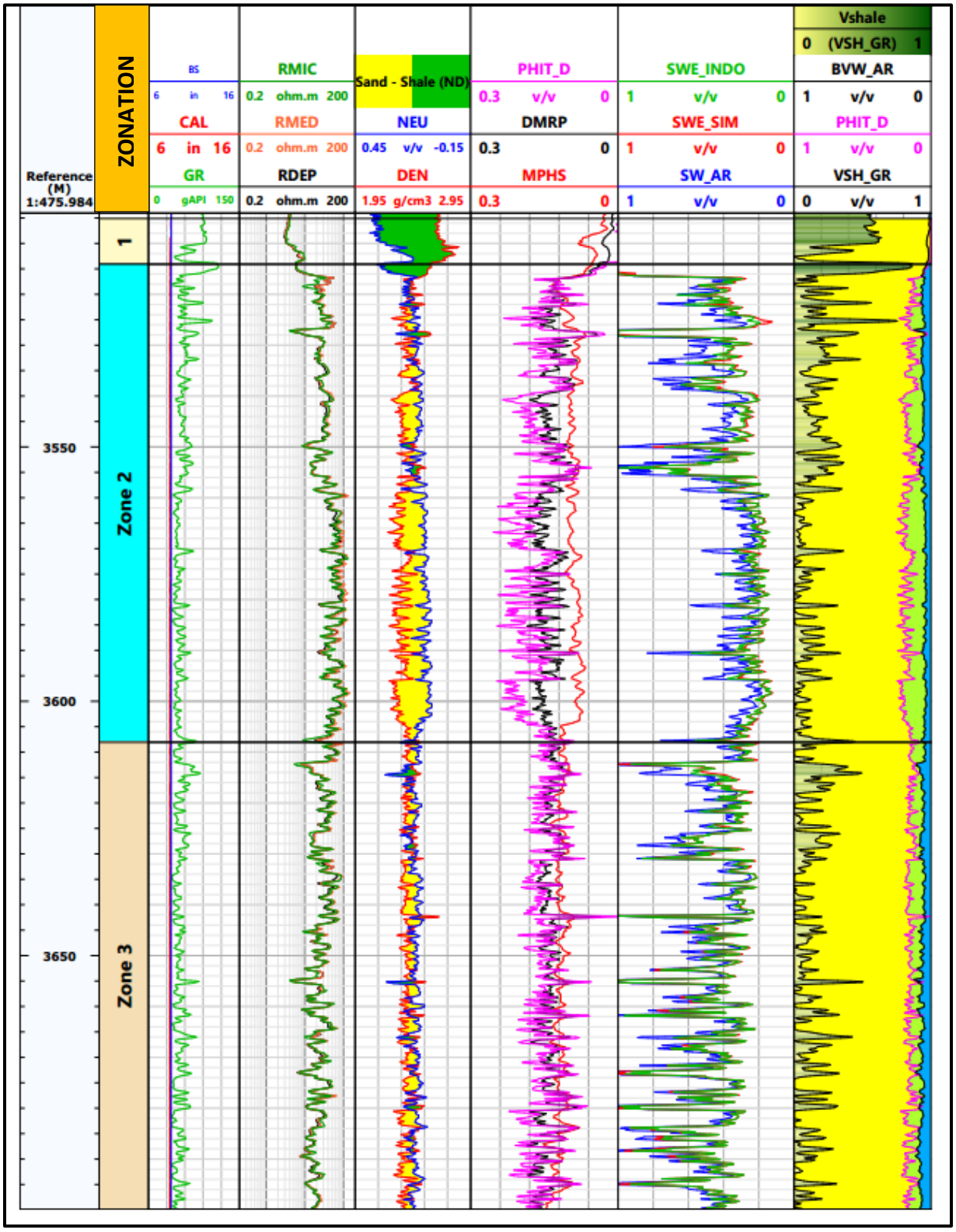

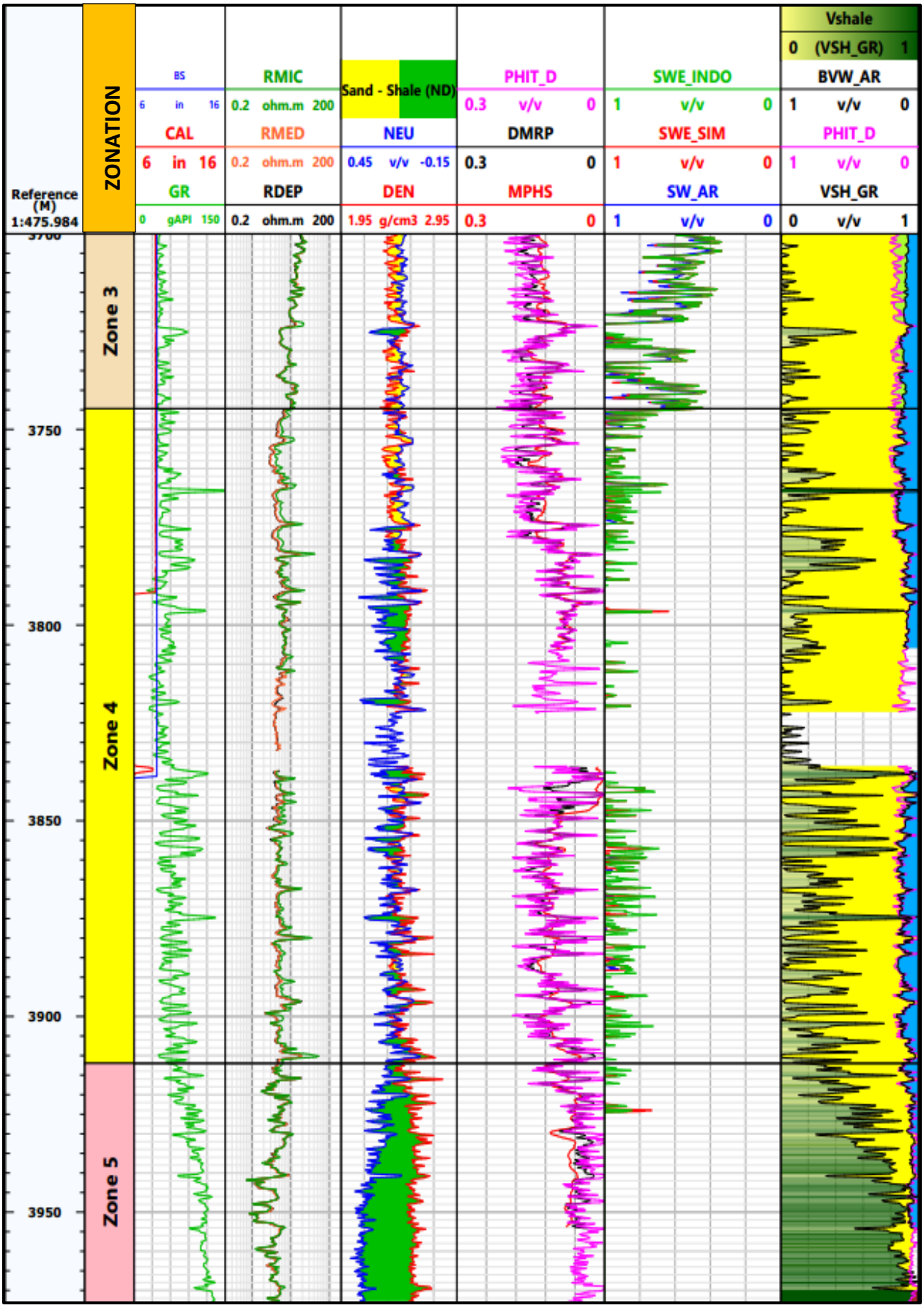
ZONATION
Reference (M)
1:475.984
BS
6 in 16
CAL
6 in 16
GR
0 gAPI 150
RMIC
0.2 ohm.m 200
RMED
0.2 ohm.m 200
RDEP
0.2 ohm.m 200
Sand - Shale (ND)
NEU
0.45 v/v -0.15
DEN
1.95 g/cm3 2.95
PHIT_D
0.3 v/v 0
DMRP
0.3 0
MPHS
0.3 0
SWE_INDO
1 v/v 0
SWE_SIM
1 v/v 0
SW_AR
1 v/v 0
Vshale
0 (VSH_GR) 1
BVW_AR
1 v/v 0
PHIT_D
1 v/v 0
VSH_GR
0 v/v 1
Zone 3
Zone 4
Zone 5
3750
3800
3850
3900
3950

A2: Density-Neutron cross plot in the gas zone of well 6406/12-3S

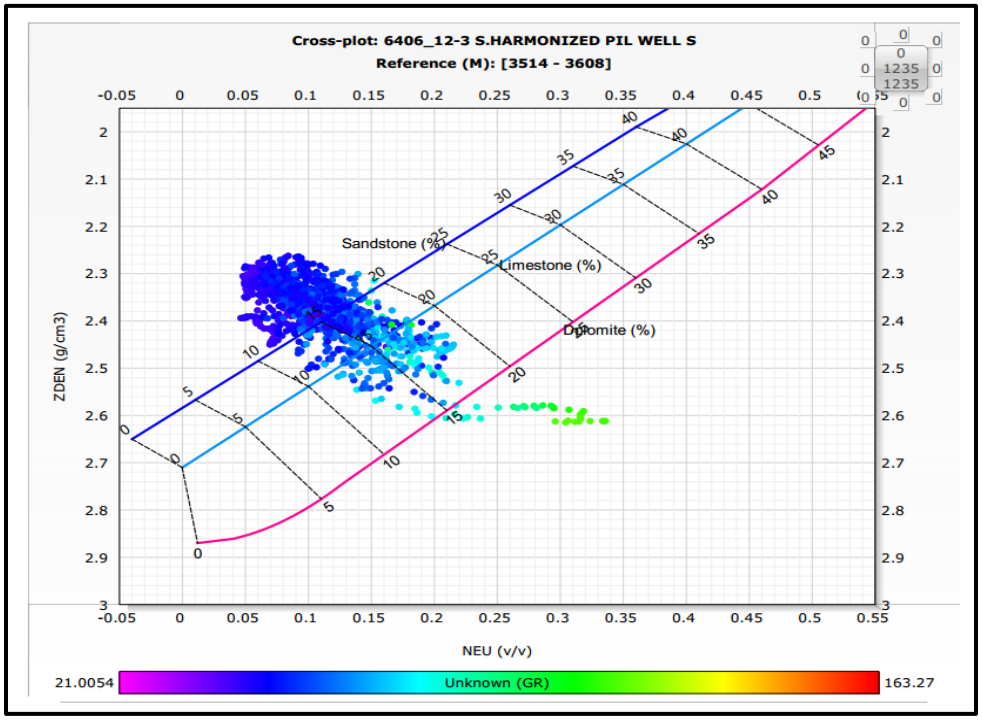

A3: Density-Neutron cross plot in the oil zone of well 6406/12-3S

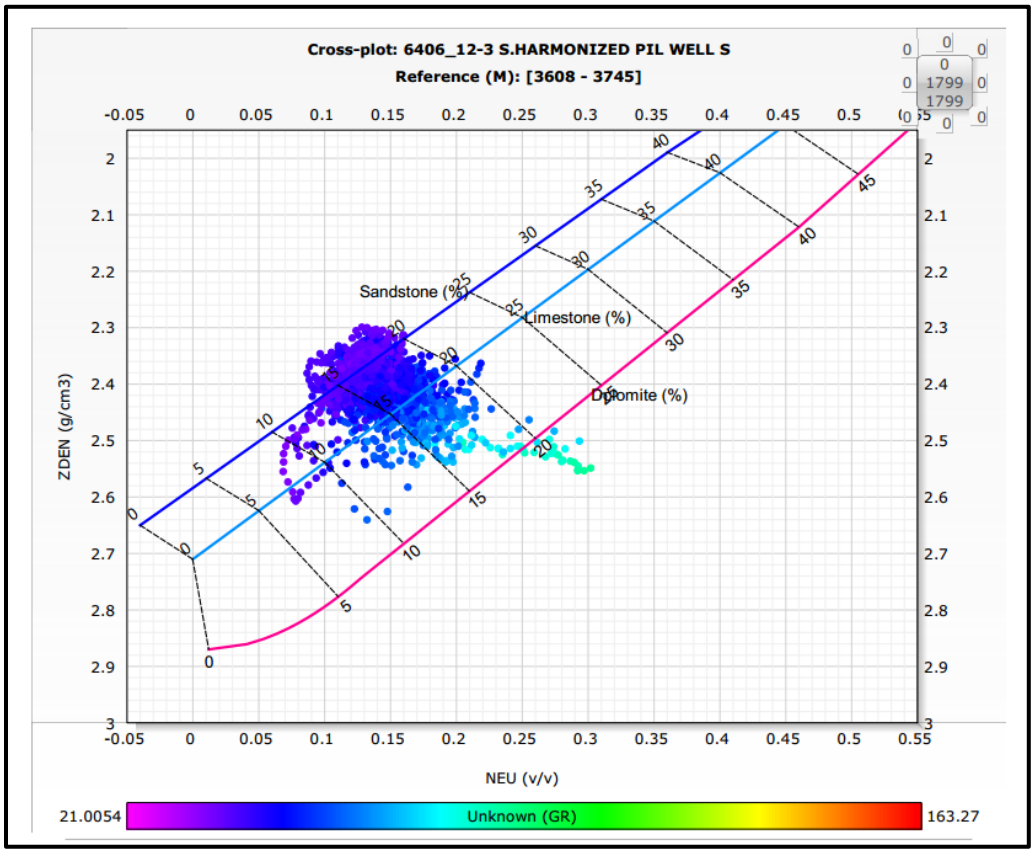

A4: Density-Neutron cross plot in the water zone of well 6406/12-3S

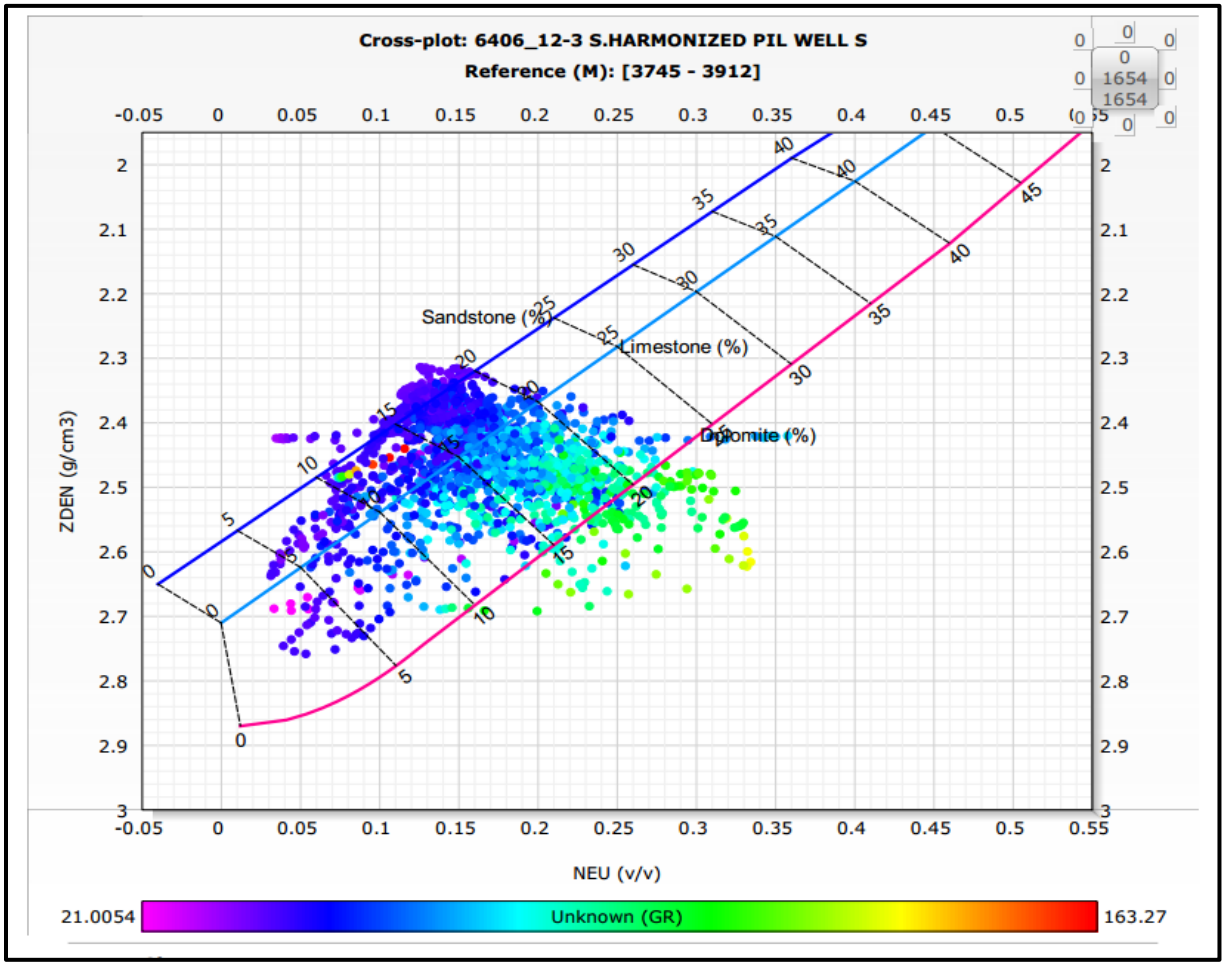

A5: Comparison of water saturation at different Rw values

Zone	Depth	Rw=0.08		Rw=0.10		Rw=0.12	
		Sw_AR	SWE_INDO	Sw_AR	SWE_INDO	Sw_AR	SWE_INDO
GAS ZONE	**3520**	0.47	0.43	0.52	0.47	0.57	0.51
	3525	0.27	0.21	0.35	0.22	0.33	0.24
	3530	0.37	0.32	0.44	0.35	0.45	0.37
	3535	0.37	0.32	0.44	0.35	0.45	0.37
	3545	0.37	0.32	0.44	0.35	0.45	0.37
	3550	0.37	0.32	0.44	0.35	0.45	0.37
	3555	0.37	0.32	0.44	0.35	0.45	0.37
	3560	0.37	0.32	0.44	0.35	0.45	0.37
	3565	0.37	0.32	0.44	0.35	0.45	0.37
	3570	0.34	0.29	0.44	0.31	0.42	0.33
	3575	0.22	0.21	0.28	0.23	0.27	0.25
	3580	0.35	0.31	0.42	0.33	0.43	0.36
	3585	0.23	0.21	0.32	0.24	0.28	0.25
	3590	0.45	0.37	0.56	0.40	0.55	0.43
	3595	0.31	0.27	0.40	0.30	0.37	0.32
	3600	0.16	0.16	0.23	0.17	0.19	0.19
	3605	0.26	0.26	0.33	0.28	0.32	0.31

In the oil zone:

	Depth	Rw=0.08		Rw=0.10		Rw=0.12	
		Sw_AR	SWE_INDO	Sw_AR	SWE_INDO	Sw_AR	SWE_INDO
OIL Zone	3615	0.39	0.35	0.47	0.39	0.47	0.42
	3620	0.29	0.29	0.36	0.33	0.36	0.36
	3625	0.31	0.29	0.39	0.32	0.38	0.35
	3630	0.63	0.57	0.68	0.62	0.75	0.67
	3635	0.29	0.28	0.36	0.31	0.36	0.34
	3640	0.29	0.28	0.36	0.31	0.35	0.34
	3645	0.45	0.41	0.56	0.45	0.55	0.49
	3650	0.45	0.43	0.55	0.47	0.55	0.51
	3655	0.73	0.69	0.78	0.72	0.79	0.74
	3660	0.53	0.49	0.61	0.54	0.65	0.58
	3665	0.47	0.40	0.56	0.43	0.57	0.46
	3670	0.35	0.34	0.43	0.37	0.43	0.41
	3675	0.28	0.28	0.34	0.31	0.34	0.34
	3680	0.50	0.47	0.57	0.52	0.57	0.55

In the water zone:

Zone	Depth	Rw=0.08		Rw=0.10		Rw=0.12	
		Sw_AR	SWE_INDO	Sw_AR	SWE_INDO	Sw_AR	SWE_INDO
Water Zone	3745	0.83	0.78	0.91	0.84	0.91	0.88
	3750	0.48	0.45	0.56	0.49	0.57	0.52
	3755	0.84	0.84	0.99	0.91	0.97	0.97
	3760	0.97	0.96	1.00	0.99	1.00	1.00
	3765	0.99	0.94	1.00	0.96	1.00	0.97
	3770	0.90	0.84	1.00	0.92	0.99	0.97
	3775	0.99	0.98	1.00	0.99	1.00	1.00
	3780	1.00	0.94	1.00	0.97	1.00	0.99
	3785	1.00	0.97	1.00	0.98	1.00	0.99
	3790	1.00	1.00	1.00	1.00	1.00	1.00
	3795	1.00	1.00	1.00	1.00	1.00	1.00
	3800	1.00	1.00	1.00	1.00	1.00	1.00

Appendix B: Well 6406/12-3B

B1: The whole interval display of the logging measurements and zonation of well 6406/12-3B

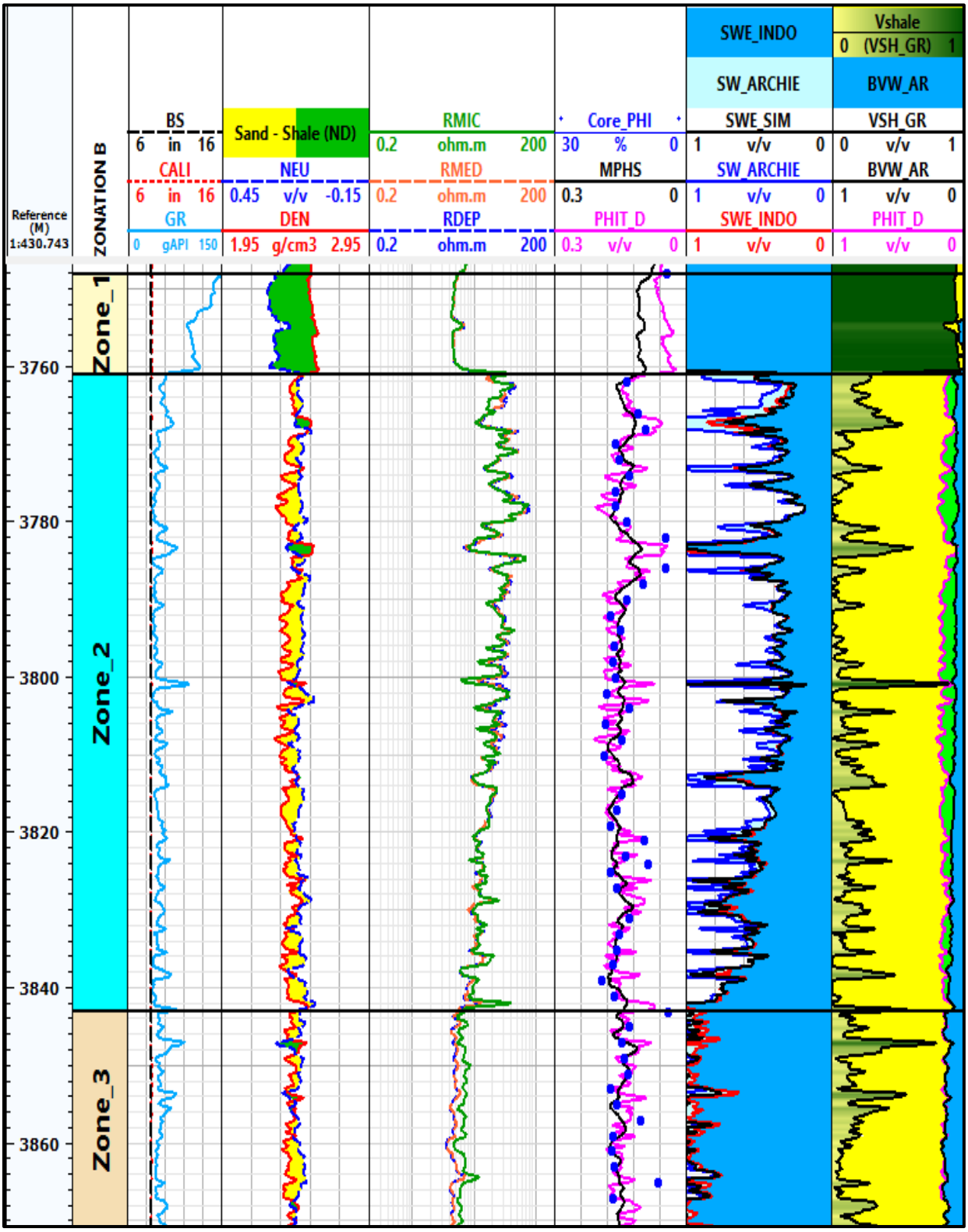

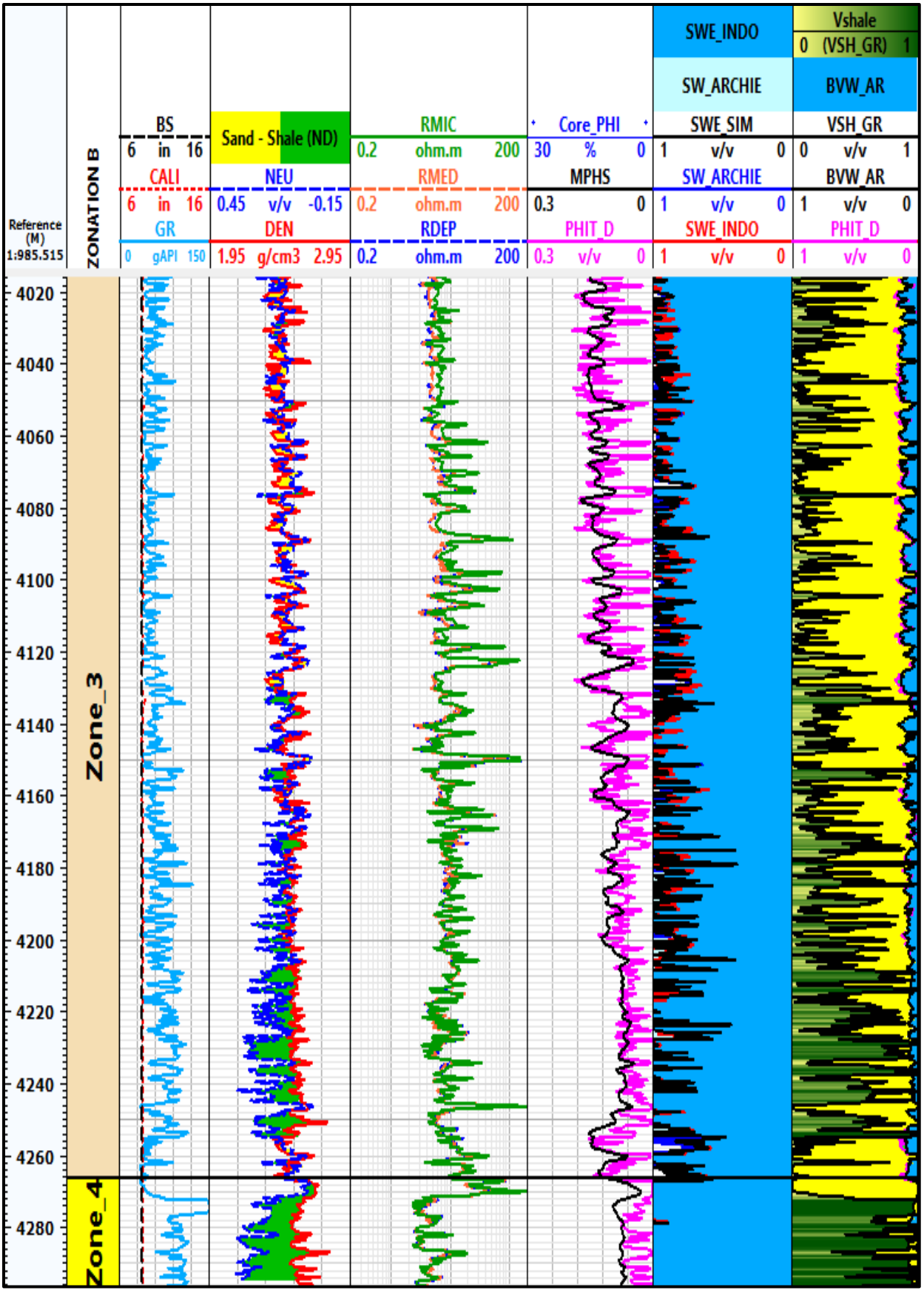
Reference (M) 1:985.515
ZONATION B
BS
6 in 16
CALI
6 in 16
GR
0 gAPI 150
Sand - Shale (ND)
NEU
0.45 v/v -0.15
DEN
1.95 g/cm3 2.95
RMIC
0.2 ohm.m 200
RMED
0.2 ohm.m 200
RDEP
0.2 ohm.m 200
Core_PHI
30 % 0
MPHS
0.3 0
PHIT_D
0.3 v/v 0
SWE_INDO
SW_ARCHIE
SWE_SIM
1 v/v 0
SW_ARCHIE
1 v/v 0
SWE_INDO
1 v/v 0
Vshale
0 (VSH_GR) 1
BVW_AR
VSH_GR
0 v/v 1
BVW_AR
1 v/v 0
PHIT_D
1 v/v 0
4020
4040
4060
4080
4100
4120
4140
4160
4180
4200
4220
4240
4260
4280
Zone_3
Zone_4

Appendix C: Well 6406/12-3A

C1: The whole interval display of the logging measurements and zonation of well 6406/12-3A

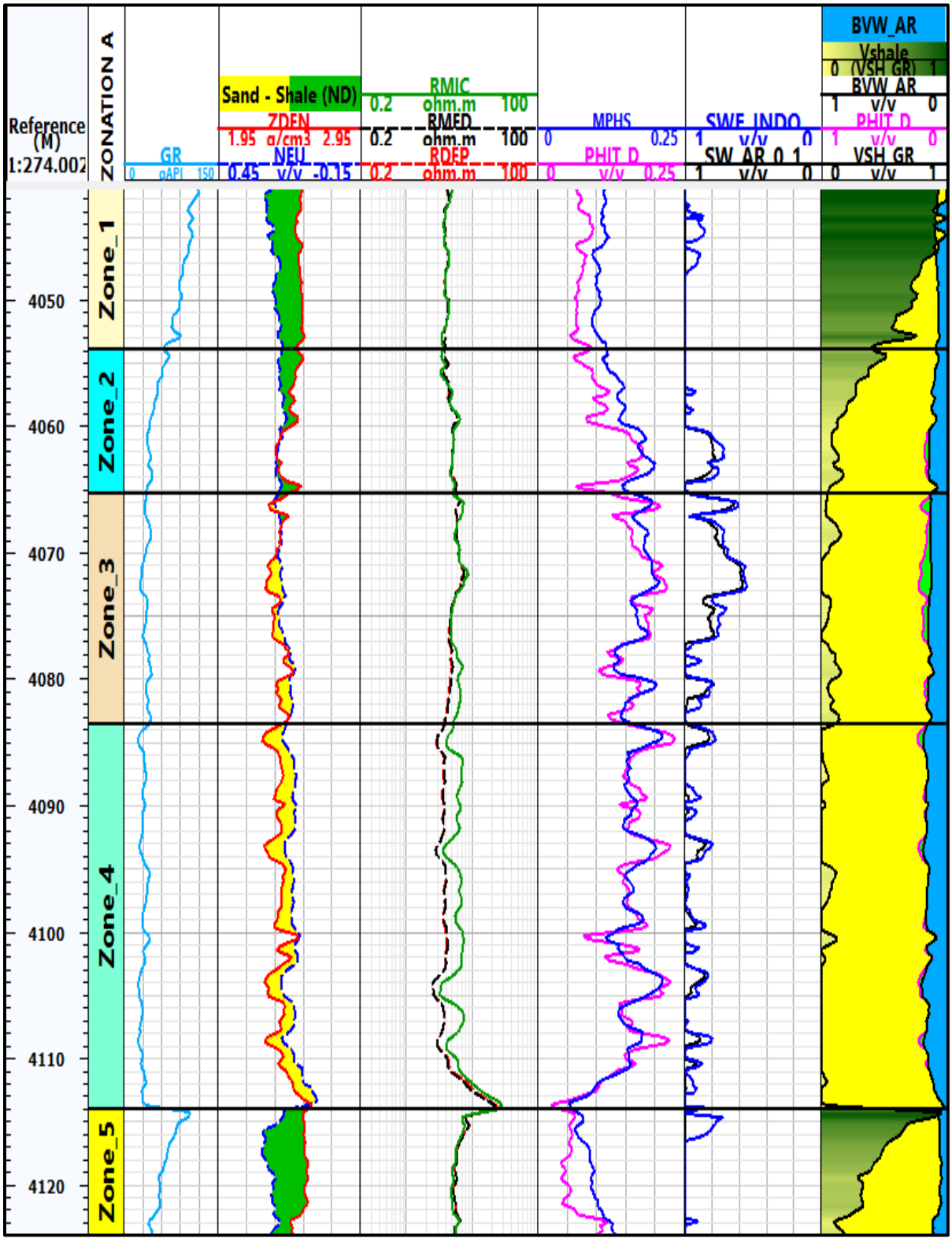

C2: Comparison of water saturations at different Rw values

MD	Rw = 0.08		Rw = 0.1		Rw = 0.12	
	Sw_AR	SWE_INDO	Sw_AR	SWE_INDO	Sw_AR	SWE_INDO
M	v/v	v/v	v/v	v/v	v/v	v/v
4065	0.76	0.71	0.78	0.79	0.89	0.85
4066	0.64	0.61	0.72	0.68	0.78	0.75
4067	0.81	0.74	0.85	0.82	0.96	0.89
4068	0.73	0.65	0.77	0.72	0.89	0.78
4069	0.68	0.63	0.73	0.70	0.83	0.76
4070	0.59	0.57	0.65	0.63	0.72	0.69
4071	0.52	0.50	0.59	0.56	0.63	0.62
4072	0.51	0.50	0.58	0.55	0.62	0.61
4073	0.71	0.67	0.80	0.75	0.88	0.82
4074	0.69	0.65	0.80	0.72	0.84	0.79
4075	0.71	0.68	0.82	0.75	0.87	0.82
4076	0.71	0.69	0.81	0.77	0.87	0.85
4077	0.94	0.89	0.99	0.97	1.00	1.00
4078	0.94	0.85	1.00	0.93	1.00	0.99
4079	0.98	0.94	0.99	0.98	1.00	0.99
4080	0.77	0.73	0.82	0.81	0.95	0.88
4081	0.83	0.77	0.94	0.86	0.98	0.93
4082	0.94	0.89	1.00	0.95	1.00	0.99
4083	0.93	0.89	0.97	0.95	1.00	0.99